The role of *Notch1* and *Vestigial-like1* in vertebrate limb development

Jeffrey Charles Francis

The Division of Developmental Biology,

MRC The National Institute For Medical Research (NIMR),

Mill Hill,

UCL.

Submitted in 2006 for the degree of Doctor of Philosophy

ProQuest LLC
789 East Eisenhower Parkway
P.O. Box 1346
Ann Arbor, MI 48106-1346

Acknowledgements

There are many people who have helped me throughout my PhD project. I have to say a big thank you to my supervisor Malcolm Logan for giving me the opportunity to work in his laboratory and for his motivation, guidance and support. Thank you to the past and present members of the laboratory for their helpful discussions and making it such a great place to work; Anna, April, Babis, Jo, Jutta, Peleg, Steve. A special thank you to Carolina for her encouragement, advice and for getting me through it. I am grateful to all the staff in the animal house in LLG for their tremendous work. Thank you to Freddy Radtke for generously giving us the *Notch1* conditional mice and to Brian Crenshaw for the *Brn4-Cre* mice. I also have to thank all my friends who have been with me throughout this work, especially Ali and Amir, for helping me when I really needed it. I am indebted to my parents and Rich, without them I would not have made it this far.

Abstract

Comparative studies of *Drosophila* genes and their vertebrate orthologues have shown that they can play analogous roles during embryonic development. Good examples are found during the development of the *Drosophila* wing, which can be considered analogous to the vertebrate limb. The *Drosophila melanogaster* genes *vestigial* and *Notch* are essential for proximal-distal outgrowth of the wing. I have investigated whether vertebrate orthologues, *Vestigial-like1* (*Vgl1*) and *Notch1*, respectively, are involved in vertebrate limb development.

In the fly, Notch signalling at the dorsoventral boundary of the wing activates downstream targets, such as *vestigial* and *wingless*. Similarly, vertebrate *Notch1* is expressed in a specialised region of cells at the dorsoventral boundary of the limb, the apical ectodermal ridge (AER). Classical embryological studies and genetic manipulation has demonstrated that the AER is required for proximal-distal outgrowth of the vertebrate limb. However, the role of *Notch1* in the vertebrate limb is poorly understood since the conventional knockout of *Notch1* dies before the onset of limb development. I have used a conditional allele of *Notch1* and exploited Cre/lox technology to delete Notch1 function in either the ectoderm or mesenchyme of the developing limb. My results demonstrate that *Notch1* is required to regulate the size of the AER, but is not required for the development of any of the mesenchyme derivatives.

Genetic studies in the fly have shown that *vestigial* is necessary and sufficient for wing morphogenesis. I have shown that chick *Vgl1* is expressed in a subpopulation of ectoderm cells, the periderm. Misexpression of various forms of *Vgl1* in the developing chick limb, using the chick retroviral system, has revealed a potential role for *Vgl1* and the periderm in the formation of the AER.

Declaration

I, Jeffrey Charles Francis, confirm that the work presented in this thesis is my own, performed in the laboratory of Malcolm Logan, MRC NIMR. Where information/reagents have been derived from other sources, I confirm that this has been indicated in the thesis. This work has been submitted in 2006 for the degree of Doctor of Philosophy.

Contents

List of figures and tables

Abbreviations

AER	apical ectodermal ridge
BMP	bone morphogenetic protein
CSL	CBF1/RBP-JΚ, Suppressor of Hairless (Su(H)), LAG-1
DIG	digoxigenin
DV	dorsal-ventral
EGF	epidermal growth factor
EST	expressed sequence tag
FGF	fibroblast growth factor
FGFR	fibroblast growth factor receptor
IPCD	interdigit programmed cell death
LPM	lateral plate mesoderm
LRP	LDL-like receptor
NICD	notch intracellular domain
PCR	polymerase chain reaction
PD	proximal-distal
SEM	scanning electron microscopic
SHFM	split-hand/ split-foot malformation
TEF	transcription enhancer factor
UTR	untranslated region
ZPA	zone of polarizing activity

1. Introduction

1.1 The vertebrate limb as a model system

During embryonic development, the individual cells that comprise an organism form complex multi-cellular structures through coordinated gene activation that directs the fate of individual cell types. This is a result of the precise control of cellular processes within an embryo, including proliferation, differentiation, cell survival and morphogenesis. The developing vertebrate limb provides a useful model environment to study these processes since they can be relatively easily manipulated and gene expression can be studied. An additional advantage is that development of the limbs can be altered or disrupted, without affecting the viability of the developing embryo. Classical embryological experiments and more recently experiments using advanced genetic manipulation methods have allowed insights into the mechanisms that regulate growth and patterning of the limbs. Many genes and signalling pathways, such as members of the bone morphogenic protein (BMP), fibroblast growth factor (FGF), WNT and hedgehog (HH) families have been shown to play important roles during limb development. These pathways are conserved between organisms and are utilized in many other developmental processes throughout embryogenesis. However, the specific regulation and function of many of the genes required for normal embryological development remains unclear. The study of vertebrate limbs allows us to analyze how these genes control various developmental processes.

The vertebrate limb originates as a bud of undifferentiated mesenchyme cells covered by ectoderm that grows out, perpendicular from the body of the embryo. Later in development, some of the mesenchyme cells condense and

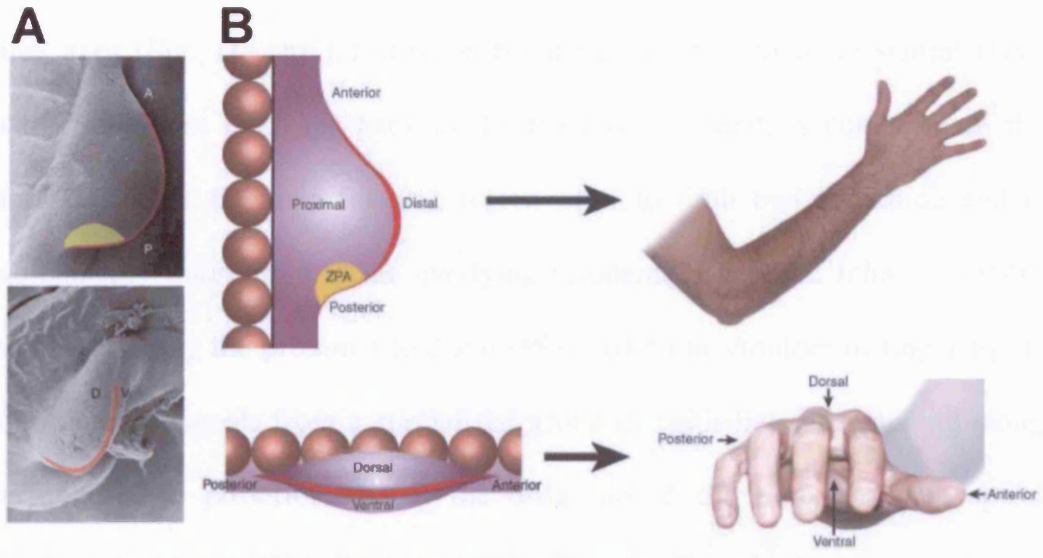

Figure 1. The vertebrate limb is patterned along three axes. (**A**) Scanning electron microscope picture of an E10.5 limb bud with the apical ectodermal ridge (AER) in red and the zone of polarising activity (ZPA) in yellow. Top picture is a dorsal view of the limb bud and the bottom is a distal view. (**B**) Schematic diagram of limb bud with the three cardinal axes and the human limbs that forms. The AER (red) runs from anterior to posterior at the distal tip of the limb bud and controls proximal-to-distal (PD) axis, from shoulder to finger tip. The ZPA (yellow) controls patterning along the anterior-to-posterior (AP) axis, the thumb-to-little finger. The ectoderm controls the dorsal-to-ventral (DV) axis, which runs from the back to the front of the hand. The AER is at the border between the dorsal and ventral ectoderm. A=Anterior, P=Posterior, D=Dorsal, V=Ventral. Adapted from (Logan, 2003).

differentiate into cartilage precursors of the limb skeleton. These precursors are subsequently mineralised to form the axial skeleton. The vertebrate limb is comprised of three skeletal domains, the proximal stylopod (humerus/femur), the zeugopod (radius and ulna/tibia and fibula) and, at the distal extreme of the limb, the autopod (wrist and fingers/ankle and toes).

Normal development of the vertebrate limb is a result of patterning along three axes (Fig. 1). The information for patterning the dorsal-to-ventral (DV) axis, which runs from the back to the front of the hand, is contained in the mesenchyme of the limb-forming region prior to limb bud formation and is subsequently transmitted to the overlying ectoderm (Chen and Johnson, 1999). Patterning along the proximal-to-distal (PD) axis from shoulder to finger tip, is controlled by signals from a specialised group of epithelial cells running along the anterior to posterior axis at the distal tip of the limb bud, the apical ectodermal ridge (AER) (Martin, 1998) (Fig. 1). The third axis, anterior-to-posterior (AP) or thumb-to-little finger, is patterned by a group of cells at the posterior of the limb mesenchyme called the zone of polarizing activity (ZPA). The cells within the ZPA pattern the AP axis by secreting the signalling molecule, Shh (Riddle et al., 1993) (Fig. 1).

The proximal-distal outgrowth of the vertebrate limb begins with the initiation of the limb bud, and then the formation of the AER that directs the continued outgrowth of the limb. Since my work is focused on the formation and function of the AER, I will first introduce limb bud initiation, and then describe what is known about the origin of the AER cells, how this structure forms and its role in outgrowth of the vertebrate limb.

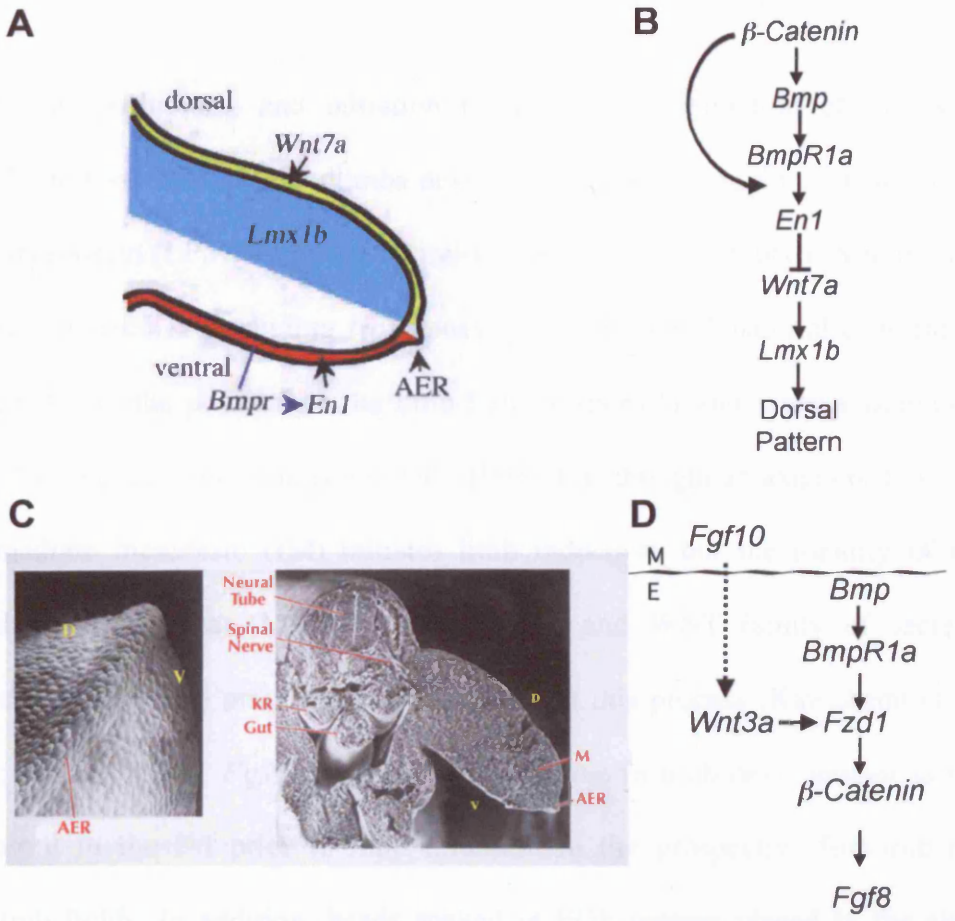

Figure 2. The molecular pathways that pattern the dorsal-ventral axis and the apical ectodermal ridge (AER) of the vertebrate limb. (**A**) A schematic diagram representing the expression domains of the genes involved in the dorsal-ventral (DV) patterning of the vertebrate limb. (**B**) The molecular relationship of the genes involved in DV patterning. *β-Catenin* acts upstream, or in parallel to, BMP signalling in the ventral limb ectoderm, which induces the expression of *Engrailed1* (*En1*). Ventrally expressed *En1* represses the expression of *Wnt7a* to the dorsal ectoderm, which induces *Lmx1b* (*Lmx1* in chick) in the dorsal mesenchyme and specifies dorsal pattern. (**C**) Scanning electron microscope pictures of the AER. The right picture shows the ridge of cells at the DV boundary of the limb bud. The left picture is a transverse section of an embryo illustrating the AER at the distal tip of the limb. (**D**) Mesenchymal Fgf10 signals to the overlying ectoderm to induce the expression of *Wnt3a*. BMP signalling in the ventral ectoderm is required for the expression of *Frizzled1* (*Fzd1*). Wnt3a signals through Frizzled receptors, presumably including Fzd1, via the canonical β-Catenin pathway. This results in the formation of the AER and expression of *Fgf8* in the pre-AER cells. D-Dorsal, V=Ventral, KR=Kidney Rudiment, M=Mesenchyme, E=Ectoderm. Adapted from Ahn et al., 2001, Barrow et al., 2003 and Soshnikova et al., 2003.

1.2 Limb bud initiation

Limb bud positioning and initiation occur prior to induction of the AER. Vertebrate forelimbs and hindlimbs develop from specific regions of the lateral plate mesoderm (LPM) along the rostral-caudal axis of the embryo. A number of different molecules (including *Hox* genes) produce a combinatorial code that is thought to set the position of the limb field (Capdevila and Izpisua Belmonte, 2001; Cohn et al., 1997; Rancourt et al., 1995). It is thought an axial cue from the intermediate mesoderm (IM) initiates limb induction, but the identity of this signal is still unclear. Members of the FGF and WNT family of secreted molecules have been proposed to be involved in this process (Kawakami et al., 2001; Martin, 1998). *Fgf8* may play this early role in limb development as it is expressed in the IM prior to limb initiation in the prospective forelimb and hindlimb fields. In addition, beads soaked in FGF protein placed in the chick inter-limb region are capable of inducing an ectopic limb (Crossley et al., 1996; Vogel et al., 1996). However, conditional deletion of *Fgf8* in the region of the embryo that includes cells that give rise to the IM have no effect on the initiation of limb outgrowth and the limbs develop normally (Boulet et al., 2004). In the chick, two WNT molecules are expressed in the IM and lateral plate mesoderm prior to the initiation of limb outgrowth, *Wnt2b* in the forelimb and *Wnt8c* in the hindlimb. Misexpression of these genes in the inter-limb flank leads to the ectopic expression of downstream limb mesenchyme markers and the growth of an ectopic limb, similar to that produced by an FGF bead (Kawakami et al., 2001). However, no mouse orthologues of *Wnt2b* and *Wnt8c*, or other WNT family members, have been described that have a similar expression pattern in the LPM. Furthermore, in a mouse knockout of *Lef1* and *Tcf1*, two nuclear

components of WNT signalling, limb bud outgrowth is still initiated (Galceran et al., 1999). In the mouse there maybe another WNT expressed in the LPM yet to be described, perhaps signalling via different nuclear constituents. Alternatively, WNT signalling may not play a comparable role in the mouse as it has been reported to do in the chick.

In response to the early axial cue from the IM, two members of the T-box family of transcription factors are expressed in the limb-forming region of the LPM, *Tbx5* in the forelimb and *Tbx4* in the hindlimb. Mouse mutants for these genes have shown they are required for limb bud formation. In *Tbx5* knockout mice the forelimbs fail to initiate (Agarwal et al., 2003; Rallis et al., 2003). Similarly, if *Tbx4* is deleted in mouse embryos the hindlimbs fail to develop (Naiche and Papaioannou, 2003). Further experiments have recently shown that although *Tbx5* and *Tbx4* have forelimb and hindlimb restricted expression patterns, they play equivalent roles in forelimb and hindlimb initiation, respectively (Minguillon et al., 2005).

Tbx5 in the forelimb and Tbx4 in the hindlimb activate the expression of *Fgf10*, which is expressed in the limb-forming region of the LPM. Expression of *Fgf10* in this region of the LPM is absent in the *Tbx5* mutant (Agarwal et al., 2003; Rallis et al., 2003). Deletion of *Fgf10* results in mice with truncations of the forelimbs and hindlimbs and, in addition, the lung buds fail to form (Min et al., 1998; Sekine et al., 1999). In these mutant mice the AER does not form, and as a result there is no proximal-distal growth of the limb bud.

1.3 Induction of the AER

Once limb bud outgrowth has been initiated, the AER is induced from cells of the overlying ectoderm. Several lines of evidence have demonstrated that mesenchymal *Fgf10* activates the expression of *Wnt3a* in the chick (*Wnt3* in mouse) in the overlying ectoderm, and that Wnt3a/Wnt3 signalling is required for the expression of *Fgf8* in the AER precursor (pre-AER) ectoderm cells (Fig. 2C and 2D). Firstly, the temporal expression pattern of these genes is consistent with this epistatic relationship; *Fgf10* is expressed first in the mesenchyme, subsequently *Wnt3a* is expressed in the overlying ectoderm and finally *Fgf8* in the ectoderm of the pre-AER cells. *Fgf10*-expressing cells placed in the inter-limb flank induce *Wnt3a* expression in 12 hours, while *Fgf8* expression is activated 18 hours after this operation (Kawakami et al., 2001). Misexpression experiments in the chick have shown that *Wnt3a* can ectopically induce AER-marker genes, such as *Fgf8*, *Fgf4* and *Bmp2* in broad patches of ectoderm. Misexpression of *Wnt3a* also disrupts AER formation and induces ectopic AERs in the dorsal and ventral ectoderm. However, misexpression of *Fgf8* in the prospective limb field is not able to induce the expression of *Wnt3a*, as expected if *Fgf8* is downstream of *Wnt3a* (Kengaku et al., 1998).

In the chick, misexpression of either a dominant-active form of *β-catenin* or *Axin*, a negative regulator of β-catenin, have demonstrated that Wnt3a signals via the β-catenin pathway. WNTs signal through the Frizzled receptors that function together with the LRP (LDL-like receptor) co-receptors. In a cell that is not responding to WNT signal, the complex of Axin, APC, and GSK3β promotes the degradation of β-catenin via the ubiquitin pathway. When a WNT ligand

binds to the Frizzled/LRP receptor complex, β-catenin is uncoupled from the Axin/APC/GSK3β complex, through a process that is not fully understood. This results in the accumulation of β-catenin, which translocates to the nucleus and interacts with the transcription factors Tcf/Lef to activate target genes (reviewed in Church and Francis-West, 2002; Nelson and Nusse, 2004; Sharpe et al., 2001). Misexpression of activated *β-catenin* induces the expression of *Fgf8* and other AER markers genes, in a similar fashion to the misexpression of *Wnt3a.* Misexpression of *Axin* prior to AER formation has no effect on *Fgf10* expression in the mesenchyme, while the expression of *Fgf8* in the ectoderm is downregulated and the AER is disrupted. This supports a model in which *Fgf10* induces the expression of *Fgf8* in the ectoderm via WNT/β-catenin signalling (Fig 2D) (Kengaku et al., 1998; Kawakami et al., 2001).

Mouse mutants for *Wnt3* and *β-catenin* have also shed light on the role of these genes in AER formation and maintenance. Mice that have *Wnt3* conditionally deleted from the ectoderm and AER of the limb have severe limb defects, including some examples in which the limbs are absent (Barrow et al., 2003). In some mutant embryos *Fgf8* expression is present throughout the AP length of the AER, although the DV axis is thinner. In other *Wnt3* mutant embryos *Fgf8* expression is lost or only present in small patches. After the deletion of *Wnt3*, some of the pre-AER cells do not express *Fgf8* and do not form a thickened ectoderm, demonstrating *Wnt3* has a role in the formation of the AER. The variability in the phenotypes could be due to differences in the temporal and spatial activity of the Cre line used to delete *Wnt3* from the limb ectoderm. *Wnt3* is expressed throughout the limb ectoderm and can signal in a cell non-autonomous fashion. During AER formation Wnt3 may only need to

signal to the ectoderm cells that will form the ridge. Therefore, regions of limb ectoderm in which *Wnt3* is not deleted could still signal to the population of ectodermal cells that are required for AER formation (Barrow et al., 2003). Mice that have *β-catenin* conditionally deleted from the limb ectoderm phenocopy *Wnt3* mutant mice, consistent with Wnt3 signalling through the canonical β-catenin pathway in AER formation. In the hindlimbs of these conditional knockouts, the *β-catenin* gene is deleted from the ventral ectoderm prior to AER formation. This is sufficient to abolish all *Fgf8* expression and produce mice with a no hindlimb phenotype that is completely penetrant. This illustrates that WNT signalling, through β-catenin, is only required in the ventral ectoderm for AER formation (Barrow et al., 2003). Mice that have a gain-of-function mutation for *β-catenin*, where an activated form is expressed in the ectoderm, exhibit an expanded AER (Barrow et al., 2003).

Although there is complete loss of hindlimbs in the *β-catenin* mutants, the Cre activity in the forelimb ectoderm occurs after induction of the AER, so that a ridge of cells forms that are expressing *Fgf8*. However, analysis of limb buds at later stages of development show a progressive decrease in the amount of *Fgf8* signal, until it eventually disappears. This work indicates that WNT/β-catenin signalling is required for the maintenance as well as the initiation of the AER (Barrow et al., 2003; Soshnikova et al., 2003).

Mice that carry a conditional deletion of the *bone morphogenic protein receptor 1a* (*Bmpr1a*) gene in the limb ectoderm also have disruptions in the AER, although this phenotype is not 100% penetrant. The expression of *Fgf8* varies in the AER of these mutant animals, with some having nearly complete loss of *Fgf8*

expression while others are almost normal. Most mutant embryos have large areas of *Fgf8* expression with gaps of non-expressing cells along the ridge (Ahn et al., 2001). In the chick, *Bmp2*, *Bmp4* or *Bmp7* are expressed in the ventral ectoderm of the early limb bud. Misexpression experiments in the chick using a dominant-active *Bmpr* results in a partial or complete loss of the AER, leading to truncated or notched limbs (Pizette et al., 2001). Interestingly, this dominant-active construct also results in ectopic *Fgf8* expression in the dorsal ectoderm where *Bmp*s are not normally expressed. Misexpression of a BMP antagonist, *Noggin*, results in AER disruptions and the formation of ectopic AERs ventrally. These experiments indicate that either loss of BMP signalling ventrally or ectopic BMP signalling dorsally is sufficient to induce ectopic *Fgf8* expression. Taken together, it is thought a boundary between ventral *Bmp*-expressing cells and dorsal non *Bmp*-expressing cells is required for correct AER formation (Pizette et al., 2001). The gain- and loss-of-function misexpression experiments in the chick have also shown that BMP signalling regulates the expression of the transcription factors *Msx1* and *Msx2* in the ventral limb ectoderm (Pizette et al., 2001). *Msx* genes are known targets of BMP signalling in other locations in the developing embryo (Lallemand et al., 2005). However, the mouse *Msx1*$^{-/-}$; *Msx2*$^{-/-}$ double knockout does not have disruptions in AER initiation (Lallemand et al., 2005).

Soshnikova et al. found that activated β-catenin could rescue the AER disruptions in mice that have *Bmpr1a* conditionally deleted from the limb ectoderm. In these compound mutants *Fgf8* and *Bmp4* are expressed in the limb ectoderm prior to AER formation, and continue to be expressed in a similar fashion to embryos that have the activated form of β-catenin misexpressed in the

limb ectoderm. From these experiments it is possible to put *Bmpr1a* upstream of WNT/β-catenin signalling in AER formation (Fig. 2D). In the *Bmpr1a* mutants, *Wnt3* was normally expressed in the limb ectoderm, but the expression of the WNT receptor *Frizzled1* (*Fzd1*) was lost from the ventral ectoderm. This indicates a complex interaction between BMP signalling and WNT/β-catenin signalling during AER induction, and that *Fzd1* is involved in this crosstalk (Soshnikova et al., 2003) (Fig. 2D).

1.4 The origin and maturation of the AER

Prior to limb outgrowth the embryo is covered by a single layer of ectoderm that later in development consists of two layers; an irregular cuboidal layer of cells and an overlying simple squamous periderm (Koster and Roop, 2004; Todt and Fallon, 1984; Todt and Fallon, 1986). When the limb ectoderm cells have been induced to form an AER, the pre-AER cells comprise a broad patch of thickened ectoderm. These cells migrate and form a ridge of multilayered columnar epithelium at the DV boundary (Tickle and Altabef, 1999). Several studies have begun to identify where the AER cells originate from and the compartment boundaries that are necessary to form a normal AER at the distal tip of the limb bud.

Chick-quail chimera experiments have shown the ridge progenitors are initially spread over a wide area of ectoderm covering the limb-forming region of the LPM. These experiments also indicate there is a lineage restriction between dorsal and ventral cells of the AER, ensuring these cells do not mix (Michaud et

al., 1997). Further fate-mapping experiments in the chick using DiI labelling have also demonstrated the AER progenitors come from a large domain of ectoderm cells, that contains both ridge and non-ridge progenitors (Altabef et al., 1997). Ectoderm cells labelled prior to limb development are found in either the dorsal or ventral limb ectoderm, demonstrating there are two early ectodermal compartments. These dorsal and ventral compartments extend down the body and include the inter-limb region. The AER precursor cells come from both the dorsal and the ventral ectoderm. At stages 13 to 16 ridge progenitors are spread broadly over the future limb ectoderm and are mixed with ectoderm cells that will not comprise the ridge. Cells labelled in the ventral ectoderm never crossed the middle of the ridge into the dorsal side of the AER. However, in contradiction to the chick-quail study, dorsally labelled ectoderm cells are found throughout the AER (Altabef et al., 1997).

Cre/LoxP based fate-mapping and retroviral cell marking experiments in the mouse have suggested there are two lineage boundaries that are required for correct AER formation (Kimmel et al., 2000). *En1* is expressed in the ventral ectoderm and the ventral half of the AER. Expression analysis of an *En1* knock-in allele using a *lacZ* reporter mouse has shown that from E9.5 to E11.5, *En1* expressing cells do not cross from the ventral to the dorsal side of the AER, similar to the chick fate-mapping results. At later stages of development, as the AER begins to degenerate, some *lacZ* positive cells are found in the dorsal side of the AER. In a different approach, ultrasound was used to inject a replication-defective *lacZ* expressing retrovirus into the amniotic fluid of wild-type E8.5 mouse embryos. This allowed the random infection of the *lacZ* retrovirus into the

surface ectoderm of embryos. It was assumed that small clusters of cells (average of 8) were the descendents of a single infected cell and the position of clusters was analysed within the AER. At E10.5, *lacZ* expressing cells are found in either the dorsal or ventral AER, but by E11.5 cells are distributed in both the dorsal and ventral AER. This work suggests there is a transient lineage restriction at the middle of the AER (Kimmel et al., 2000). This boundary within the AER is consistent with the chick-quail chimera experiments, in which no mixing was seen between dorsal and ventral AER cells. However, in the chick DiI cell labelling experiment mixing of dorsal cells was observed but, as this is a transient border, cells would mix in embryos analysed at later stages of development (Kimmel et al., 2000; Altabef et al., 1997).

There is a second boundary at the dorsal margin of the AER that prevents mixing of AER cells with ectoderm cells (Kimmel et al., 2000). A tamoxifen-inducible version of a promoter thataa drives Cre expression specifically in the developing and mature AER, *Msx2-Cre*, allowed labelling of the pre-AER cells. These experiments showed that at E10.5 and E11.5 there is dense staining in the AER and also scattered staining in ventral pre-AER cells. However, no cells are stained dorsally, indicating there is a restriction of cell movement at the dorsal boundary of the AER. The labelled cells that persist in the ventral pre-AER after AER formation demonstrate that not all the cells that initially express AER genes become incorporated into the AER. Labelling cells after AER formation results in staining primarily in the AER, demonstrating the cells in the mature AER (cells that are expressing *Msx2*) become restricted to the ridge (Kimmel et al., 2000).

These fate-mapping experiments of the limb ectoderm indicate that while in both the mouse and chick the AER precursor cells are mixed with ectoderm cells prior to ridge formation, there is a difference in the origin of the pre-AER cells. In the chick they appear to be distributed over the dorsal and ventral ectoderm, while in the mouse the AER seems to be formed from cells of the ventral ectoderm. This work illustrates a requirement for the selection of ridge cells and their movement to form a mature AER at the distal tip of the limb. The transcription factor *En1*, expressed in the ventral ectoderm of the limb bud and ventral half of the AER has been implicated in this process. In *En1* mutants, the pre-AER cells express AER-marker genes, but they never form a ridge at the DV boundary of the limb bud. Instead, the ventral ectoderm is broader, thickened and sometimes forms a second ridge, while the dorsal part of the AER forms normally (Loomis et al., 1996). In these *En1* mutants, *Wnt7a*, which is normally restricted to the dorsal ectoderm of the limb bud, is misexpressed in the ventral ectoderm. Interestingly, in $En1^{-/-}$; $Wnt7a^{-/-}$ double knockouts a relatively normal AER forms, suggesting that *Wnt7a* plays a role in the formation of the ectopic ridges and could be involved in endogenous AER formation. However, this is still unclear, as when *Wnt7a* is deleted alone a normal AER forms (Cygan et al., 1997; Loomis et al., 1998).

En1 is important in establishing the two lineage boundaries, which are required to form the mature AER (Kimmel et al., 2000). In transgenic mice that misexpress a single copy of the *En1* gene throughout the AER, the ridge becomes fragmented with only patches of *Fgf8* expression present and *Fgf8*-expressing cells found dorsal and ventral relative to the DV boundary. This loss

of AER formation could reflect a disruption of the boundary within the AER, normally established by *En1* expression restricted to the ventral cells of the AER. Sections of these limb buds show in some cases the ridges are flattened and have low levels of *Fgf8* expression, while in others there is no ridge and *Fgf8* expression is absent. The fragmented AER in these transgenics are characterised by the formation of ridges dorsal to the DV margin, which could be a result of the misexpression of *En1* in the dorsal half of the AER. En1 in the ventral ectoderm and AER normally represses the expression of *Wnt7a* which is restricted to the dorsal ectoderm. Misexpression of *En1* in the dorsal AER also results in the expression domain of *Wnt7a* at the dorsal edge of the AER being shifted proximally (Kimmel et al., 2000). In homozygous transgenic mice that express higher levels of *En1* in the AER, *Fgf8* expression is lost early in AER formation in the pre-AER. The majority of these transgenic mice lacked hindlimbs. This failure to form an AER could be due to the high levels of *En1* misexpressed in the dorsal AER preventing signalling that normally takes place between dorsal and ventral cells within the ridge. Alternatively, the proximal shift in *Wnt7a* expression in the dorsal ectoderm could affect the formation of the ridge (Kimmel et al., 2000).

This work is consistent with misexpression of *En1* in the chick (Altabef et al., 2000). Ectopically expressed *En1* prevents the formation of a morphological AER and the expression of ridge-associated genes. Subsequently, the limb buds fail to develop. However, lineage tracing after *En1* misexpression does not alter the segregation of dorsal and ventral ectodermal compartments. This demonstrates that while *En1* is required for AER formation it is not involved in compartment maintenance (Altabef et al., 2000).

1.5 Function of the AER during limb outgrowth

The role of the AER during vertebrate limb development has been shown in embryological experiments in the chick. Following surgical removal of the AER, limb outgrowth is disrupted and a truncated limb forms. If the AER is removed at early stages of limb bud outgrowth the limb is severely truncated, with only the most proximal structures present. However, if the AER is removed at later stages of development more distal structures develop (Saunders, 1998; Summerbell, 1974). The limb truncation phenotype can be rescued if an exogenous source of fibroblast growth factor (FGF) is supplied after removal of the AER. These results suggest that FGFs expressed by cells in the AER play essential roles in maintaining limb outgrowth (Fallon et al., 1994; Martin, 1998; Niswander et al., 1993). Four members of the FGF family are expressed in the AER; *Fgf4*, *Fgf8*, *Fgf9* and *Fgf19*. *Fgf8* is the first FGF to be expressed in the AER. Genetic studies using conditional deletion of *Fgf8* and *Fgf4* in the AER have also demonstrated the importance of these factors in PD development of the limb (Sun et al., 2002). The Cre line used in this study deletes all *Fgf8* and *Fgf4* from the mutant hindlimbs. However, in this line Cre activity starts after forelimb AER formation, so there is transient expression of *Fgf8* and *Fgf4* in the forelimbs. None of the $Fgf8^{-/-}$; $Fgf4^{-/-}$ double mutants have hindlimbs, while the forelimbs contain hypoplastic stylopod, zeugopod and autopod elements. These conditional deletion experiments in the mouse demonstrate that *Fgf8* and *Fgf4* are involved limb outgrowth. Analysis of proliferation and apoptosis in 36 somite embryos suggest that a major function of FGFs in the limb is cell survival. In the mutant hindlimbs, which never see any Fgf8 and Fgf4, a

morphological AER is formed and maintained, although hindlimb structures fail to form.

Human limb malformations have provided further evidence of the importance of FGFs and their receptors, fibroblast growth factor receptors (FGFRs), during vertebrate limb development (reviewed in Wilkie et al., 2002). Mutations in *FGFR1* and *FGFR2* can lead to Pfeiffer syndrome. These individuals have a range of phenotypes including broad first digits, fused phalanges and cutaneous syndactyly. Patients with Aperts syndrome also have mutations in *FGFR2* and suffer from broad digits, complex bony syndactyly and the fusion of adjacent bones in the limb. Recently, a double mutation in *FGFR2* has been reported, in which individuals exhibit syndactyly of the hand and feet. These mutations and their phenotypic consequences likely arise as a result of a number of different factors, including FGF affinity and selectivity for its receptor, the level of constitutive receptor activation and the pattern of receptor expression (Wilkie et al., 2002).

There are two proposed models to explain the patterning of the vertebrate limb along the proximal-distal axis, both requiring the AER. According to the progress zone model, mesenchymal cells at the distal tip of the vertebrate limb proliferate under the influence of the AER and they measure time to assess their proximal-distal position. The progress zone is thought to be a region of undifferentiated cells approximately 300 microns deep at the tip of the limb. An internal clock that is only active while cells remain in the progress zone controls the change in positional identity. The undifferentiated cells in the zone are dividing so that cells continually leave, the internal clock is switched off and

cells obtain a fixed positional value. Cells that leave the progress zone early form proximal structures while cells that remain the longest develop into digits (Tickle and Wolpert, 2002). The second model, the progenitor model, proposes that the segments that comprise the vertebrate limb are specified early in development as distinct domains of cells in the distal region of the bud. As the limb develops, the AER directs outgrowth by expanding the domains of the progenitors (Dudley et al., 2002).

1.6 AER dynamics

Fate map studies have demonstrated that during limb outgrowth the cells that constitute the AER are dynamic and that there is some movement of ridge cells (Vargesson et al., 1997). AER cells were labelled at different positions along the anterior-posterior axis of the limb bud. Small patches of cells labelled in the AER expanded slightly to form a compact band of cells. Labelling two populations of cells demonstrated that this mixing only occurs locally, and does not involve the movement of cells throughout the whole ridge. It was noted that AER cells do not mix with the mesenchyme, but cells labelled in the anterior part of the ridge leave the AER to the non-ridge ectoderm. Further, the labelling of cells in the AER and underlying mesenchyme demonstrated that ridge cells end up more anterior compared to the mesenchyme. This suggests that during development the AER does not stay in a fixed position relative to the underlying mesenchyme but moves anteriorly, and that at stage 20 the posterior two-thirds of the ridge ultimately make up the whole AER (Vargesson et al., 1997).

1.7 Regression of the AER

Further lineage marking using *Msx2-Cre* transgenic mice has demonstrated that, although the AER is a discrete population of cells, it is a transient structure. At late stages of limb development the AER regresses and the expression of AER marker genes are lost. At this time, the columnar cells of the AER flatten to become simple cuboidal epithelium once again. The ridge cells are lost from E12.5 in the interdigit region and then later, between E13.5 and E14.5, in the region at the distal tip of the digits. After the loss of the AER, dorsal and ventral compartments are maintained in the ectoderm of the limb, with the distal border in the postnatal limb being at the edge of the nail bed (Guo et al., 2003).

Members of the BMP family are thought to be involved in AER regression. Misexpression of the BMP antagonist Noggin in the ectoderm of the chick limb results in an overgrowth of soft tissue over the digit and interdigit regions (Pizette and Niswander, 1999). In the chick, AER regression in the cells over the interdigit region takes place at stage 32, and regression has finished in cells overlying the digits at stage 35. Misexpression of Noggin leads to maintenance of AER marker genes, such as *Fgf8, Fgf4* and *Bmp4* and columnar epithelium resembling a normal AER is still present. Sustained expression of *Fgf8* in Noggin infected limbs correlates with increased cell proliferation in the underlying mesenchyme. This indicates that the ectopic outgrowths are a result of prolonged proliferation caused by sustained expression of AER *Fgf*s (Pizzette and Niswander, 1999). In a complementary experiment, in transgenic mice that misexpress Noggin in the AER the expression of *Fgf8* persists in the ectoderm overlying the interdigit regions of E13.5 embryos, and patches of *Fgf8* expression are still present at E14.5 (Wang et al., 2004). In addition, mice that

carry deletions of both *Msx1* and *Msx2* genes, which are potential targets of BMP signalling, AER regression is impaired and *Fgf8* expression is prolonged (Lallemand et al., 2005).

1.8 Dorso-ventral patterning of the vertebrate limb

The AER is positioned at the DV margin of the limb bud, between the dorsal and ventral ectoderm. The invariant position of the AER at the DV border of the limb and chick and mouse mutants have indicated that these two processes could be linked (Ahn et al., 2001; Barrow et al., 2003; Soshnikova et al., 2003). In the chick limbless mutant both AER formation and DV patterning are disrupted (Laufer et al., 1997).

Transplantation of limb mesoderm and ectoderm have demonstrated that early DV signal(s) from the mesenchyme induce signals in the ectoderm that define DV patterning of the limb (reviewed in Chen and Johnson, 1999).

Recently, experiments have begun to uncover the identity of the signals that regulate the DV polarity of the limb. In addition to the role *Bmpr1a* in AER formation, the conditional deletion of this gene from the limb ectoderm has established that BMP signalling is also required for DV patterning of the limb. Unlike the disruption in AER formation, the DV patterning defects of the *Bmpr1a* mutant is completely penetrant. Mice in which *Bmpr1a* has been conditionally deleted in the limb ectoderm prior to limb outgrowth have dorsal transformations of the limb, so that ventral structures become dorsal-like (Ahn et al., 2001). Similarly, if the BMP antagonist Noggin is expressed in the limb ectoderm ventral structures become more dorsal-like, with the loss of ventral

footpads and the presence of extra nails on the ventral surface (Wang et al., 2004).

Consistent with these studies in the mouse, misexpression of *Noggin* in the chick limb bud leads a transformation of ventral limb structures to dorsal structures. This alteration in DV patterning of the limb results in the loss of *Engrailed1* (*En1*) expression from the ventral ectoderm and the ectopic expression of the dorsal markers *Wnt7a* and *Lmx1b* ventrally. In the converse experiment, misexpression of constitutively active *Bmpr1a* ventralizes the limb, so that *En1* is ectopically expressed in the dorsal ectoderm and expression of *Wnt7a* and *Lmx1b* are lost. Misexpression of *En1* in the chick limb does not alter the expression of *Bmp2*, *Bmp4* or *Bmp7* in the ventral ectoderm (Pizette et al., 2001) (Fig. 2A and 2B). This work demonstrates that BMP signalling in the limb ectoderm activates the expression of *En1* in the ventral ectoderm and is required for correct DV patterning of the limb

Recently, two groups have implicated canonical WNT/β-catenin signalling in the establishment of DV polarity (Barrow et al., 2003; Soshnikova et al., 2003). Mice that have *Wnt3* or *β-catenin* conditionally deleted from the limb ectoderm have a loss of ventral structures and a duplication of dorsal structures, including nail plates duplicated on both sides of the limb. In addition, the expression of *En1* was absent from the ventral ectoderm of the limb (Barrow et al., 2003).

The epistatic relationship between WNT and BMP signalling in DV patterning is not completely clear. In *Wnt3/β-catenin* mutant embryos at 26 somites, ectodermal *Bmp2* and *Bmp4* expression is lost in the limb bud. This suggests that WNT/β-catenin signalling is acting upstream of BMP signalling in

DV patterning of the limb ectoderm (Barrow et al., 2003). However, in a different approach, Soshnikova et al. used mice that have *Bmpr1a* conditionally deleted from the limb ectoderm and tested whether it is possible to rescue the DV patterning defects with activated β-catenin expressed via transgenic methods in the limb ectoderm. In these compound mutants, expression of *En1* is still absent from the ventral ectoderm showing that β-catenin is unable to rescue the loss of BMP receptor 1A. Together, this work suggests that β-catenin acts genetically upstream, or in parallel to BMP signalling through Bmpr1a in DV patterning (Soshnikova et al., 2003) (Fig. 2A and 2B).

Null mutations in *En1* result in the ventral domain of the limb becoming dorsalized, so that dorsally expressed *Wnt7a* and *Lmx1b* are now ectopically expressed in the ventral part of the limb. This leads to mice with limbs that have dorsal transformations of ventral paw structures (Cygan et al., 1997; Loomis et al., 1996; Loomis et al., 1998; Parr and McMahon, 1995). This work demonstrates that En1 represses the expression of *Wnt7a* to the dorsal ectoderm (Fig. 2A and 2B).

Consistent with *Wnt7a* being required for DV patterning in the dorsal ectoderm, mice with mutations in *Wnt7a* result in a distal bi-ventral limb phenotype. These bi-ventral limbs have ectopic footpads and striated epidermis dorsally and the loss of hair on the dorsal surface of the limb. In *Wnt7a* mutants the dorsal limb mesenchymal derivatives, tendons and bone, also have their identity transformed to ventral fates (Loomis et al., 1998; Parr and McMahon, 1995). Molecular and genetic analyses have shown that Wnt7a induces the expression of *Lmx1b* (*Lmx1* in the chick) in the underlying dorsal mesenchyme

(Fig. 2). Misexpression of *Wnt7a* in the ventral ectoderm of the chick is sufficient to induce *Lmx1* expression in the ventral mesenchyme. Ectopic expression of *Lmx1* in the ventral ectoderm generates a double-dorsal limb pattern, including changes in the patterning of the ventral muscles and tendons so that they resemble a dorsal-like pattern (Riddle et al., 1995).

1.9 The role of vertebrate orthologues of *Drosophila Notch* and *vestigial* in limb development

Comparative studies of *Drosophila melanogaster* genes and their vertebrate orthologues have shown they often play analogous roles during embryonic development. Parallels have been drawn between the development of the *Drosophila* wing and the vertebrate limb. The AER is considered the analogous structure to the wing margin in the *Drosophila* wing imaginal disc. Flies have been used successfully as a model to identify vertebrate genes that have been conserved through evolution and that have similar roles in embryonic development. The *Drosophila melanogaster* genes *Notch* and *vestigial* are expressed at the wing margin and are essential for proximal-distal outgrowth of the wing. My project was to investigate whether two of their vertebrate orthologues, *Notch1* and *Vestigial-like1* (*Vgl1*) respectively, are involved in vertebrate limb development.

1.10 The Notch signalling pathway

The Notch signalling pathway is involved in a large number of developmental processes including cell fate specification, cell proliferation and cell survival

decisions during development, as well as in the adult. Notch signalling is able to control these processes by regulating many targets in a context and cell-type-dependent manner. Disruption of the *Notch* receptors, their ligands and downstream signalling components of the Notch pathway have been implicated in numerous human developmental defects and adult pathologies (reviewed in Lai, 2004).

Vertebrate *Notch1* belongs to a family of four transmembrane receptors, *Notch1-4*, that signal between cells in direct contact with one another (Fig. 3). In vertebrates, Notch is constitutively cleaved in the Golgi by members of the Furin family of proteases and is then transported to the cell surface. Upon binding to one of its ligands, *Jagged1/2* (*Serrate* in invertebrates) or *Delta1/3/4*, the Notch receptor is cleaved by two proteolytic steps to release the intracellular domain of Notch (NICD). Ligand binding allows cleavage of Notch by extracellular metalloproteases, TACE (TNFα-converting enzyme) in vertebrates. The truncated Notch receptor is the substrate for γ-secretase activity, which consists of the presenilin-nicastrin-Aph1-Pen2 complex. This γ-secretase-catalysed reaction results in the cleavage of Notch within the transmembrane domain, freeing NICD (Fortini, 2002). NICD translocates to the nucleus and forms a complex with the CSL (CBF1/RBP-Jκ, Suppressor of Hairless (Su(H)), LAG-1) DNA-binding protein and the Mastermind (MAM)/Lag3 co-activator and acts as a transcriptional activator. When CSL is not bound to NICD it can recruit repressors, so that activation of Notch signalling can switch from active repression to activation of target genes. The CSL/NCID complex can bind to specific sequences in the promoter region of targets and activate their expression,

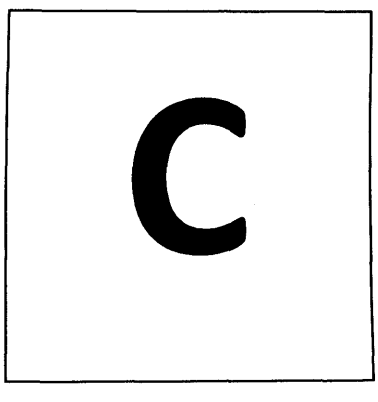
C

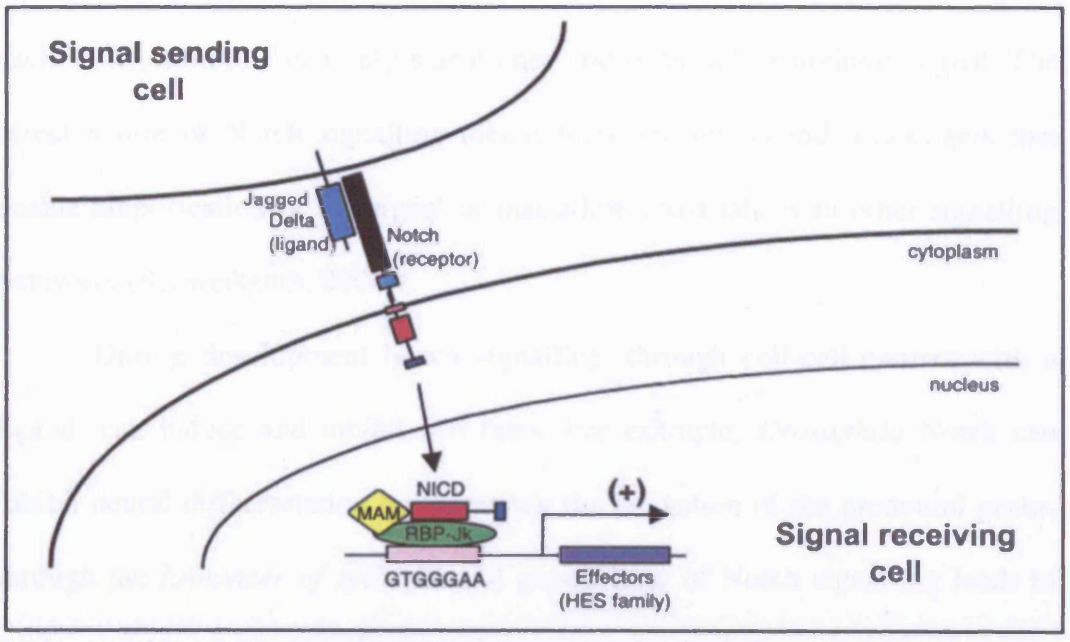

Figure 3. The vertebrate Notch signalling pathway. The extracellular domain of a Notch receptor (black) expressed on one cell, signals once bound to one of its ligands, *Jagged1/2* or *Delta1/3/4* (light blue), on an adjacent cell. Upon binding, Notch is proteolytically cleaved and the Notch intracellular domain (NICD, pink) translocates to the nucleus. There it interacts with the CSL (CBF1/RBP-Jκ, Suppressor of Hairless (Su(H), green), LAG-1) DNA-binding protein and the Mastermind (MAM, yellow) co-activator to activate the transcription of target genes, such as members of *Hes* family. Adapted from Iso et al., 2003.

such as the *Hairy/Enhancer of Split* (*Hes*) and *Hes-related repressor protein* (*Herp*) genes (for review see Lai, 2004; Schweisguth, 2004).

The method of Notch signalling, involving ligand binding, cleavage of the receptor and the direct activation of target genes has a number of characteristics. As ligand binding induces an irreversible proteolytic cleavage of the receptor, each Notch molecule can only signal once and is an 'all-or-nothing' signal. The direct nature of Notch signalling means there are no second messengers that enable amplification of the signal or that allow cross-talk with other signalling pathways (Schweisguth, 2004).

During development Notch signalling, through cell-cell contact with a ligand, can induce and inhibit cell fates. For example, *Drosophila* Notch can inhibit neural differentiation by repressing the activation of the proneural genes, through the *Enhancer of split* [*E(spl)*] genes. Loss of Notch signalling leads to the loss of this inhibitory effect and the over production of neural cells. A similar method of repression is used in vertebrates to inhibit neurogenesis, with the Notch pathway activating members of the *Hes* genes (reviewed in Lai, 2004). Notch signalling can induce new cell types, such as in the wing imaginal disc. Notch activation at the DV boundary of the wing disc at the junction between cells that express *Serrate* and cells that express *Delta* results in the activation of genes required for wing outgrowth (described in detail below). This activation of Notch signalling leads to the induction of new cell fates, as well as establishing a boundary between the dorsal and ventral compartments of the wing (reviewed in Irvine and Vogt, 1997). As in the fly wing imaginal disc, Notch signalling regulates the formation of boundaries in vertebrates. Notch signalling controls

the segmentation of somites, blocks of mesoderm along the trunk of the embryo that give rise to the vertebral column and most of the skeletal muscles. This involves the oscillation of signalling components of the Notch pathway so that somites are formed at specific time points, and leads to sharp boundaries being created between each somite (Bessho and Kageyama, 2003).

1.11 The complexity of Notch signalling

Notch signalling is often depicted as a simple pathway with receptor-ligand binding, followed by receptor cleavage, translocation to the nucleus and activation of target genes. However, numerous studies have now revealed there are many points at which this core pathway is regulated further. Modulation of the core pathway allows tight control of Notch signalling, in a context and cell specific manner during a diverse array of developmental processes.

The Notch receptors and ligands can be modulated to influence the activity of Notch signalling. The *neuralized* and *mind-bomb* genes are two ubiquitin ligases that promote the internalization and degradation of Delta. Internalization of Delta is thought to enhance Notch signalling by promoting removal of the Notch extracellular domain from the neighbouring cell, assisting the further proteolytic cleavage of Notch. Neuralized can be unequally distributed during mitosis so that daughter cells have differences in their activation of Notch (Kadesch, 2004; Le Borgne et al., 2005).

Another molecule that can regulate Notch activity and is unequally segregated during cell division is Numb. This is a phosphotyrosine binding domain adaptor protein that interacts with Notch and inhibits signalling in that cell. Two daughter cells can both express Notch and a ligand, but if one cell has

inherited Numb it will not be able to signal. An example of this occurs during the formation of *Drosophila* mechanosensory bristles, which is made up of two cell types, a shaft cell and a socket cell. The shaft cell receives Numb so it is inhibited from activating Notch signalling, but it can signal to a neighbouring socket cell to activate signalling (Wang et al., 1997).

Notch signalling requires the addition of fucose to the EGF-like repeats, a process called *O*-glycosylation, and this could be a mechanism of regulating receptor-ligand interaction. The Notch receptors can be additionally glycosylated by members of the Fringe family, which in vertebrates include *Radical Fringe*, *Lunatic Fringe* and *Manic Fringe*. This modification of the receptor increases the affinity of Notch for Delta, while reducing Jagged/Serrate affinity (Irvine, 1999). A second model for Fringe glycosylation of Notch involves the interference of Notch-ligand complexes that are thought to form in the Golgi. These complexes result in the retention of the Notch receptor in the signal-receiving cell. The retention of Notch in the Golgi would prevent the receptors from being expressed on the cell surface, leading to a decrease in signalling. Fringe may reduce these Notch-ligand interactions, allowing Notch to be trafficked to the cell surface and restoring signalling (Lei et al., 2003).

1.12 Notch is required for *Drosophila* wing outgrowth

In *Drosophila*, Notch signalling creates a specialised margin of cells at the dorso-ventral boundary of the wing imaginal disc (Fig. 4A). Imaginal discs are epithelial discs that proliferate and differentiate into the adult structures of the fly. The wing margin produces molecular cues that organise wing outgrowth, such as its downstream targets, *vestigial* (*vg*) and *wingless* (*wg*). This interaction

of Notch signalling at the DV boundary, and the subsequent induction of genes is essential for the initiation and patterning of the proximal-distal axis of the wing (Irvine, 1999; Klein, 2001) (Fig. 4).

The wing imaginal disc is comprised of two regions, a dorsal body wall and a ventral wing field. This division of the wing disc is set up by early expression of *wg* regulated in a *hedgehog* (*hh*) dependent manner. The wing field is later subdivided into dorsal and ventral compartments by the expression of the selector gene *apterous* (*ap*) specifically in the dorsal compartment. *ap* induces the expression of *fringe*, which modulates the sensitivity of activation of Notch by its ligands, Delta and Serrate. Fringe glycosylates the Notch receptor to inhibit its responsiveness to the dorsally expressed Serrate, while potentiating its ability to respond to Delta in ventral cells (Irvine and Vogt, 1997; Rauskolb et al., 1999). This results in the activation of Notch along the DV boundary, which in turn activates the expression of *vg* and *wg* (Fig. 4B).

1.13 Implication of Notch signalling in vertebrate limb development

In vertebrates, several components of the Notch signalling pathway are expressed in the developing limbs and several lines of evidence have suggested they are important in the development of individual tissues of the limb, such as the bones, muscles and vasculature (Delfini et al., 2000; Iso et al., 2003; Myat et al., 1996; Nobta et al., 2005; Vargesson et al., 1998; Watanabe et al., 2003; Williams et al., 1995) and in regulating the size of the limb (Vasiliauskas et al., 2003).

Evidence that *Notch1* and *Notch2* are involved in bone development comes from work showing they are expressed in osteoblasts, and data from work in cell lines.

Expression of NICD using an adenovirus vector in MC3T3-E1 cells, or co-culturing them with Delta-like1 expressing cells, results in a significant increase in calcified nodules (Tezuka et al., 2002). Consistent with this, inhibition of Notch signalling with the dominant-negative extracellular domain of Notch1 or siRNA results in a decrease in the expression of differentiation markers (Nobta et al., 2005). However, overexpression of NICD in mouse ST-2 stromal and MC3T3 cells using retroviral vectors inhibited BMP2 induced differentiation to osteoblasts (Sciaudone et al., 2003). Constitutively active NICD inhibits osteoblastogenesis by blocking WNT signalling and its target genes, mediated through *Hes1* (Deregowski et al., 2006). These contradictory results of Notch signalling on osteoblast differentiation could be due to differences in the cell lines used, the delivery and activation of Notch signalling, or may reflect multiple roles for Notch signalling in osteoblastogenesis (Deregowski et al., 2006). Notch1 protein is detectable in condensed mesenchymal cells that will form cartilage and in chondrocytes at the developing articulations in mouse limb buds. In chondrogenic cell lines, Notch signalling has an inhibitory effect on both differentiation and proliferation (Hayes et al., 2003; Watanabe et al., 2003). Two Notch ligands, *Delta1* and *Serrate2*, are expressed in the muscles of developing chick limbs in a similar pattern to the muscle marker *MyoD* (Vargesson et al., 1998). Further, activation of the Notch pathway in the chick limb by misexpression of *Delta1* suppresses myogenesis *in vivo* (Delfini et al., 2000). In agreement with Notch signalling having an inhibitory effect on myogenesis, several groups have shown that activated Notch signalling inhibits muscle differentiation in mouse cell lines. Constitutively active Notch1 in C_2C_{12} myoblast cells delays the expression of the myogenic markers MyoD and

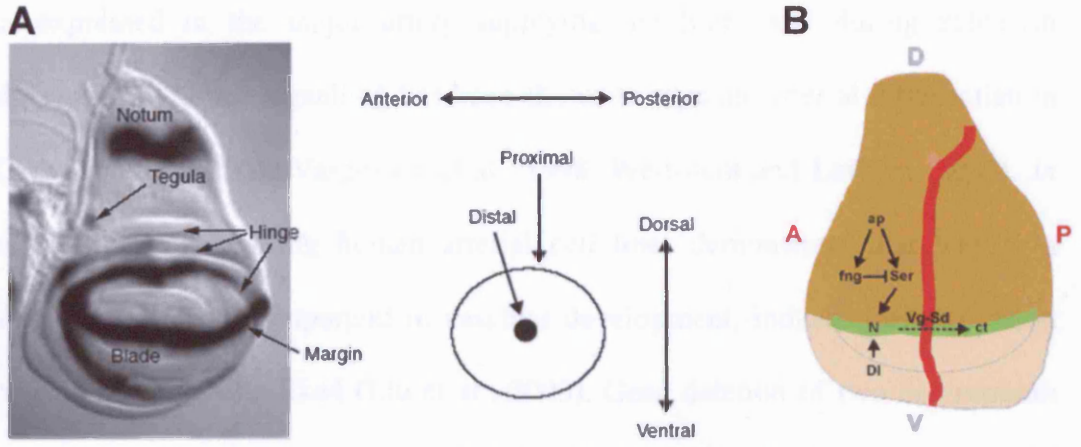

Figure 4. Patterning of the *Drosophila* wing imaginal disc. (**A**) The picture on the left is Wg expression in a late third instar wing imaginal disc. On the right is a schematic showing the orientation of the wing disc. Wg is expressed along the dorsoventral (DV) compartment boundary that will form the wing margin and in two rings surrounding the wing blade that constitutes the hinge. It is also expressed in the dorsal part of the disc that will form the Notum. To create the 3-dimentional structure of the wing, the imaginal disc is organized in a concentric manner. The distal-most point is in the centre, the wing margin, with the proximal domains, the hinge, surrounding it. (**B**) Schematic of Notch signalling components in the early wing disc. Dorsally expressed Apterous (ap) induces the expression of Fringe (fng) and Serrate (Ser) in the dorsal half of the wing disc. Fringe inhibits the responsiveness of Notch to Serrate, so that Serrate can only signal to cells ventrally. Ventrally expressed Delta (Dl) signals to dorsal cells. This leads to the activation of Notch signalling at the DV boundary of the wing disc and the activation of target genes, such as *vg* (vg) and *cut* (ct). The DV boundary is shown in green, the AP axis is in red. D=Dorsal, V=Ventral, A=Anterior, P=Posterior. Adapted from Klein, 2001 and Nagel et al., 2001.

myogenin (Kopan et al., 1994; Kuroda et al., 1999; Nofziger et al., 1999; Shawber et al., 1996).

The Notch signalling pathway has been implicated in the formation of the developing vasculature (Iso et al., 2003). In the chick, *Notch1* and *Serrate1* are co-expressed in the major artery supplying the limb, and during zebrafish development Notch signalling has been shown to regulate arterial differentiation (Lawson et al., 2001; Vargesson et al., 1998; Weinstein and Lawson, 2002). *In vitro* experiments using human arterial cell lines demonstrate that VEGF, a signalling molecule important in vascular development, induces the expression of Notch1 and Delta-like4 (Liu et al., 2003). Gene deletion of two downstream components of Notch signalling, *Hey1* and *Hey2*, leads to defects in vasculature remodelling including impaired arterial differentiation (Fischer et al., 2004). Deletion of *Notch1* using mice with a conditional allele and a Cre line driving activity under the control of an endothelial specific promoter die at E10.5 as a result of severe vascular defects. This demonstrates that *Notch1* carries out a cell-autonomous role in the endothelium to form the mature vascular network (Iso et al., 2003; Limbourg et al., 2005).

Chick *c-hairy1*, a potential target of Notch signalling, has two different splice variants expressed in the distal mesenchyme of the limb. Misexpression of one of these variants causes limb truncations with shortening of the skeletal elements. It is thought Notch signalling, via *c-hairy1*, regulates the size of the limb by controlling the differentiation of cells in the distal mesenchyme (Vasiliauskas et al., 2003). A mouse orthologue of *c-hairy1*, *Hes1*, is also expressed in the developing limb mesenchyme (Jouve et al., 2000).

A chick orthologue of *Drosophila fringe*, *Radical Fringe* (*R-fng*), is expressed in the dorsal ectoderm of the developing limb. Misexpression experiments suggest *R-fng* is involved in positioning the AER, so that the ridge forms between cells expressing *R-fng* and those that do not (Laufer et al., 1997; Rodriguez-Esteban et al., 1997). However, the mouse *R-fng*$^{-/-}$; *Lunatic Fringe*$^{-/-}$ double knockout of does not have a limb phenotype demonstrating that these genes are not required for normal limb formation in the mouse (Moran et al., 1999; Zhang et al., 2002).

Jagged2 is a Notch ligand expressed in the AER of mouse and chick embryos (Jiang et al., 1998; Vargesson et al., 1998; Williams et al., 1995). Mutations in *Jagged2* cause the AER to expand in size, which ultimately leads to digit fusions (syndactyly). This provides evidence that Notch signalling is required for proper functioning of the AER (Jiang et al., 1998; Sidow et al., 1997).

1.14 *Vestigial* is necessary and sufficient for *Drosophila* wing outgrowth

Another gene essential to the development of the *Drosophila melanogaster* wing and a target of Notch signalling is *vestigial* (*vg*). During embryogenesis *vg* is chiefly expressed in the wing and halter primordia and transiently in some neural and muscle precursors (Williams et al., 1991). Vestigial is a nuclear protein that physically interacts with Scalloped (Sd) via a 56 amino acid motif, called the scalloped-binding domain (SBD) (Paumard-Rigal et al., 1998; Simmonds et al., 1998). Scalloped and their vertebrate orthologues, transcription enhancer factors (TEF's), belong to a conserved family of proteins that contain a TEA/ATTS DNA-binding domain (Simmonds et. al. 1998; Halder and Carroll 2001;

Srivastava and Bell, 2003). The expression of *scalloped* (*sd*) is very similar to *vg* in the wing imaginal disc, but *sd* is also expressed in other tissues of the developing embryo (Campbell et al., 1992; Williams et al., 1993). The binding of Vg to Sd forms a heterotetramer on DNA that changes the binding selectivity of Sd, so that the Vg-Sd complex binds to different target sites than Sd alone. The formation of the Vg-Sd complex on DNA requires protein domains of Vg that are outside of the SBD (Halder and Carroll, 2001).

Numerous *vg* and *sd* mutants have been described that differ in the pattern and levels of Vg and Sd expression. Analysis of these mutants, such as vg^{83b27}, has enabled the characterization of the *vg* locus and the function of Vg. In the vg^{83b27} mutant, the boundary enhancer (*vg*BE) is lost and subsequently *vg* expression is absent along the DV boundary of the wing disc and there is a failure in wing outgrowth. This mutant demonstrates the essential role that *vg* plays during wing development (MacKay et al., 2003; Paumard-Rigal et al., 1998; Simmonds et al., 1997). Ectopic expression of *vestigial* in the eye, antenna or leg imaginal discs is capable of transforming them to wing tissue and inducing the expression of wing marker genes (Halder et al., 1998; Kim et al., 1996; Paumard-Rigal et al., 1998). *vg* is only able to induce these wing-like outgrowths in other imaginal discs, such as the eye, where *sd* is also expressed (Simmonds et al., 1998). However, overexpression of Sd can cause disruptions in wing growth similar to *vg* loss of function mutants, suggesting precise levels of Sd are required for correct Vg function (Paumard-Rigal et al., 1998; Simmonds et al., 1998; Varadarajan and VijayRaghavan, 1999). In addition, *sd* mutants and protein deletions of Sd and Vg have demonstrated that Sd is required to translocate Vg to the nucleus. In

flies that are *sd* mutants, or if the Sd-binding domain is deleted from Vg, Vg is found in the cytoplasm. Consistent with this, a predicted nuclear localisation signal is in the Sd TEA domain. When this Sd TEA domain is fused to Vg the fusion construct is found in the nucleus and can rescue a *vg* mutant (Srivastava et al., 2002). This data demonstrates that Vg interacts with Sd, localises to the nucleus to activate target genes, and that the Vg-Sd complex is necessary and sufficient for wing morphogenesis.

1.15 The regulation of *vestigial* in the wing imaginal disc

Drosophila vg is expressed early in wing development in the embryonic wing and halter imaginal disc precursors, and is one of the first genes to be expressed in the wing primordia (Williams et al., 1991). During larval stages *vg* is sequentially expressed, with early expression along the DV boundary regulated by the Notch/Wingless pathways and later expression in the rest of the wing pouch activated by the Decapentaplegic (Dpp) signalling pathway (Williams et. al., 1993, Kim et. al. 1996; reviewed Klien, 2001). The initiation of *vg* by the Notch signalling pathway along the DV boundary is activated through the *vg*BE, which contains a single *Su(H)* DNA binding site in the second intron (Kim et al., 1996; Williams et al., 1994). Dpp signalling, via the binding of mothers against dpp (MAD) protein, induces *vg* expression through a second enhancer, the quadrant enhancer (*vg*QE) (Kim et al., 1997a; Kim et al., 1996).

Loss of the single intronic *Su(H)* site in the *vg*BE or loss of *Su(H)* results in the absence of *vg* expression during wing development (Kim et al., 1996; Klein and Arias, 1999). However, the wing phenotype of *Su(H)* mutants are not as severe,

compared to loss of *vg* or other genes involved in Notch signalling. When the expression of *vg* is analysed earlier in development, weak, transient levels are seen. This expression of *vg* is thought to be sufficient to enable distal structures to develop and result in the weaker phenotype seen after loss of *Su(H)*. In the *Su(H)* mutants there is a de-repression of target genes, including the transient induction of *vg* expression, which is Notch independent (Koelzer and Klein, 2006). This is consistent with other work that has shown Su(H) can interact with co-repressor proteins to repress transcription (Barolo et al., 2002).

1.16 The roles of *vestigial* in *Drosophila* wing development

Multiple roles have been described for the Vg-Sd complex during wing development, such as cell fate determination, proliferation, cell survival and cell affinity. *Drosophila* mutants for *vestigial* and *scalloped* show a reduction in wing size and several mutant alleles result in the complete elimination of the wing and haltere.

The Vg-Sd complex is required for wing identity and outgrowth, and may play an important role in cell proliferation and cell survival. Recent work has confirmed that *vg* can promote proliferation in the wing and activate the expression of genes known to control cell cycle progression, such as *dE2F1* and *dihydrofolate reductase* (*DHFR*). *vg* and *sd* are also able to induce proliferation of HeLa cells, suggesting that some of the mechanisms that Vg-Sd uses to regulate the cell cycle are conserved in vertebrates (Delanoue et al., 2004). In addition, *vg* mutants or flies grown on aminopterin, an inhibitor of DHFR, have an upregulation in the pro-apoptotic gene *reaper* and a downregulation in *Drosophila* inhibitor of apoptosis (DIAP1) specifically at the DV boundary of

the wing imaginal disc. The change in the expression of *reaper* and DIAP1 leads to caspase-mediated cell death at the DV margin. Ectopic expression of DIAP1 at the DV boarder of heterozygous *vg* null mutant flies that have been reared on aminopterin rescues the loss of wing tissue. This work indicates that *vg* is also required for cell survival, and this is likely to be a major cause for the disrupted wing phenotypes (Delanoue et al., 2004).

Analysis of cells overexpressing *vg*, or mutant for *sd*, suggests that Vg-Sd could be involved in differences in cell affinities that result in the separation of the proximal wing hinge from the distal wing blade, and in establishing a gradient of affinities along the wing blade. Cells overexpressing Vg in clones in the wing blade primordia are much rounder and smoother than control clones, which normally have an irregular shape. The ability of Vg to alter the adhesion properties of the cells depends on the distance from the DV border. Vg has less of an influence on cell affinity as distance from the border increases. This graded regulation of cell affinity matches the graded expression of Vg-Sd that is highest at the DV border. This suggests that a gradient of Vg-Sd expression has an effect on the adhesion of wing blade cells (Liu et al., 2000).

Evidence has suggested that during the early phase of *vg* expression it genetically interacts with *apterous* in the formation of the DV boundary. Comparisons of the DV border in vg^{null}, a mutant that lacks any functional Vg, and vg^{83b27}, a mutant lacking the *vg*BE, showed that the early expression of *vg* prior to either the *vg*BE or the *vg*QE is involved in the formation of the DV boundary (Delanoue et al., 2002). However, although *vg* is expressed along the DV border from early stages of wing development, mutant flies with a combination of *vg* loss-of-function alleles form a smooth boundary between *ap*

expressing cells and non-expressing cells. This suggests that *vg* is not essential in the formation of the DV compartment boundary (Koelzer and Klein, 2006).

Although *vg* is not required cell-autonomously in the wing hinge the Vg-Sd complex produces a signal in the wing blade that regulates the expression of genes, such as *wg*, in wing-hinge cells and is essential for hinge development. In agreement, normal *wg* hinge expression is lost in *vg* mutants (Lui et al., 2000).

1.17 Activation of *vestigial* target genes

During wing development, Vg is thought to act in co-operation with different signalling pathways, for example Notch, to activate different target genes. Enhancers containing Vg-Sd binding sites in combination with binding sites of the transcriptional effectors of signalling pathways, such as Su(H), are able to activate the expression of genes in specific domains of the wing (Halder et al., 1998; Kim et al., 1997b; Paumard-Rigal et al., 1998; Simmonds et al., 1998). This is elegantly demonstrated in the fly by analysing wing specific regulatory elements and different combinations of enhancers to drive expression of reporters in different domains of imaginal discs. The early expression of *vg* in the wing disc could genetically interact with the effectors of the Notch and Dpp signalling pathway, Su(H) and Mad proteins, to direct the wing-specific expression of *vg* during larval stages (Bray, 1999; de Celis, 1999).

Truncated versions of Vg can activate transcription in a yeast one-hybrid assay and significant activation is only seen with the N- and C-terminal domains of the protein (Vaudin et al., 1999). Further, transgenic flies expressing different deletion constructs of the *vg* open reading frame have been tested for their ability

to ectopically express Sd, to ectopically produce wing-like outgrowths in the eye and to rescue *vg* mutants. Results from these *in vivo* experiments, which are consistent with the results from the *in vitro* studies, identify three domains that are required for Vg function; the SBD (residues 278-335), an N-terminal domain (approximately residues 1-65) and a C-terminal domain (residues 335-453). This work also demonstrated that a large portion of the Vg protein, residues 187 to 287, is dispensable for normal Vg function (MacKay et al., 2003).

1.18 Vertebrate orthologues of *vestigial*

To date, four vertebrate *vestigial-like* genes, also called *Tondu*, have been identified. All of these genes contain a region of sequence homologous to the SBD of *vg* and human VESTIGIAL-LIKE1 (VGL1) directly interacts with all mammalian TEFs via this domain (Vaudin et al., 1999). VGL1 is expressed in foetal kidney and lung, while in human adult tissues it is detected in the placenta. A VGL1-GAL4 fusion protein activates the expression of a UAS reporter in *Drosophila* S2 cells, suggesting that it may act as a transcriptional activator in vertebrates. Transgenic flies expressing *VGL1* can activate the expression of a target of *vg, cut*, in the presumptive wing margin and partially rescue the wings of a *vestigial* null mutant (Vaudin et al., 1999). Importantly, the *VGL1* rescued wings have correct patterning of veins and wing margin, suggesting that *VGL1* can activate multiple targets of *Drosophila vg* in the wing imaginal disc. Human VGL1 however, is unable to replicate the ability of *vg* to induce wing tissue outgrowths when ectopically expressed in other imaginal discs. VGL1 is able to increase the size of the eye tissue in a Sd-dependent manner and suggests that, like Vg in flies, can induce proliferation (Vaudin et al., 1999).

Mutations in the *VGL1* gene may be associated with a human congenital limb malformation, split-hand/split-foot malformation (SHFM). SHFM, also called ectrodactyly, is characterized by the absence of part or all of one or more of the digits. In addition to this, there are a number of other distal limb phenotypes associated with SHFM including, syndactyly, aplasia and/or hypoplasia of the phalanges, metacarpal and metatarsals. In humans a large number of gene defects can cause SHFM, and so far, five loci have been identified; SHFM1 (chromosome 7q21), SHFM2 (chromosome Xq26), SHFM3 (chromosome 10q24), SHFM4 (chromosome 3q27) and SHFM5 (chromosome 2q31). SHFM2 has been mapped to a 5.1Mb region of Xq26 and *VESTIGIAL-LIKE1* (*TONDU1*) is a candidate gene as it lies within this locus. Analysis of this 5.1Mb region in patients with SHFM2 showed there are no mutations in the exons and exon/intron boundaries of 19 candidate genes, including *VESTIGIAL-LIKE1* (Faiyaz-Ul-Hauqe, 2005). However, the possibility remains that mutations could be in a regulatory region of the *VESTIGIAL-LIKE1* gene (Duijf et al., 2003; Faiyaz-Ul-Haque et al., 2005).

A number of studies have demonstrated that *Vestigial-like2* (*Vgl2*) plays an important role during muscle differentiation. *Vgl2* is expressed in adult skeletal muscle, and during mouse embryogenesis is expressed in the pharyngeal arches and co-expressed with myogenin in differentiated muscle (also see results). Upon differentiation of the mouse myoblast cell line C_2C_{12}, *Vgl2* expression is induced (Maeda et al., 2002; Mielcarek et al., 2002). In addition, Vgl2 protein localises to the cytoplasm of myoblast cells, while it is detected in the nucleus of differentiated myotube cells (Maeda et al., 2002). Deletion of putative nuclear

localisation and nuclear export signals in the C-terminus results in cytoplasmic retention of the protein. The Vgl-TEF interaction was confirmed in a yeast two-hybrid assay, which shows a strong interaction between Vgl1 and Vgl2 with TEF-1 factors. Vgl2 interacts with MEF2, a transcription factor expressed in muscle, and activates TEF1 and MEF2-dependent promoters in differentiated muscle cells (Maeda et al., 2002). Vgl2 affects the DNA binding ability of different TEFs, in a similar fashion to Vg binding to Sd. Changes in the DNA binding site of TEFs could be a method to achieve selective activation of downstream targets. Downregulation of Vgl2 *in vitro* by siRNA or antisense morpholino (MO) in myogenic cell lines, and *in vivo* with the use of a MO in chick embryos results in a decrease in muscle-specific gene expression and blocked muscle differentiation (Chen et al., 2004; Gunther et al., 2004).

Vestigial-like4 has recently been implicated in the regulation of cardiac myocytes. *Vgl4* is the only member of the Vestigial-like family that is expressed in the heart and has two Scalloped-binding domains. A BLAST search using the *Drosophila vestigial* gene also identified a sequence on human chromosome 3 that is related to the Scalloped-binding domain of *Vgl1* and *Vgl2*, called *Vgl3*. Northern blot analysis demonstrated that this transcript is enriched in human placenta (Maeda et al., 2002; Chen et al., 2004).

The four vertebrate TEF factors, TEF1/TEF3/TEF4/TEF5, all contain a highly conserved TEA domain and also have a high degree of sequence conservation in the C-terminal half of the protein (Jacquemin et al., 1996; Kaneko and DePamphilis, 1998). Human TEF1 can rescue the lethality and wing blade defects seen in different Sd fly mutants. TEF1 can also activate the expression of

a *sd* reporter in the wing imaginal disc as effectively as Sd, suggesting that their functional domains have been conserved during evolution (Deshpande et al., 1997). Mouse *TEF1* (chick *RTEF1*) is widely expressed from early stages in development, with high levels of expression in cardiac and skeletal muscle and in some parts of the forebrain, hindbrain and spinal cord (Jacquemin and Davidson, 1997). In mouse embryos *TEF3* is expressed in the myogenic compartments of the somites, the lung and liver, while in adult chicks (the chick orthologue called *NTEF1*) transcripts have been detected in the cardiac and skeletal muscle. *TEF4* is widely expressed early in mouse development and then becomes restricted to proliferating neuroblasts, and several developing organs including the kidney. *TEF5* (chick *DTEF1*) is expressed in the developing heart, lung and placenta (Jacquemin and Davidson, 1997).

1.19 Project Aims

Since the deletion of *Notch1* is lethal prior to limb bud stages, its role in development remains poorly understood (Huppert et al., 2000; Swiatek et al., 1994). The Cre/Lox system allows specific temporal and spatial recombination of appropriately targeted mouse alleles making it possible to disrupt genes in specific tissues at distinct times so that tissue-specific gene function can be assessed (Sauer, 1998). To address the role of *Notch1* in the developing limb, I have used a conditional allele of *Notch1*, *Notcth1*$^{lox/lox}$ (Radtke et al., 1999), in combination with two distinct Cre transgenic lines that enable me to separately delete *Notch1* function in either the limb mesenchyme or the limb ectoderm during early stages of limb development.

I have obtained two chicken orthologues of *vestigial*, *Vestigial-like1* (*Vgl1*) and *Vestigial-like2* (*Vgl2*). Firstly, to investigate whether *Vesigial-like1* and *Vestigial-like2* are involved in vertebrate limb development, I analysed their expression pattern. I produced an eGFP-Vgl1 fusion construct to investigate the sub-cellular localisation of Vgl1. Finally, I have used a gene misexpression approach in the chick to study the role *Vestigial-like1* in vertebrate limb development.

2. Materials and Methods

2.1 Mouse and chick embryos

Mouse embryos were staged according to Kaufman (Kaufman, 2001). Noon on the day a vaginal plug was observed was taken to be E0.5 days of development. Mice carrying the conditional *Notch1* allele, *Notch1*$^{lox/lox}$ (Radtke et al., 1999), were crossed with either of the two Cre deleter lines; the limb mesenchyme-restricted *Prx1-Cre* line (Logan et al., 2002) and the limb ectoderm-restricted *Brn4-Cre* line (Ahn et al., 2001). To produce mice null for *Notch1*, mice homozygous for the conditional *Notch1* allele (*Notch1*$^{lox/lox}$) were crossed with mice heterozygous for the conditional *Notch1* allele and hemizygous for the *Cre* transgene (*Notch1*$^{lox/wt}$; *Prx1-Cre* or *Brn4-Cre*). Cre activity was analysed by crossing Cre lines with the Z/AP reporter line (Lobe et al., 1999). The Z/AP transgenic mice express the *lacZ* reporter under the control of a constitutively active promoter. After Cre-mediated recombination, a cassette flanked by loxP sites and containing *lacZ* and followed by three polyAdenylated signals is removed and human alkaline phosphatase (AP) is expressed. To detect AP embryos were incubated at 70°C for 30 minutes in PBT to heat inactivate endogenous AP, washed 3 times for 10 minutes with NTMT (100mM NaCl, 100mM Tris HCl pH9.5, 50mM $MgCl_2$) and then stained with AP substrates, NBT (0.075g/1ml 70% dimethyl formamide) and BCIP (0.05g/ml H_20). Fertilised chicken eggs (Needle's farms, Winter's farms) were incubated at 37°C and staged according to Hamburger Hamilton (HH) (Hamburger and Hamilton, 1951).

2.2 Tail and embryo sac DNA preparations

Tails were digested overnight at 55°C in 0.5ml lysis buffer (50mM Tris pH7.5. 50mM EDTA, 100mM NaCl, 0.3% SDS) with 0.1mg/ml proteinase K. The DNA was then precipitated with 0.5ml isopropanol at room temperature and centrifuged at 4000rpm for 3 minutes. The pellet was washed in 70% ethanol, air dried and re-suspended in 100µl 10mM Tris pH7.5. Embryo sacs were digested overnight in 200µl of lysis buffer with the same concentration of proteinase K. To precipitate the DNA 500µl ethanol, 10µl sodium acetate and 1µl glycogen were added to the digested sac and left at –20°C for 1 hour. They were then spun for 10 minutes at 14000rpm, washed in 70% ethanol, air dried and re-suspended in 50µl 10mM Tris pH7.5.

2.3 Genotyping

To genotype mouse lines a PCR reaction was carried out on tail and embryo sac DNA. Three primers were used to produce a 285bp product from a *wt* allele, a 350bp product from the *Notch1* floxed allele and a 500bp product from the *Notch1* floxed-out (recombined) allele (Radtke et al., 1999). The sequence of the primers used to genotype the floxed *Notch1* mice were; (1) 5' CTG ACT TAG TAG GGG GAA AAC 3' and (2) 5' AGT GGT CCA GGG TGT GAG TGT 3'. The null allele was detected with the addition of a third primer; (3) 5' TAA AAA GCG ACA GCT GCG GAG 3'. The PCR reaction mix was; 3µl DNA, 2.5µl 10x PCR buffer, 1µl dNTP 25mM each, 1µl primer1 (50pmol), 1µl primer2 (50pmol), 1µl primer3 (50pmol), 2.5µl DMSO, 1µl Taq (ABgene), 12µl of H_20. The 10x PCR buffer was; 166µl 1M ammonium sulphate, 670µl 1M Tris pH8.8,

67µl 1M $MgCl_2$, 3.9µl β-mercaptoethanol, 0.13µl 0.5M EDTA, 93µl H_20. The PCR programme was; (1) 93°C for 3 minutes, (2) 93°C for 1 minute, (3) 62°C for 1 minute, (4) go to (2) for 40 cycles, (5) 68°C for 3 minutes and 30 seconds. *Brn4-Cre* (Ahn et al., 2001) and the *Prx1-Cre* (Logan et al., 2002) were genotyped using the following *Cre* specific primers; (1) 5' ATC CGA AAA GAA AAC GTT GA 3' and (2) 5' ATC CAG GTT ACG GAT ATA GT 3'. The PCR reaction mix was 1µl DNA, 1µl primer1 (10pmol), 1µl primer2 (10pmol), 0.2µl Taq, 10µl 5x PCR buffer, 36.8µl H_20. The PCR buffer was; 250µl 1M KCl, 50µl 1M Tris pH8.4, 12.5µl 1M $MgCl_2$, 10µl 100mM dNTP each, 85µl BSA (10mg/ml), 562.5µl H_20. The PCR programme was; (1) 94°C for 2 minutes, (2) 94°C for 30 seconds, (3) 54°C for 30 seconds, (4) 72°C for 90 seconds (5) go to 2 for 30 cylces.

2.4 Plasmid DNA preparations

DNA preparations were carried out using the Qiagen mini-prep kit following the manufacturer's protocol.

2.5 Reverse Transcriptase-PCR (RT-PCR) analysis

Chick embryos at Hamilton and Hamberger stages 14, 15, 16, 17, 19, 25 and 32 were harvested in PBT and dissected with forceps (also see Results Fig. 18A). Lateral plate mesoderm was dissected from the prospective forelimb field from stage 14 and 16 chicks, between somites 15 and 19. Whole limb buds were removed and the distal tip of the bud was processed for the stage 17 and 25 embryos. A limb bud was removed from a stage 19 embryo and the ectoderm and

AER was separated from the mesenchyme using a sharp glass needle, which was made using a glass pipette puller (KOPF). The heart and a limb were dissected from a stage 32 embryo. This limb was further dissected with a sharpened glass needle so that tissue was taken from the interdigit area and from the distal part of the forming digit. RNA preparations were made using Trizol (Gibco) following manufacturers instructions and RT-PCR was performed using the Qiagen OneStep RT-PCR kit. Tissue was homogenised in 0.8ml Trizol, incubated at room temperature for 5 minutes and then centrifuged at 12000rpm for 10 minutes. To perform phase separation 160µl of chloroform was added to the supernatant, vortexed for 15 seconds and incubated at room temperature for 2 minutes. This was then centrifuged for 15 minutes at 12000rmp and the aqueous phase removed and precipitated with isopropanol. The pellet was washed with 70% ethanol and re-suspended in 50µl of RNAse free water. RNA was quantified prior to RT-PCR reactions using the NanoDrop ND-1000 spectrophotometer (Labtech). Primers for c*Vestigial-like1* forward; 5' TGA GGT TGT TGT CCC GAA GC 3' and reverse; 5' TGA TGA TAC ACC GGG CTG GTG 3' detected a 249bp fragment, c*Wnt3a* forward; 5' ACA GGC ACA ACA ATG AAG CTG G 3' and reverse; 5' TCG TAT GCA TTC CTG GCA GCG 3' detected a 482bp fragment, primers for c*Fgf8* forward; 5' ACG GTA AGG AAG GAC GCG GC 3' and reverse; 5' TGG CGC TGG AGT TTC GAG TCC 3' detected a 376bp fragment. PCR products were run out on a 2% agarose gel.

2.6 RNase protection assays

Two ^{32}P-labelled c*Vgl1* probes were used; c*Vgl1ΔC* probe is made from the first 180bp of the open reading frame (ORF) of c*Vgl1* and c*Vgl1 3'* is a 305bp fragment of the 3' untranslated region. The reaction mix for probe synthesis was; 1μl 0.5mg/ml linearized template, 2.5μl ^{32}P-UTP (50 μCi/mmol), 0.25μl 250mM DTT, 0.25μl RNAsin, 0.5μl 10mM rNTPs (A, C and G), 0.5μl transcription buffer (400mM tris pH7.5, 60mM $MgCl_2$, 20mM spermidine), 0.5μl polymerase. The reactions were incubated for 1 hour at 37°C, 1μl DNaseI was added and incubated for 10 minutes at 37°C and then run on a 6% acrylamide gel. The gel was exposed to film and the full length labelled transcript excised. The probe was eluted with 0.4ml elution buffer (0.5ml NH_4Ac, 1mM EDTA, 0.1% SDS) overnight. The eluted probe was precipitated with 1ml ethanol on dry ice for 30 minutes, then spun down, washed in 70% ethanol and resuspended in 50μl TE. RNA from stage 19 and stage 22 limb buds was hybridised with the radiolabelled probe, digested with RNase A and then run on a 6% acrylamide gel. The hybridisation reactions were; 15μl 2x PES (50mM pipes pH6.8, 2M NaCl, 2mM EDTA), 1μl probe, equal amounts of RNA (5μg). The reactions were hybridised at 80°C for 1 hour, digested with RNase A (with 10mM tris HCl pH7.5, 5mM EDTA, 300mM NaCl, 5μg T1 RNA) for 30 minutes at 37°C, phenol extracted and precipitated in 100% ethanol overnight. The hybridisation mixes were washed with 70% ethanol, resuspended in 2μl TE and 2μl formamide dye and loaded onto a gel (0.5x TBE 37.5μl, 2.5x TBE 12.5μl, 100μl 10% APS, 100μl TEMED). The gel was dried and then exposed to xomat film (Kodak), with intensifying screens, at -70°C.

2.7 Whole-mount *in situ* hybridisation

Whole-mount *in situ* hybridisations were carried out essentially as previously described (Riddle et al., 1993). Care was taken with proteinase K (PK) treatment so as not to damage ectoderm. Stage 14-16 chick embryos were treated in 2μg/ml PK for 1-2 minutes, while stage 17-24 embryos were incubated for 5-8 minutes. Embryos were processed with no PK treatment to detect outer ectodermal cells. E10.5 and E11.5 mouse embryos that were processed by whole-mount *in situ* hybridisations to detect genes expressed in ectodermal tissue were treated with 2μg/ml PK 5-8 minutes, while to detect genes expressed in mesenchymal tissue embryos were treated with 10μg/ml PK 10-15 minutes. E12.5 and E13.5 embryos were treated with 10μg/ml PK 15-20 minutes.

The DIG-UTP labelling mix routinely used to *in vitro* transcribe riboprobes is a 35% labelled DIG-UTP 10X mix that consists of 10mM GTP, 10mM ATP, 10mM CTP, 6.5mM UTP and 3.5mM DIG-UTP. A series of labelling mixes were made-up with increasing amounts of labelled DIG-UTP; 80% labelled DIG-UTP (2mM UTP, 8mM DIG-UTP), 70% labelled DIG-UTP (3mM UTP, 7mM DIG-UTP), 60% labelled DIG-UTP (4mM UTP, 6mM DIG-UTP) and 50% labelled DIG-UTP (5mM UTP, 5mM DIG-UTP). These nucleotide mixes were added to the transcription reaction as normal. No probes were transcribed when using the 80% and 70% DIG-UTP mix, this could be because high levels of DIG interfere with transcription, but a product for each probe was made when using the 60% DIG-UTP mix. These probes were used to analyse the expression of *Vgl1*. DIG-UTP labelled, unincorporated nucleotides

were removed from probe preparations using ProbeQuant G-50 columns (Amersham Biosciences).

DNA templates for anti-sense RNA probes were as follows; m*Fgf8* (Crossley and Martin, 1995); m*Notch1* is a 1.2kb fragment digested with *EcoR*I and transcribed with T7 RNA polymerase; m*Jagged2* is full-length sequence digested with *BamH*I, transcribed with T7 RNA polymerase; m*Jagged1* (Mitsiadis et al., 1997); m*Hes1* (Sasai et al., 1992); m*Bmp2* (Lyons et al., 1989); m*Bmp4* (Jones et al., 1991); m*Bmp7* (Dudley and Robertson, 1997); m*Hoxa13* (Ma et al., 1998); c*Fgf8* (Vogel et al., 1996); c*Wnt3a* (Hollyday et al., 1995); c*Msx1* (Ros et al., 1992); c*Bmp2* (Schlange et al., 2002); c*Engrailed1* (Noramly et al., 1996); c*Lmx1* (clone ID; ChEST100c17); *NTEF1* (ChEST332b16); *RTEF1* (ChEST905i10); *DTEF1* (ChEST371b16); c*Vgl2* (clone ID; ChEST976P9) are EST's from (http://www.chick.umist.ac.uk), which were digested *Not*I and transcribed using T3 RNA polymerase. The full-length c*Vgl1* isolated from a limb cDNA library (A. Brent and M. Logan, unpublished) was digested *Nco*I and transcribed using T7 RNA polymerase.

2.8 Section *in situ* hybridisation

Embryos were fixed overnight in 4% paraformaldehyde (PFA) at 4°C, washed in PBS, left in 30% sucrose overnight and then embedded in OCT (BDH, Merck). Section *in situ* hybridizations were carried out on 10μm cryosections essentially as previously described (Schaeren-Wiemers and Gerfin-Moser, 1993). No proteinase K treatment was used on sections. After detection, slides were washed twice with PBT and post-fixed with 4% PFA and 0.1% glutaldehyde for one

hour. Slides were then mounted with Aquatex (BDH) or using Vectashield with DAPI (Vector Labs). Slides were analysed using an Axiophot microscope, photographed using a Jenoptik camera (Jena) and Openlab software.

2.9 Microtome sections

Wax microtome (Leica) sections (10μm) of mouse and chick embryos were cut that had been previously processed by whole-mount *in situ* hybridisation.

2.10 Histology and immunohistochemistry assays

The cartilage and bone elements of newborn mouse pups were stained with alcian blue and alizarin red, respectively, essentially as described (Hogan, 1994). Pubs were skinned and eviscerated and dehydrated in 95% ethanol overnight and then acetone overnight. Samples were stained (5ml alcian blue (0.3% w/v alcian blue in 70% ethanol), 5ml alizarin red S (0.1% w/v alizarin red S in 95% ethanol), 5ml glacial acetic acid and 85ml 70% ethanol) overnight at 37°C. Skeletons were cleared by washing three times for 30 minutes with 95% ethanol at room temperature and 1% KOH overnight or until clear. Skeletons were stored in glycerol. To study the muscle pattern, E14.5 embryos were fixed overnight in 4% paraformaldehyde, washed in PBT and dehydrated through a methanol series. The muscle pattern was analysed using the monoclonal My32 antibody (Sigma), essentially as previously described (Kardon, 1998). Embryos were fixed in 4% PFA and stored in methanol. After removing the skin, embryos were rehydrated in 50% PBT/methanol and then 100% PBT. Embryos were incubated in 100% PBT at 70°C for 1 hour to inactivate endogenous alkaline-phosphatase

and then bleached using Dents bleach (1 part H_2O_2: 2 parts Dents fix) overnight at 4°C. They were washed with 100% methanol, 5 times for 10 minutes and fixed using Dents fix (1 part DMSO: 4 parts methanol) at 4°C, overnight. The embryos were washed in PBT, 3 times for 5 minutes and then 3 times for 1 hour and incubated in My32 antibody (1:400) in blocking solution (5% goats serum, 75% PBT, 20% DMSO) overnight at room temperature. They were then washed in PBT 3 times 5 minutes, 5 times 1 hour and then overnight at 4°C. To detect antibody, embryos were washed with NTMT and incubated with BCIP and NBT.

Vasculature was analysed using an anti-PECAM-1 antibody. First, E12.5 mouse embryos were fixed for 1 hour in 4% paraformaldehyde at room temperature, washed in PBS, left in 30% sucrose overnight and then embedded in OCT (BDH, Merck). Transverse frozen cryostat sections (12 μm) were processed using an α-mouse (CD31) PECAM-1 monoclonal antibody (Pharmigen) (1:1000) and a HRP-conjugated anti-rat secondary antibody (Calbiochem), essentially as previously described (Zimmermann et al., 2001).

To detect pERK staining, an anti-p44/p42 MAPK rabbit polyclonal antibody (Cell Signalling, #9101) was used on E11.5 embryos, and processed as described (Corson et al., 2003). Essentially, embryos were dissected in cold PBS and fixed in 8% paraformaldehyde overnight at 4° C. They were then washed in PBS containing 0.5% NP40 twice for 10 min, dehydrated through methanol, bleached in 5% hydrogen peroxide for 1 hour at 4° C, rehydrated and blocked in PBSST (5% sera, 0.1% Triton in PBS) for 1 hour at 4°C. They were then incubated in 1:350 dilution of p44/p42 MAPK antibody in PBSST overnight at 4°C, washed 6 times for 1 hour, incubated with 1:350 dilution of HRP donkey anti-rabbit overnight at 4°C in PBSST, washed 6 times in PBS and then stained

with DAB. The DAB stain consists of one 10mg DAB tablet (Sigma) in 10ml 0.1M Tris pH7.2 added to an equal volume of 3.4μl 30% H_2O_2 in 5ml water.

2.11 TUNEL and Phospho-Histone H3 analysis

Programmed cell death was assayed by TdT-mediated dUTP nick end labelling (TUNEL), using a Q-BIOgene kit. E11.5 mouse embryos were fixed overnight in 4% paraformaldehyde, washed in PBS, left in 30% sucrose overnight and embedded in OCT. Transverse sections (12 μm) were assayed by TUNEL according to the manufacturer's protocol. Essentially, sections were fixed in 4% paraformaldehyde at room temperature for five minutes, washed with PBS and then fixed with 1:1 ethanol/acetic acid at –20°C for 15 minutes. They were then re-hydrated in PBS, and incubated in equilibration buffer (Q-BIOgene), 5 minutes at room temperature. The sections were then incubated with the TdT enzyme for 1 hour in a humidified chamber at 37°C. The reaction was stopped by washing in stop solution (Q-BIOgene), and then three 1 minute washes in PBS. The reaction was visualised by incubating the sections in an anti-DIG-fluorescein antibody for one hour (Q-BIOgene), washing five times with PBS, and then mounted using Vectashield with DAPI (Vector Labs). To detect cells in mitosis, a rabbit anti-phosphorylated histone H3 primary polyclonal antibody (Upstate Biotechnology) and Cy3-conjugated goat anti-rabbit IgG secondary antibody (Jackson Lab) were used following the protocol described previously (Yamada et al., 1993). Essentially, sections were washed in PBT 3 times for 5 minutes, blocked for 1 hour in 10% sheep serum and incubated overnight in antibody (1:400) diluted in block. Sections were then washed in PBT 5 times for 5 minutes

and incubated with Cy3 secondary antibody for 1 hour (1:400). The sections were then washed with PBT 5 times for 5 minutes and mounted with vectorshield with DAPI.

The average number of cells positive for TUNEL staining was calculated over an equal area in 10 comparable sections of control and mutant limbs. The mean number of TUNEL positive cells found per control section was 7.18, while in mutants it was 2.7. A student T-test on the number of TUNEL positive cells on sections of control and mutant limbs gave a p value of 5.74E-06, demonstrating there is a significant difference in the number of apoptotic cells. A similar analysis was done on 6 comparable sections of control and mutant limbs stained with PH3 antibody. The mean number of positive cells in the AER per control section was 1 while the mean number of positives cells in mutant AERs was 0.83. In 5 comparable sections of control and mutant limbs stained with PH3 the mean number of positive cells in the mesenchyme was 11.8 and 11.2 respectively. A T-test on the PH3 positive cells in the AER of control and mutant limbs gave a p value of 0.30, while a T-test on the PH3 positive cells in mesenchyme gave a p value of 0.37, demonstrating no significant difference in the number of cells undergoing mitosis.

2.12 Production of pSlax-λ-eGFP construct

The full-length 714bp *eGFP* was cloned into *pSlax* using PCR with primers that contained a *Pst*I restriction site in the forward primer (5' ACG CTG CAG ATG GTG AGC AAG GGC GAG GAG 3') and a *Hind*III restriction site in the reverse primer (5' ACG AAG CTT TTA CTT GTA CAG CTC GTC CAT GCC

3'). A 130bp bacteriophage *λ-hinge* fragment was then cloned in-frame with the N-terminal end of the *eGFP* by using a forward primer with an *EcoR*I site (5' ACG GAA TTC GTT AGT ATG CAG CCG TCA CTT 3') and a reverse primer with a *Pst*I site (5' ACG CTG CAG GGA TCT GCT TAC CCA TCT CTC 3'). This strategy produced a construct where a gene of interest can be cloned into the *Nco*I/*EcoR*I site resulting in a fusion with the *λ-hinge* and *eGFP*. The λ-hinge is predicted to aid in flexibility of the fusion construct and may help to ensure correct folding of the eGFP and the gene of interest fused to it (Ohashi et al., 1994). Full-length chick *Vestigial-like1* was cloned into the *Nco*I/*EcoR*I site of the *pSlax-λ-eGFP* fusion construct, which was then cloned into *pcDNA* (also see Results Fig. 24).

Ligations were carried out using T4 DNA ligase (New England Biolabs) with the supplied buffer at room temperature for 1 hour. Ligation reactions were performed in a volume of 10μl, with 1μl of ligase. After incubation, 5μl of the ligation reaction was added to 30μl of DH5α competent cells and left on ice for 15 minutes. The cells were heat shocked by placing at 42°C for 60 seconds, placed on ice for 2 minutes, incubated in 300μl of antibiotic free 2xTY at 37°C for 1 hour and then plated on agar plates with ampicillin at 37°C overnight.

2.13 Transfection of Cos-1 and DF1 cells

Cos-1 cells and DF1 cells (an immortalised chick fibroblast cell line) (Himly et al., 1998; Schaefer-Klein et al., 1998) were transfected with 10μg of either *pCS2-eGFP* or *pcDNA-λ-eGFP-Vgl1* DNA using Superfect (Qiagen) following the

manufactures instructions. After 48 hours the cells were washed with PBS and fixed for 15 minutes in 4% paraformaldehyde. The cells were then incubated with Rhodamine Phalloidin (1:200) for 15 minutes and then washed with PBS. They were then mounted using Vectashield with DAPI (Vector Labs).

2.14 Retroviral production and misexpression

Cloning of retroviral constructs and production of concentrated retroviral supernatants were carried out as described previously (Logan and Tabin, 1998). Cloning of the *Vestigial-like1* viral constructs was carried out by A. Brent and M. Logan (unpublished). The full-length chick *Vgl1* construct contains all 729 bp of the chick *Vgl1* clone that was obtained from a limb library. The *Vgl1ΔC* construct contains 180bp of the full-length *Vgl1* clone. The *Vgl1-Engrailed* construct contains the 5' 180bp of the full-length *Vgl1* clone fused to a.a. 2-298 of the *Drosophila* Engrailed protein (Jaynes and O'Farrell, 1991). The *Vgl1-VP16*$_4$ contains 180bp of *Vgl1* fused to a duplex of the lambda hinge region and VP16 (Ohashi et al., 1994). To establish the role of *Vestigial-like1* during limb development, the various constructs of *Vestigial-like1* were misexpressed in developing chick embryos using concentrated viral supernatants as previously described (Logan and Tabin, 1998). Essentially, DF1 cells were grown until 50%-70% confluent in a 6cm tissue culture plate (Nunc) and transfected with a retroviral construct using Superfect (Qiagen). Cells were then expanded to six 15cm plates and grown until over-confluent. 10ml of low serum (1/10) media was placed on each plate and harvested the next day. This was repeated for three days. The supernatants were filtered using 0.45μm units (Nalgene) and then

concentrated by ultracentrifugation using a SW40 rotor, 21,000rpm. Chick embryos were injected with one of the retroviral c*Vestigial-like1* constructs at stage 9-11 or stage 16 of development into the prospective forelimb region. To target the ectodermal cells virus was injected just underneath the vitelline membrane and over the prospective limb ectoderm. After 48-72 hours, the embryos were harvested and fixed overnight in 4% paraformaldehyde.

3. Results

3.1 Components of the Notch signalling pathway are expressed in the limbs

My work on the deletion of *Notch1* in the mouse limb ectoderm and mesoderm has been peer reviewed and subsequently published:
Jeffrey C. Francis, Freddy Radtke, and Malcolm P.O. Logan (2005). *Notch1* signals through *Jagged2* to regulate apoptosis in the apical ectodermal ridge in the developing limb bud. *Dev. Dynamics* 234; 1006-1015.

Previous studies have shown that in vertebrates *Notch1* is expressed in the AER and several of its ligands are expressed in the limbs, both in the AER and in the underlying mesenchyme (Jiang et al., 1998; Myat et al., 1996; Vargesson et al., 1998; Williams et al., 1995). However, the function of *Notch1* in the developing vertebrate limb remains unclear. Since I am interested in understanding the molecules that are involved in the formation and maintenance of the specialised group of cells that comprise the AER, I investigated if *Notch1* has a role in this process.

Previous expression analysis of *Notch1* and its ligands have been carried out at a limited number of embryonic stages in the developing mouse limb, or have been undertaken in chick embryos (Jiang et al., 1998; Myat et al., 1996; Vargesson et al., 1998; Williams et al., 1995). To begin this study, I first carried out detailed expression analysis of *Notch1* and its ligands in the developing mouse limb using whole-mount *in situ* hybridization. At E10.5, weak levels of *Notch1* transcripts are detectable in the AER and ectoderm (Fig. 5A and 5A'). By E11.5, expression of *Notch1* is clearly observable in the AER while lower levels of expression are apparent in the ectoderm (Fig. 5B and 5B'). I was unable to detect the expression of the other Notch receptors (*Notch2-4*) by whole-mount *in*

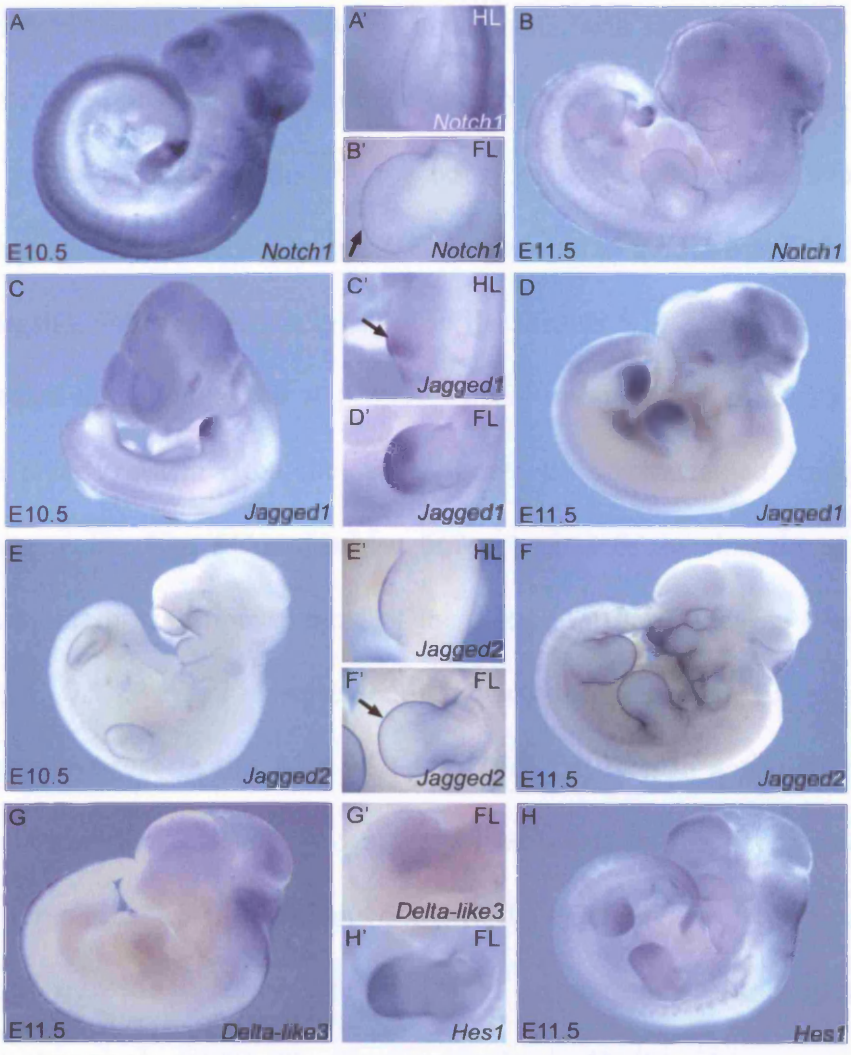

Figure 5. *Notch1*, *Jagged1*, *Jagged2*, *Delta-like3* and *Hes1* are expressed during mouse limb development. At E10.5, *Notch1* (**A** and **A'** detail) is expressed in the AER of the forelimb and hindlimb. At E11.5, *Notch1* (**B** and **B'** detail, arrow) expression is still detected in the AER of the developing forelimb and hindlimb, and low levels in the dorsal and ventral ectoderm. At E10.5, *Jagged1* (**C** and **C'** detail, arrow) is expressed in the distal mesenchyme, but is excluded from the AER of the developing forelimb and hindlimb. At E11.5, *Jagged1* (**D** and **D'** detail) transcripts increase in the distal mesenchyme and are still absent from the AER. At E10.5, *Jagged2* (**E** and **E'** detail) expression is detected in the AER of the developing forelimb and hindlimb, and low levels are detected in the dorsal and ventral ectoderm, in a similar pattern to *Notch1*. At E11.5, *Jagged2* (**F** and **F'** detail, arrow) expression increases in the AER, and low levels of transcript are still found in the dorsal and ventral ectoderm. At E11.5, *Delta-like3* (**G** and **G'** detail) is expressed in the deep, medial limb mesenchyme. At E11.5, *Hes1*, a downstream target of Notch signalling, is also expressed in the distal mesenchyme in an overlapping pattern to *Jagged1*. Left lateral views of embryos are shown in all cases. FL forelimb, HL hindlimb

situ hybridisation in the developing mouse limb, although expression of these genes was seen in other regions of the embryo. I was able to detect three Notch ligands in the developing mouse limb buds, in non-overlapping domains. Two Notch ligands, *Jagged1* and *Jagged2*, are expressed in the limb at E10.5. A third Notch ligand, *Delta-like3*, is expressed in the limb at E11.5. *Jagged1* transcripts are detected in a small patch of posterior distal mesenchyme of E10.5 limb bud and are clearly absent from the AER, shown by the unstained stripe of non-expressing cells (Fig. 5C and arrow 5C'). At E11.5, the domain of *Jagged1* expression increases to cover most of the distal limb mesenchyme (Fig. 5D and 5D'). At E10.5, *Jagged2* is expressed in the ectoderm and the AER and levels of expression increase in the AER at E11.5 (Fig. 5E-5F), in a similar pattern to *Notch1*. *Delta-like3* is expressed at very low levels in the deep, medial limb mesenchyme at E11.5 (Fig. 5G and 5G'). In the chick, a downstream component of Notch signalling, *Hairy1*, is expressed in the distal limb mesenchyme (Vasiliauskas et al., 2003). The mouse orthologue *Hes1* is also expressed in the distal limb mesenchyme in an overlapping domain with *Jagged1* (Fig. 5H and

Notch Receptor	Notch Ligand	Potential downsteam Notch target
Notch1 ✓	*Jagged1* ✓	*Hes1* ✓
Notch2	*Jagged2* ✓	*Hes5*
Notch3	*Delta-like1*	
Notch4	*Delta-like3* ✓	
	Delta-like4	

Table 1. Expression analysis of the *Notch* receptors, ligands and potential downstream targets in mouse limb buds. Whole-mount *in situ* hyridisation of components of the Notch signalling pathway. *Notch1* and *Jagged2* are expressed in the AER and ectoderm of the mouse limb, while *Jagged1* and *Hes1* are ecpressed in overlapping domains in the distal mesenchyme of the limb bud. *Delta-like3* is expressed in the medial mesenchyme of the limb bud. ✓ indicates the gene is detected by whole-mount *in situ* hyridisation in mouse limb buds.

5H', Jouve et al., 2000). I was unable to detect the expression of *Delta-like1* and *Delta-like4* in the developing mouse limb by whole-mount *in situ* hybridisation (data not shown).

3.2 *Notch1* appears not to be required in the limb mesenchyme

Although I was unable to detect *Notch1* expression in the limb mesenchyme at stages E9.5 to E14.5, roles for *Notch1* and components of the Notch signalling pathway have been implicated in the development of bone, muscle and vasculature. To study if *Notch1* has a role in the development of any of these limb mesenchyme derivatives, I used a conditional allele of *Notch1* (*Notch1*$^{lox/lox}$) (Radtke et al., 1999) and a *Cre* transgenic line that is capable of expressing Cre recombinase throughout the developing limb mesenchyme, *Prx1-Cre* (Fig. 6) (Logan et al., 2002). This gene deletion approach tests the requirement of *Notch1* in the mesenchyme of the developing limb. The *Prx1-Cre* has been successfully used with other conditional alleles to efficiently delete genes in the mesenchyme of the developing limb (Akiyama et al., 2002; Compagni et al., 2003; Rallis et al., 2003; Selever et al., 2004). In this line, Cre activity is first detectable by E9.0 and is throughout the limb mesenchyme of the forelimb by E9.5 (Fig. 6A and Logan et al., 2002). By E10.5, there is Cre-mediated recombination throughout the hindlimb mesenchyme (Logan et al., 2002). Since Cre activity is detectable at relatively early stages, all the descendents of these cells, that will give rise to the, tendon, cartilage/bone, vasculature and muscle, will have had conditional alleles deleted via Cre-catalysed recombination. At E13.5, Cre activity can clearly be seen throughout most of the cells of the limb mesenchyme, with blood cells Cre negative (Fig. 6B). Importantly, in the *Prx1-Cre* line, Cre expression is restricted

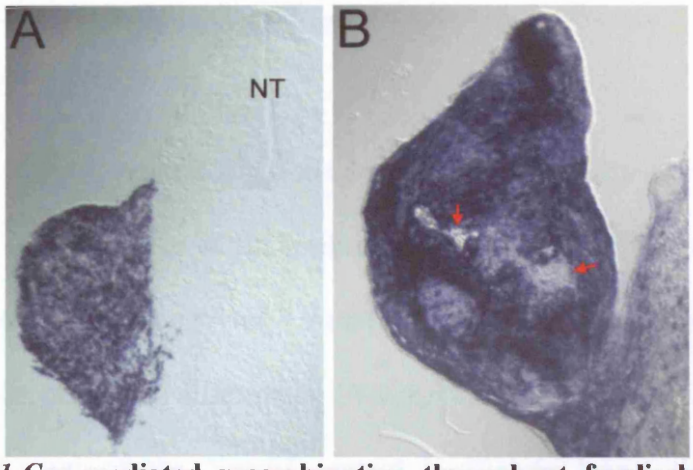

Figure 6. *Prx1-Cre* mediated recombination throughout forelimb mesenchyme. Alkaline-phosphatse staining of *Z/AP; Prx1-Cre* mice demonstrating Cre-mediated recombination in sections of E9.5 (**A**) and E13.5 (**B**) limb buds. At E9.5 there is a high level of Cre activity throughout the limb bud mesenchyme. At E13.5 there continues to be high levels of Cre–mediated recombination in the limb mesenchyme, with no Cre activity in blood cells (red arrows). Both tranverse 10μm frozen cryostat sections. NT=neural tube. Alkaline-phosphatse staining and sections carried out by M. Logan.

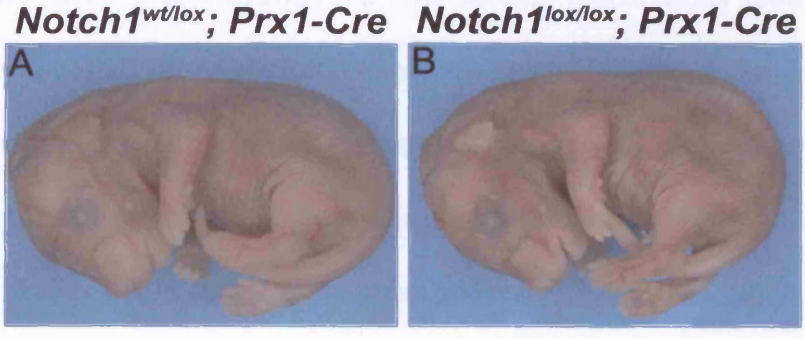

Figure 7. E17.5 embryos have no apparent phenotype after deletion of *Notch1* in the limb mesenchyme. (**A**) E17.5 *Prx1-Cre; Notch1*$^{lox/wt}$ control littermate. (**B**) E17.5 *Prx1-Cre; Notch1*$^{lox/lox}$ conditional knockout. Deletion of *Notch1* in the mesenchyme of the developing limb with the *Prx1-Cre* line does not produce a phenotype when compared to a control littermate.

to the mesenchyme and no cells in the AER or limb ectoderm are exposed to Cre activity. Using the *Prx1-Cre* it is possible to distinguish the effects of specifically deleting *Notch1* in the limb mesenchyme.

Surprisingly, despite reports suggesting that Notch1 activity is required for the development of derivatives of the limb mesenchyme, E17.5 embryos mutant for *Notch1* in the limb mesenchyme (*Notch1*$^{lox/lox}$; *Prx1-Cre*) are indistinguishable from the limbs of control littermates (*Notch1*$^{wt/lox}$; *Prx1-Cre*) (compare Fig. 7A with 7B). The ear of the *Notch1* mutant is slightly larger than the control littermate. This could be due to the deletion of *Notch1* in regions of the head where the *Prx1-Cre* is also active (Logan et al., 2002). Since *Notch1* has been implicated in the development of cartilage/bone, vasculature and muscle, I investigated in detail if these mesenchymal derivatives are affected in these mutant mice. To analyse the bone elements after deletion of *Notch1* from the mesenchyme, I carried out skeletal preparations on control and mutant mice at E16.5 with Alcian blue/Alizarian red. The skeletal preparations show that in the mutant embryos all of the skeletal elements of the forelimb and hindlimb appear normal, compared to a control littermate (Fig. 8A-H). To study the muscle patterning in the *Notch1*$^{lox/lox}$; *Prx1- Cre* embryos, anti-muscle myosin antibody staining was carried out on control (*Notch1*$^{wt/lox}$; *Prx1-Cre*) and mutant (*Notch1*$^{lox/lox}$; *Prx1-Cre*) E14.5 embryos (Fig. 8I-L). All the muscles of the mutant limb are present and are the correct shape and position, compared to the control littermate. This demonstrates that the patterning of the limb musculature is unaltered in embryos where *Notch1* has been deleted from the limb mesenchyme.

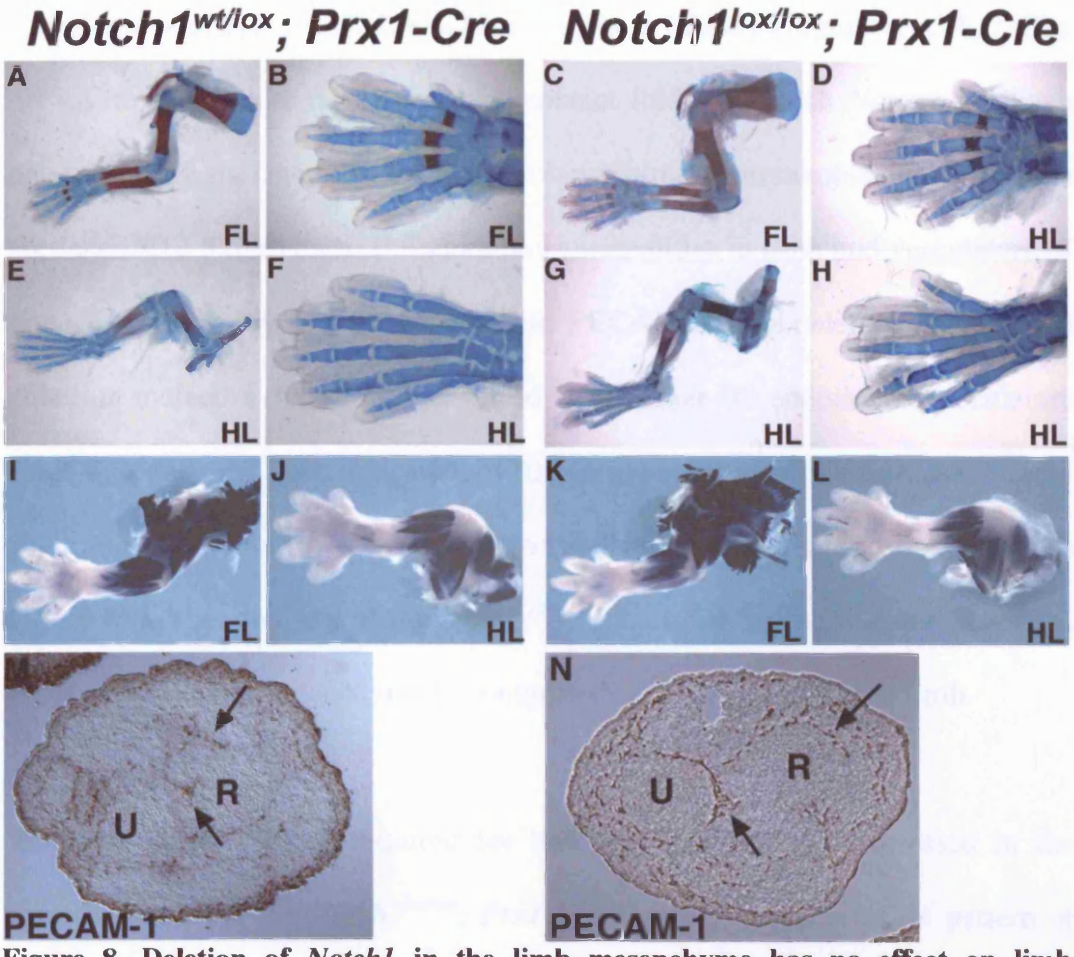

Figure 8. Deletion of *Notch1* in the limb mesenchyme has no effect on limb development. Alcian blue/Alizarin red staining of the forming skeletal elements in control (*Notch1*$^{wt/lox}$; *Prx1-Cre*: **A**, **B**, **E**, **F**) and mutant (*Notch1*$^{lox/lox}$; *Prx1-Cre*: **C**, **D**, **G**, **H**) embryos at E16.5. Forelimb (**A**) and detail of the forefoot (**B**), hindlimb (**E**) and detail of the hindfoot (**F**) from a *Notch1*$^{wt/lox}$; *Prx1-Cre* embryo. Forelimb (**C**) and detail of the forefoot (**D**) and hindlimb (**G**) and detail of the hindfoot (H) from a *Notch1*$^{lox/lox}$; *Prx1-Cre* embryo. Immunohistochemical staining of the limb muscles in forelimb (**I**) and hindlimb (**J**) from a *Notch1*$^{wt/lox}$; *Prx1-Cre* embryo at E14.5. Identical staining of forelimb (**K**) and hindlimb (**L**) from a *Notch1*$^{lox/lox}$; *Prx1-Cre* embryo. No difference in PECAM-1 staining, a marker of vascular endothelial cells, on comparable transverse sections of E12.5 control (**M**) and mutant (**N**) forelimbs (arrows mark assembled endothelial vasculature). U=Ulnar, R=Radius, FL=forelimb, HL=hindlimb

The Notch signalling pathway has also been implicated in angiogenesis, where *Notch1* carries out a cell-autonomous role in the endothelium to form the mature vascular network (Iso et al., 2003; Limbourg et al., 2005; Vargesson et al., 1998). To assess vasculature development in mutant limbs in which *Notch1* has been deleted in all the mesenchymal cells, I performed immunohistochemistry on sectioned E12.5 limb buds. I observe no abnormalities in limb bud vasculature of these mutant embryos, as assessed with PECAM-1, a platelet/endothelial cell adhesion molecule (CD31 antigen) used as a marker for endothelial vasculature (Fig. 8M and 8N). As indicated by the arrows in Figure 8N, these *Notch1* conditional mice start to assemble the vasculature, comparable to the control in Figure 8M. This analysis of the *Notch1*$^{lox/lox}$; *Prx1-Cre* mice indicates *Notch1* is not required in the mesenchyme for outgrowth and patterning of the limb.

To confirm that signals required for limb development are expressed in the correct manner in the *Notch1*$^{lox/lox}$; *Prx1-Cre* mutants, the expression pattern of two secreted signalling molecules was analysed at early limb bud stages. *Fgf8* and *Shh* are expressed in two key signalling centres of the limb bud. *Fgf8* is expressed in the apical ectodermal ridge (AER) and is required for proximal-distal outgrowth of the limb (Martin, 1998). *Shh* is expressed in the zone of polarising activity (ZPA) and is required for anterior-posterior patterning of the limb (Riddle et al., 1993). *Fgf8* expression is identical in the AER of the *Notch1*$^{lox/lox}$; *Prx1-Cre* mice, compared to a control littermate (Fig 9A-9D). Similarly, *Shh* is expressed normally in the mutant mice (Fig. 9E-9H). Consistent with my analysis of the bone, muscle, vasculature and molecular data, mutant newborn pups also have no evident phenotype compared to control littermates. In

addition, mutant animals develop to adulthood apparently normally. In contrast to previous data suggesting a role for Notch signalling during bone, muscle and vasculature development (Delfini et al., 2000; Nobta et al., 2005; Pereira et al., 2002; Vargesson et al., 1998; Watanabe et al., 2003), these results demonstrate that *Notch1* is not required for the development of the limb mesenchyme and its derivatives *in vivo*. Furthermore, it does not appear to be required at postnatal stages for continued maturation and homeostasis of these limb tissues.

3.3 *Notch1* is required in the limb ectoderm/AER

Notch1 is expressed in the AER (Williams et al., 1995) and my expression analysis using whole-mount *in situ* hybridisation has shown that mRNA transcripts are detected in the AER by E10.5 and expression can be clearly seen in the ridge at E11.5. To delete *Notch1* in this ectodermal derivative, I used the conditional *Notch1*$^{lox/lox}$ mouse in combination with a *Brn4-Cre* transgenic mouse line that expresses the *Cre* recombinase in the ectoderm and AER (Ahn et al., 2001). In the *Brn4-Cre* line, Cre-catalysed recombination is first detected in the limb ectoderm at E9.75, a stage when the forelimb has already begun to form but prior to the initiation of the hindlimb bud (Ahn et al., 2001). Cre activity is detected in the hindlimb at E10, particularly robustly at the distal tip of the limb in the region of cells that will give rise to the AER. By E10.5, Cre activity is detected throughout the hindlimb AER and ventral ectoderm, with more limited activity in the dorsal ectoderm (Fig 10A, 10C, 10E). Forelimb buds of E10.5 embryos have patchy Cre activity in the AER and ventral ectoderm, with little or no activity in the dorsal ectoderm (Fig 10A, 10B, 10D). At E11.5 and E12.5, while Cre is broadly active in the hindlimb AER and ventral ectoderm there is

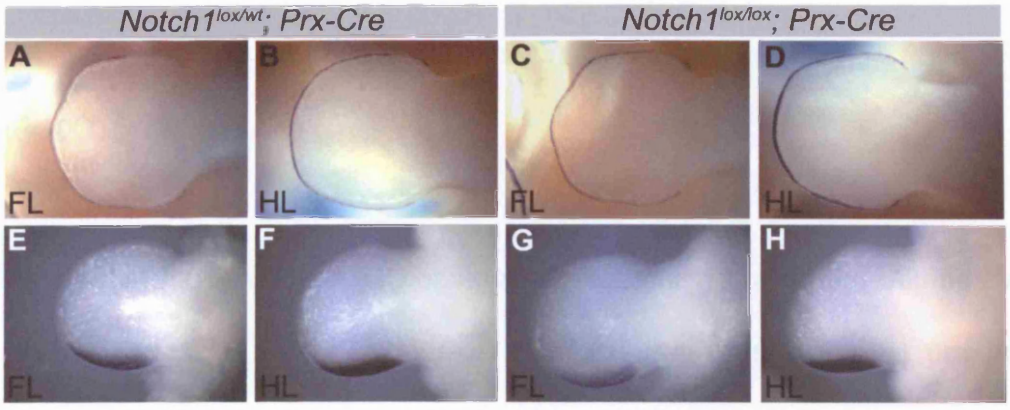

Figure 9. Signalling centres are unaffected after deletion of *Notch1* in the limb mesenchyme. Mutant E11.5 limb buds processed by whole-mount *in situ* hybridization display no difference in the expression of *Fgf8* in the AER or in *Shh* expression in the ZPA. *Fgf8* expression in control (*Notch1*$^{wt/lox}$; *Prx1-Cre*: **A**, **B**) and mutant (*Notch1*$^{lox/lox}$; *Prx1-Cre*: **C**, **D**) limbs, and *Shh* expression in control (**E**, **F**) and mutant limb buds (**G**, **H**). Left lateral views of embryos are shown in all cases. FL=forelimb, HL= hindlimb

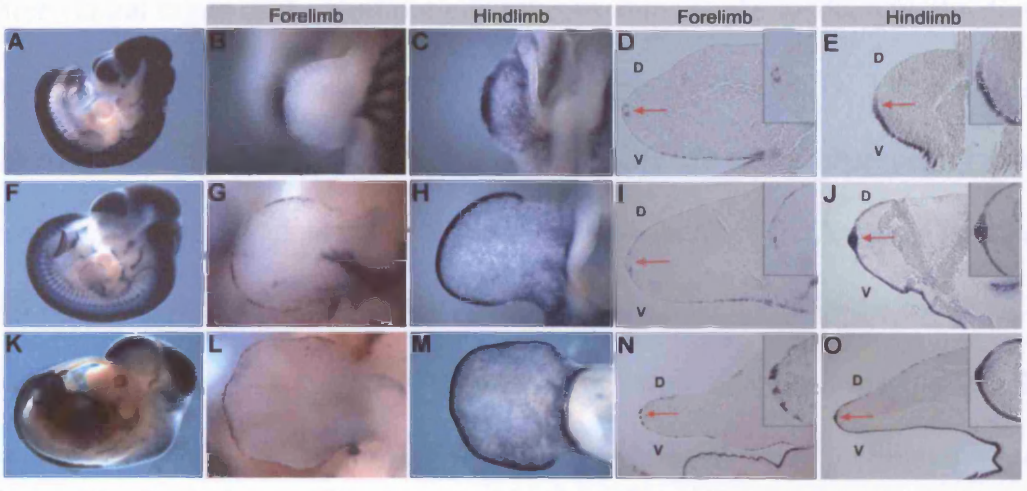

Figure 10. *Brn4-Cre* mediated recombination throughout hindlimb AER and ventral ectoderm, but low levels of activity in the forelimb. Alkaline-phosphatase staining of *Z/AP*; *Brn4-Cre* mice demonstrating Cre-mediated recombination in E10.5 (**A-E**), E11.5 (**F-J**) and E12.5 (**K-O**) embryos. 10μm transverse wax sections of forelimbs (**D**, **I**, **N** and inset AER detail) showing patchy Cre activity in the AER and ventral ectoderm, while the hindlimbs (**E**, **J**, **O** and inset AER detail) have strong activity in the AER and ventral ectoderm. Very little Brn4-Cre activity is seen in the dorsal ectoderm of forelimbs or hindlimbs. (**A**, **F**, **K**) Left lateral views of embryos, (**B**, **G**, **L**) dorsal view of forelimbs and (**C**, **H**, **M**) ventral view of hindlimb. Red arrows indicate AER, D=dorsal, V=ventral.

only weak activity in the dorsal ectoderm. At these stages in the forelimb, there continues to be just a few cells where a Cre-catalysed event has occurred (Fig. 10F-10O).

P0 pups that have had *Notch1* conditionally deleted from the developing limb ectoderm and AER (*Notch1*$^{lox/lox}$; *Brn4-Cre*) have apparently normal proximal elements, but distally the digits are affected (Fig. 11B, 11D and 11F). The hindlimbs of the *Notch1*$^{lox/lox}$; *Brn4-Cre* mutants have bent digits that are closer together and are restricted along the anterior-posterior axis compared to control mice. The hindfeet have a "clenched foot " phenotype, with a fibular deviation of the first digit and a tibial deviation of the fifth digit (Fig. 11D and 11F). The three central digits of the hindfoot exhibit complete simple syndactyly, the digits being joined by soft tissue along their entire length (Fig. 11D, 11F and 11I). Osseous fusions between bones of adjacent digits are never observed in these mutants. Analysis of embryos at E14.5 demonstrates that syndactyly of the three central digits are evident by this stage (Fig. 11H). The digits in the footplate of the control embryo are clearly defined with large interdigit spacing. In the *Notch1*$^{lox/lox}$; *Brn4-Cre* mutants the digits have much less interdigital space between them. The vascular patterning in the hindlimb of the *Notch1*$^{lox/lox}$; *Brn4-Cre* mutant also appears slightly different to the *Notch*$^{wt/lox}$; *Brn4-Cre* control (Fig. 11G and 11H). A highly penetrant and reproducible phenotype is only observed in hindlimbs of mutant animals. Bent digits or syndactyly are never seen in the forelimbs of the *Notch1*$^{lox/lox}$; *Brn4-Cre* mutants. I therefore concentrated my analysis on hindlimbs of the *Notch1*$^{lox/lox}$; *Brn4-Cre* mutants to study the role *Notch1* in the AER.

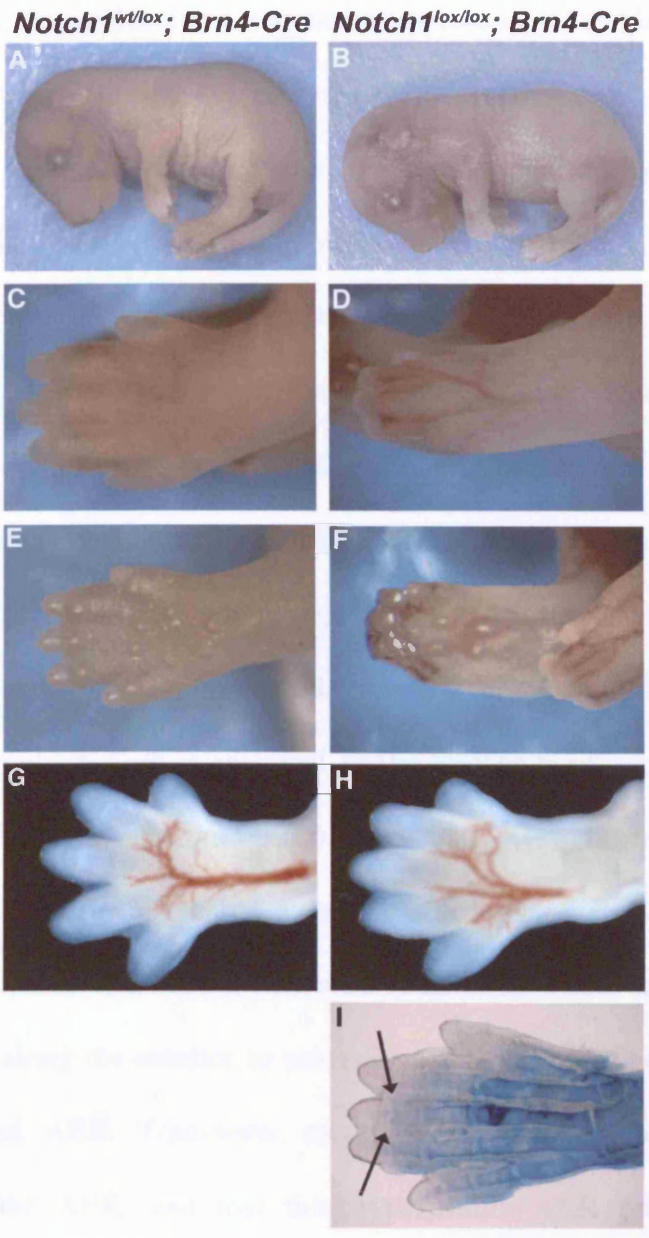

Figure 11. Deletion of *Notch1* in the limb ectoderm leads to syndactyly. Hindlimb defects of *Notch1*$^{lox/lox}$; *Brn4-Cre* embryos. Left lateral (**A**), dorsal (**C**) and ventral (**E**) views of *Notch1*$^{wt/lox}$; *Brn4-Cre* (control) P0 pups. Left lateral (**B**), dorsal (**D**) and ventral (**F**) views of *Notch1*$^{lox/lox}$; *Brn4-Cre* (mutant) embryos. As a result of a failure of interdigital cell death that normally frees the digits, the phalangeal elements of the mutant hindfoot are brought together to form an arched footplate rather than the flattened footplate in the control. The footplate of a control (**G**) and mutant (**H**) E14.5 embryo. The failure in normal interdigital cell death is already evident and is most obvious between the three central digits. (**I**) Alcian blue staining of the skeleton of a E17.5 mutant embryo. Syndactyly between the three central digits is obvious although there are no fusions between the phalangeal bones (arrows). Hindlimbs are shown in all cases and the anterior digit 1 is uppermost in all panels.

To understand the molecular mechanisms that lead to syndactyly following deletion of *Notch1* in the AER, I analysed the expression of *Fgf8* (Fig. 12A-H). *Fgf8* is a gene molecular marker of the AER and is required for proximal-distal outgrowth of the limb. At E10.5, the hindlimb AER has been initiated, but has not yet formed a ridge of cells at the DV margin of the limb bud. At this stage, *Fgf8* is expressed in a broad domain at the distal tip of the limb. At E10.5, the domain of *Fgf8* expression is identical in the mutant hindlimb, compared to a control littermate (Fig. 12A and 12B). By E11.5, the expression domain of *Fgf8* becomes restricted to a sharp border along the anterior to posterior extent of the AER that divides the dorsal and ventral ectoderm. In a dorsal view at E11.5, the expression domain of *Fgf8* is identical in the mutant hindlimb, compared to a control littermate (Fig. 12C and 12D). In a distal view however, there is an expansion along the dorsal-ventral axis of the domain of *Fgf8*-expressing cells (Fig. 12F), compared to a control littermate (Fig. 12E). These areas of expanded AER can vary along the anterior to posterior extent of the ridge, resulting in an irregular shaped AER. Transverse sections of mutant limbs show a clear expansion of the AER, and that this hyperplastic AER protrudes into the mesenchyme of the limb (Fig. 12H). The hyperplastic AER phenotype is strikingly similar to that reported for mice mutant for the Notch ligand, *Jagged2* (Jiang et al., 1998; Sidow et al., 1997).

3.4 Hyperplastic AERs form in *Notch1* mutants due to a decrease in programmed cell death

Notch1$^{lox/lox}$; *Brn4-Cre* hindlimbs were analysed determine whether the hyperplastic AER is due to an increase in cell proliferation or a decrease in cell

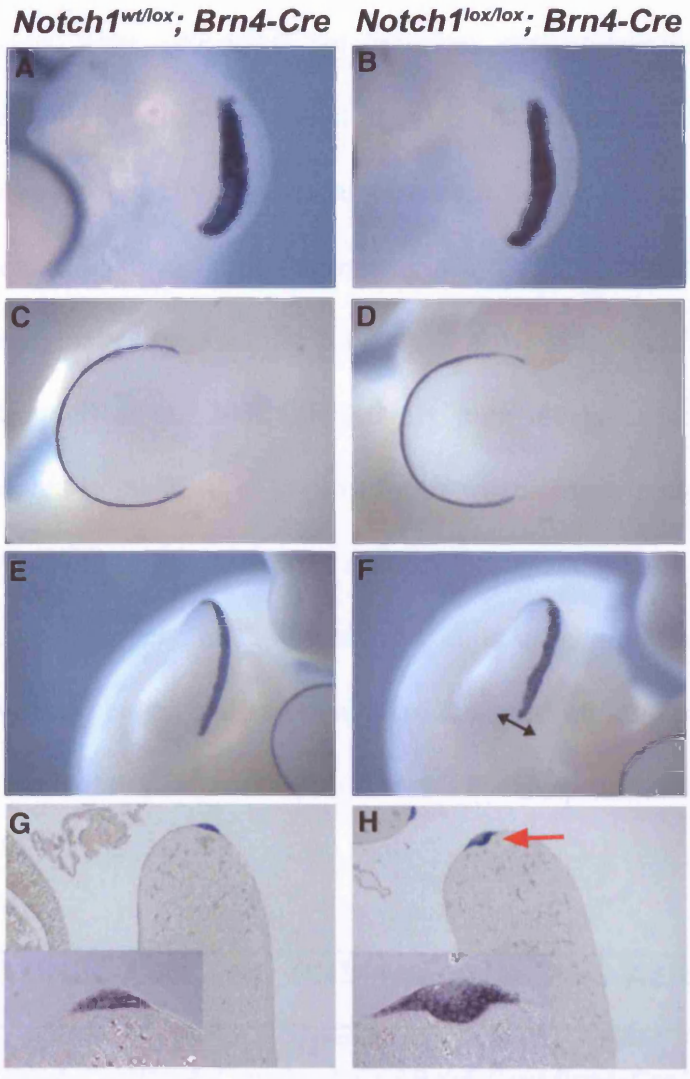

Figure 12. Deletion of *Notch1* in the ectoderm leads to the formation of a hyperplastic AER. Hyperplasia of the AER is evident by the expanded expression of *Fgf8* in mutant E11.5 hindlimbs. No difference in comparable distal views of E10.5 control (*Notch1*$^{wt/lox}$; *Brn4-Cre*) (**A**) and mutant (*Notch1*$^{lox/lox}$; *Brn4-Cre*) (**B**) limbs processed by whole-mount *in situ* hybridisation with an *Fgf8* probe. Dorsal views of E11.5 control (**C**) and mutant (**D**) limbs demonstrate that the anterior to posterior extent of *Fgf8* expression is unaffected. However, views of the apex of the limb show the expanded domain of *Fgf8*-expressing cells in the mutant limb (arrow in **F**) when compared with the same view of a control limb (**E**). In sections of the limb, the extent of the AER hyperplasia is evident. The AER is expanded and protrudes into the mesenchyme (**H** red arrow and inset detail 40X magnification) compared with the normal AER morphology in the control limb (**G** and inset detail 40X magnification). A=anterior, P=posterior.

apoptosis within the ridge. To determine apoptotic cells, E11.5 mutant and control embryos were processed for terminal deoxynucleotidyl transferase (TdT)-mediated dUTP nick end labelling (TUNEL) staining. When a cell is eliminated by apoptosis, DNA fragmentation occurs prior to cell death. TUNEL staining detects cells undergoing apoptosis via DNA strand breaks that are detected by enzymatically labelling the free 3'-OH with modified nucleotides using TdT (Gavrieli et al., 1992). Relatively high levels of programmed cell death are observed in the AER of control limbs when compared to the rest of the limb ectoderm (Fig. 13A). A similar section through a mutant limb indicates there is a marked decrease in the number of cells undergoing apoptosis in the AER (Fig. 13B). When several samples were analysed and the mean number of apoptotic cells calculated, almost 3-fold more TUNEL-positive cells are present

	TUNEL AER +ve cells		**PH3 +ve cells**		**PH3 AER +ve cells**	
Sample #	*N1*$^{wt/lox}$; *Brn4-Cre*	*N1*$^{lox/lox}$; *Brn4-Cre*	*N1*$^{wt/lox}$; *Brn4-Cre*	*N1*$^{lox/lox}$; *Brn4-Cre*	*N1*$^{wt/lox}$; *Brn4-Cre*	*N1*$^{lox/lox}$; *Brn4-Cre*
1	9	3	11	13	2	0
2	6	4	13	12	0	1
3	4	2	10	9	1	1
4	7	1	9	12	1	1
5	8	3	14	10	2	0
6	9	5	14		0	2
7	11	1				
8	6	2				
9	5	4				
10	8	2				
11	6					
Mean	7.18	2.7	11.83	11.2	1	0.83

Table 2. After deletion of *Notch1* in the AER there is no change in proliferation, but a decrease in apoptosis. There is almost a three-fold decrease in TUNEL positive cells in the AER of mutant limbs (*N1*$^{lox/lox}$; *Brn4-Cre*), compared to control (*N1*$^{wt/lox}$; *Brn4-Cre*). There is no difference in the levels of phospho-histone H3 (PH3) in the AER or distal mesenchyme of mutant limbs. +ve=positive

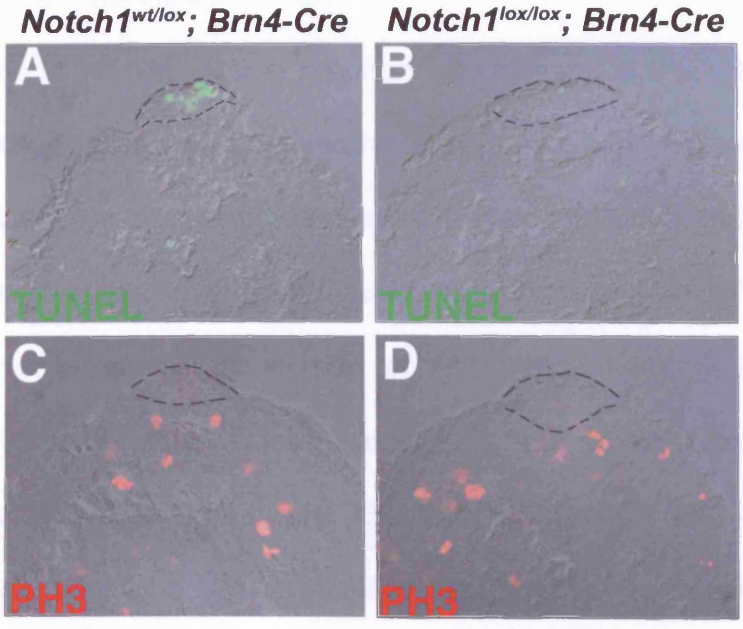

Figure 13. Deletion of *Notch1* in the AER/ectoderm leads to reduced programmed cell death in the AER. A higher number of TUNEL positive (apoptotic) cells are observed in the control (*Notch1*$^{wt/lox}$; *Brn4-Cre*) AER (**A**) than mutant (*Notch1*$^{lox/lox}$; *Brn4-Cre*) AER (**B**). Using phospho-histone-3 (PH3) as a marker of cells committed to mitosis, no difference in the number of cells undergoing cell division is observed between the AER in control (**C**) and mutant (**D**) hindlimbs. The AER is outlined on sections with a dashed line, transverse sections of E11.5 hindlimbs. 40X magnification.

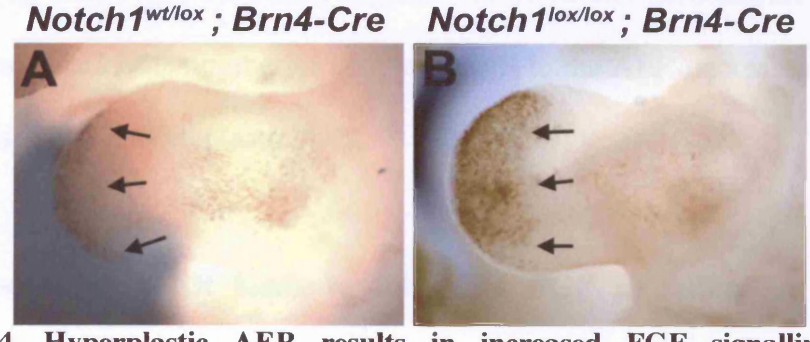

Figure 14. Hyperplastic AER results in increased FGF signalling in the mesenchyme under the AER. pERK staining shows FGF signal receiving cells in the distal mesenchyme of control (*Notch1*$^{wt/lox}$; *Brn4-Cre*) limb (**A**), which is increased in the mutant (*Notch1*$^{lox/lox}$; *Brn4-Cre*) limb (**B**). Black arrows mark the proximal level of pERK staining. Left lateral views of E11.5 hindlimbs.

in the control limbs than mutant limbs (student T-test p value of 5.74E-06) (Table 2 and Materials and Methods).

I used an antibody against phophorylated histone H3 (PH3) to analyse the number of cells undergoing proliferation in the hyperplastic AER of the mutant hindlimb. The covalent phosphorylation of histone H3 has been implicated in chromosome condensation during mitosis, and is a good marker of proliferating cells (Choi et al., 2005). In sections of E11.5 mutant embryos there is no difference in the number of cells stained for PH3 in the AER (Fig. 13D), compared to control littermates (Fig. 13C) (mutant mean 0.8 PH3+ cells/section versus control mean 1 PH3+ cells/section and a T-test gave a p value of 0.30 and Table 2). This demonstrates that there is no change in the number of proliferating cells in the AER following deletion of *Notch1*. Most of the proliferating cells in the developing limb detected with PH3 are found within the underlying mesenchyme. I also detect no difference in the number of PH3-positive cells in the mesenchyme of control and mutant limbs (11.8 and 11.2 PH3+ cells/section, respectively and Table 2). Taken together, these results demonstrate that in the absence of *Notch1* the number of apoptotic cells in the AER decreases, leading to the formation of a hyperplastic AER.

3.5 Hyperplastic AER leads to increased FGF signalling in the distal mesenchyme

To determine whether the larger AER produces increased levels of FGF signalling that may affect the distal limb bud, I analysed the levels of phospho-ERK (pERK). An antibody against the diphosphorylated forms of ERK1 and ERK2 was used as a read-out of FGF-dependent signalling. FGF ligands bind

and activate fibroblast growth factor receptors (FGFR) and signalling is transduced via activation of the receptors cytoplasmic tyrosine kinase domain. This results in an intracellular cascade, including the sequential phosphorylation of a number of protein kinases, leading to the activation of ERK. Active pERK is involved in a number of cellular processes, such as gene activation, translation and cytoskeleton re-arrangement (Marshall, 1995). The use of an antibody against pERK enables the identification of cells that are actively responding to FGF signalling.

pERK staining in the mouse is initially detected in the surface ectoderm at E9.0. At E9.5, a gradient of pERK signalling is established in the mesenchyme underneath the AER. pERK is also detected in the surface ectoderm, but little staining is seen in the AER. A similar pattern of pERK is seen at E10.5, with staining present in mesenchyme adjacent to the AER. This pERK staining diminishes in the presence of the FGFR-specific inhibitor, SU5402 (Corson et al., 2003). The levels of pERK vary between control (*Notch1*$^{wt/lox}$; *Brn4-Cre*) and mutant (*Notch1*$^{lox/lox}$; *Brn4-Cre*) embryos that have a hyperplastic AER (Fig. 14). In the *Notch1* conditional mutants there is a larger domain of pERK staining that is expanded proximally, compared to the control. This suggests that there is an increased level of AER-derived FGF signalling, resulting in a larger domain of pERK activation.

3.6 The AER regresses normally in *Notch1* mutants

Between E12.5 and E13.5 the AER begins to regress, resulting in the gradual loss of *Fgf8* expression from the distal tip of the limb (Sun et al., 2002; Guo et

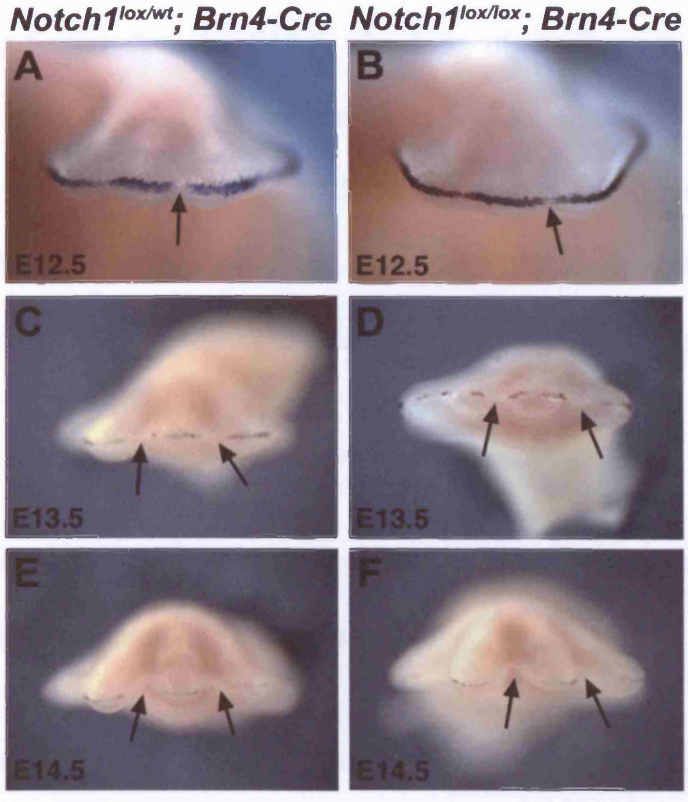

Figure 15. AER regression occurs normally after deletion of *Notch1* in the AER/ectoderm. Distal views of limbs processed by whole-mount *in situ* hybridisation with an *Fgf8* probe show that at E12.5 AER regression begins in both the control (*Notch1*$^{wt/lox}$; *Brn4-Cre*) (**A**) and the mutant (*Notch1*$^{lox/lox}$; *Brn4-Cre*) (**B**). AER regression can be more clearly seen at E13.5 and E14.5 in between the digits, where similar amounts of *Fgf8* expressing AER cells are lost in the mutant (**D**, **F**) compared to the control littermate (**C**, **E**). Arrows indicate lost *Fgf8* expression. Distal views of limbs are shown in all cases.

al., 2003). To investigate whether the decrease in the levels of programmed cell death in the AER of the *Notch1*$^{lox/lox}$; *Brn4-Cre* hindlimbs also results in a persistence of the AER, the expression of *Fgf8* was analysed from E12.5 to E14.5 (Fig. 15). At E12.5, the first signs of a downregulation of *Fgf8* are seen in the interdigit area of both a control and a mutant hindlimb (Fig. 15A and 15B). Later, at E13.5 and then at E14.5, the loss of *Fgf8* expression becomes progressively more obvious between the digits of the control and the *Notch1*$^{lox/lox}$; *Brn4-Cre* mutant hindlimbs (Fig. 15C-15F). Together, this demonstrates that there is no difference in the timing and extent of *Fgf8* downregulation and AER regression after *Notch1* has been deleted from the AER, compared to a control littermate.

3.7 Expression patterns of Notch signalling components are unaffected following deletion of *Notch1* in the ectoderm

Studies on the regulation of the Notch signalling components have shown there are often feedback loops between the Notch receptors and their ligands that regulate, and often refine, their expression domains (de Celis and Bray, 1997; Jen et al., 1999; Panin et al., 1997; Ross and Kadesch, 2004). To determine if the removal of *Notch1* from the limb ectoderm and AER has an effect on the expression patterns of its ligands, I analysed their expression by whole-mount *in situ* hybridisation. *Jagged2* is expressed in cells of the AER (Fig. 16A and 5F) in a pattern that overlaps with that of *Notch1*. *Jagged2* expression is unaffected *Notch1*$^{lox/lox}$; *Brn4-Cre* hindlimbs (Fig. 16B), indicating that *Notch1* is not required to regulate expression of *Jagged2* in the AER. *Jagged1* (Fig. 16C and 16D) and *Hes1* (Fig. 16E and 16F), which are expressed in the distal

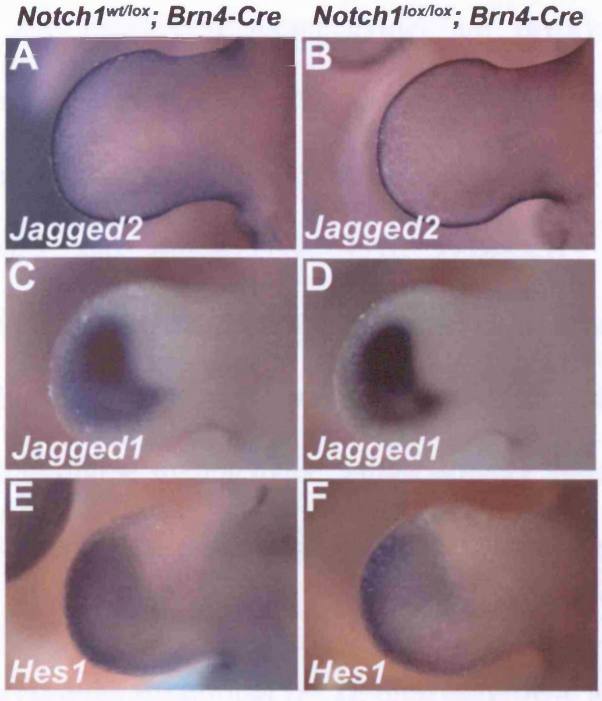

Figure 16. Expression of *Jagged1*, *Jagged2* and *Hes1* are not affected following deletion of *Notch1* in the AER/ectoderm. Control (*Notch1*$^{wt/lox}$; *Brn4-Cre*) hindlimbs are shown in panels **A**, **C** and **E**. Mutant (*Notch1*$^{lox/lox}$; *Brn4-Cre*) hindlimbs are shown in panels **B**, **D** and **F**. The expression of the Notch ligands *Jagged2* (**A**, **B**), *Jagged1* (**C**, **D**) and a downstream target, *Hes1*, (**E**, **F**) are identical in the mutant, compared to the control. Left lateral views of E11.5 hindlimbs are shown in all cases.

mesenchyme of the limb, are also unaffected following deletion of *Notch1* in the AER.

3.8 Deletion of *Notch1* in the ectoderm has consequences on gene expression in the limb mesenchyme

Three bone morphogenetic proteins (BMPs), *Bmp2*, *Bmp4* and *Bmp7*, expressed in the cells of the interdigital mesenchyme, are involved in controlling interdigital programmed cell death (IPCD) and normal digit formation (Buckland et al., 1998; Ganan et al., 1998). In E13.5 mutant hindlimbs (*Notch1*$^{lox/lox}$; *Brn4-Cre*) *Bmp2*, *Bmp7* and *Bmp4* (Fig. 17B, 17D, 17F, respectively) are downregulated in the interdigital limb mesenchyme. In all examples the domains where expression is most obviously downregulated are limited to the distal-most extremes of the interdigital mesenchyme, either directly underneath or close to the hyperplastic AER and in the interdigital space between digits 2 and 3 and digits 3 and 4.

Hoxa13 is required for normal IPCD, digit outgrowth and chondrogenesis of the limb (Fromental-Ramain et al., 1996; Stadler et al., 2001). *Hoxa13* controls IPCD by regulating *Bmp2* and *Bmp7* expression (Knosp et al., 2004). *Notch1*$^{lox/lox}$; *Brn4-Cre* mutant embryos show a decrease in the expression *Hoxa13* expression at E12.5 (Fig. 17H). Interestingly, *Hoxa13* is most obviously downregulated in the interdigital space between digits 2 and 3 and digits 3 and 4, precisely the same location where *Bmp2*, *Bmp7*, and *Bmp4* are most profoundly downregulated.

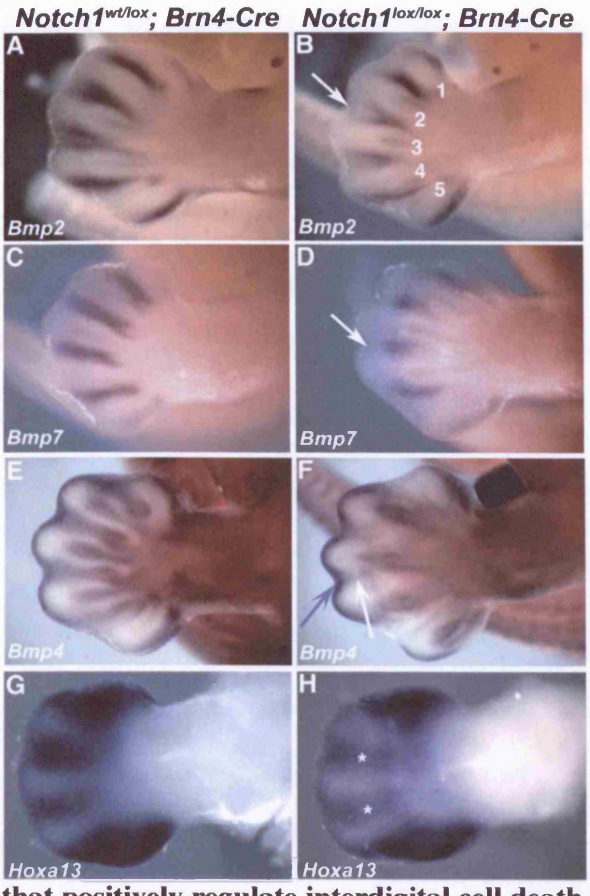

Figure 17. Factors that positively regulate interdigital cell death are downregulated following deletion of *Notch1*. *Bmp2*, which is expressed in the interdigital mesenchyme of control limbs (**A**), is downregulated in the mutant limb (*Notch1*$^{lox/lox}$; *Brn4-Cre*) (**B**). This downregulation is most apparent in the interdigital regions between digits 2 and 3 (white arrow) and 3 and 4. The forming digits are numbered 1-5. *Bmp7*, expressed in the interdigital mesenchyme (**C**), is downregulated in the mutant (**D**). The interdigital space between digits 3 and 4 is indicated with an arrow. Similarly, the expression of *Bmp4*, expressed in the interdigital mesenchyme, (**E**), is downregulated in the mutant (**F**) (white arrow). *Bmp4* is also expressed in the AER and this expression domain is expanded in the mutant (blue arrow) (**F**). *Hoxa13*, expressed in the interdigital space in a control limb (**G**), is downregulated in the mutant limb (**H**) most profoundly in the interdigital space between digits 2 and 3 and 3 and 4 (denoted with *). Left lateral views of hindlimbs are shown in all cases. (**A**-**F**) E13.5 embryos, (**G**, **H**) E12.5 embryos.

These results demonstrate that after deletion of *Notch1* in the limb mesenchyme there is no apparent phenotype in any of the mesenchymal derivatives, which constitute cartilage/bone, muscle and vasculature. Subsequently, these mutants develop normal limbs to adulthood. However, after deletion of *Notch1* in the AER/ectoderm, the hindlimbs of mutant mice have hyperplastic AERs due to a decrease in the number of apoptotic cells in the ridge. Mutants with this expanded AER have a larger domain of FGF signalling in the underlying distal limb mesenchyme, but the AER regresses normally. The expression of *Hoxa13*, *Bmp2*, *Bmp4* and *Bmp7* are downregulated in the interdigit region of the hindlimb autopod, and P0 pups display soft tissue syndactyly.

3.9 *Vestigial-like1* is expressed in the developing chick embryo

To identify chick *Vestigial-like* (*Vgl*) genes expressed in the developing vertebrate limb, a limb lambda phage cDNA library was screened (using a human IMAGE clone as a probe, db EST ID; 589455) and a full-length chick *Vgl* gene was isolated (A. Brent and MPL unpublished, Fig.18). A phylogenetic tree of this chick sequence with the human, mouse and zebrafish *Vgl* orthologues shows that this gene is most similar to *Vestigial-like1* (*Vgl1*). A *Vestigial-like2* (*Vgl2*) expressed sequence tag (EST) was obtained from the chick BBSRC EST database (clone ID; ChEST976p9, http://www.chick.umist.ac.uk). To determine whether these vertebrate orthologues of the *Drosophila* gene *vestigial* are involved in limb development, I examined the expression pattern of these two orthologues, *Vgl1* and *Vgl2*.

To examine the temporal and spatial expression of *Vgl1* in the developing chick embryo, I used both whole-mount and section *in situ* hybridisation techniques. Initial experiments using these methods on embryos from stage 10 to stage 23 with a probe against the full-length 729bp *Vgl1* ORF did not produce a detectable signal. I therefore used reverse transcriptase-polymerase chain reaction (RT-PCR) to analyse the expression of *Vgl1*. This method is more sensitive than RNA *in situ* hybridisation to detect mRNA transcripts. RNA was extracted from different regions of chick embryos; the lateral plate mesoderm (LPM) adjacent to somites 15 to 19, the prospective limb-forming region, at (Hamburger and Hamilton) stage 14 and stage 16, a limb bud stage 17, an apical ectodermal

A

MEETRKLSPKPCKSKEPVKTEWGAQSVVFTYFQGDINSVVDEHFSRALSNARNPQDLST
KHKSEVVVPKHDSMSPHQWNFSSHCSKPYPSSSSTSMSNSALDFPAVAMAGQYQPAALR
THPAQPADLWPFPSLGTPSLTSPVYHHAVPDLHVVDEPISDRKYRSLLGLLQQERCLMS
MQECAVKQHSSSTCMTGPARLQNISQSSVPGGERKASSYQGSENPSASHATAGIQIHDR
RRDLYF.

B

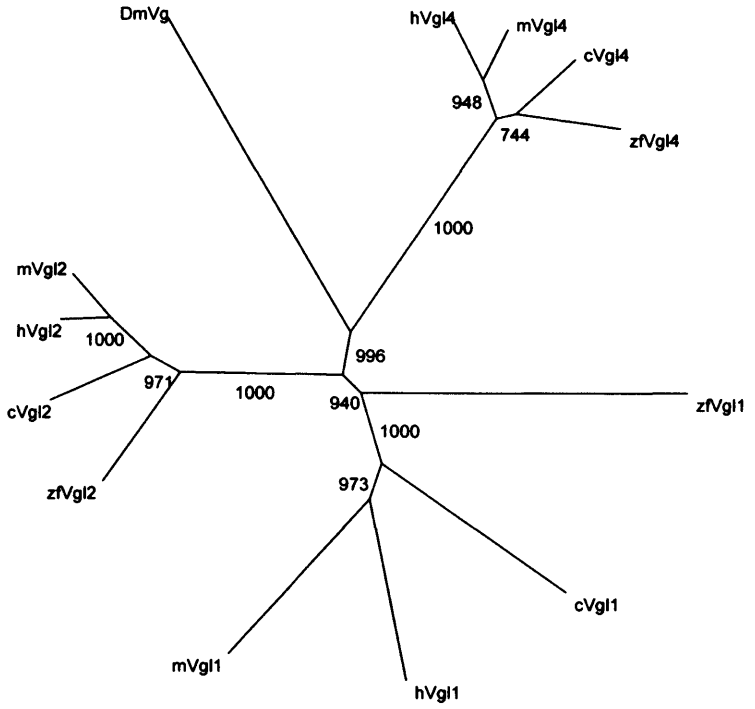

Figure 18. Predicted peptide sequence of the full-length chick Vestigial-like1 and phylogenetic tree of Vgl proteins. (**A**) Full-length Vestigial-like1 peptide sequence. The scalloped-binding domain (SBD) is highlighted in yellow. The last amino acid of the truncated version of Vestigial-like1, Vgl1-ΔC, is marked in red. The *Drosophila* Engrailed repressor domain and $VP16_4$ activator domains were fused in-frame at this position. (**B**) ClustalX neighbour-joining unrooted phylogenetic tree of *Drosophila*, human, mouse, chick and zebrafish Vgl1, Vgl2 and Vgl4. The numbers represent 1000 bootstrap replicates.

ridge (AER) stage 19, limb mesenchyme stage 19, a limb bud stage 25, the distal part of a digit stage 32, the interdigit region stage 32 and a heart stage 32 (Fig. 19A). Primers were designed that spanned two exons (from exons 3 and 4 of *Vgl1*, 2 and 3 of *Wnt3a* and 3 and 4 of *Fgf8*) so that amplification from genomic DNA could be discriminated from the cDNA fragment of interest. Three sets of primers were used, one that would amplify a fragment of the *Vgl1* gene (249 base pair (bp)), as well as one pair for *Wnt3a* (482 bp) and one for *Fgf8* (376 bp) (Fig.19B). The RT-PCR experiments were carried out in multiplex, so that all three primer sets were used in the same reaction. This enabled the amplification of a fragment of all three genes and a comparison of the expression of *Vgl1* with that of *Wnt3a* and *Fgf8*, two genes that are required for AER formation and function (as discussed in Introduction) for each RNA sample. Expression of *Wnt3a* is first detected by whole-mount *in situ* hybridization in the ectoderm covering the LPM of the prospective limb-forming region at stage 15 (Kengaku et al., 1998). Later, at stage 17, once the limb bud has formed *Fgf8* is expressed in the ectoderm cells of the pre-AER (Martin, 1998).

By RT-PCR, I detect the expression of *Vgl1* and *Wnt3a* in the prospective limb-forming LPM of stage 14 and 16 embryos (Fig. 19B, lanes 2 and 3). The larger band between 1033bp and 653bp is likely to be from the amplification of genomic DNA of *Vgl1*, which from annotation of the genomic sequence I predict to produce a fragment of 844bp. The expression of *Wnt3a* at stage 14 is earlier than I could detect by whole-mount *in situ* hybridization and that has been previously described (Kengaku et al., 1998). This is probably due to the fact that

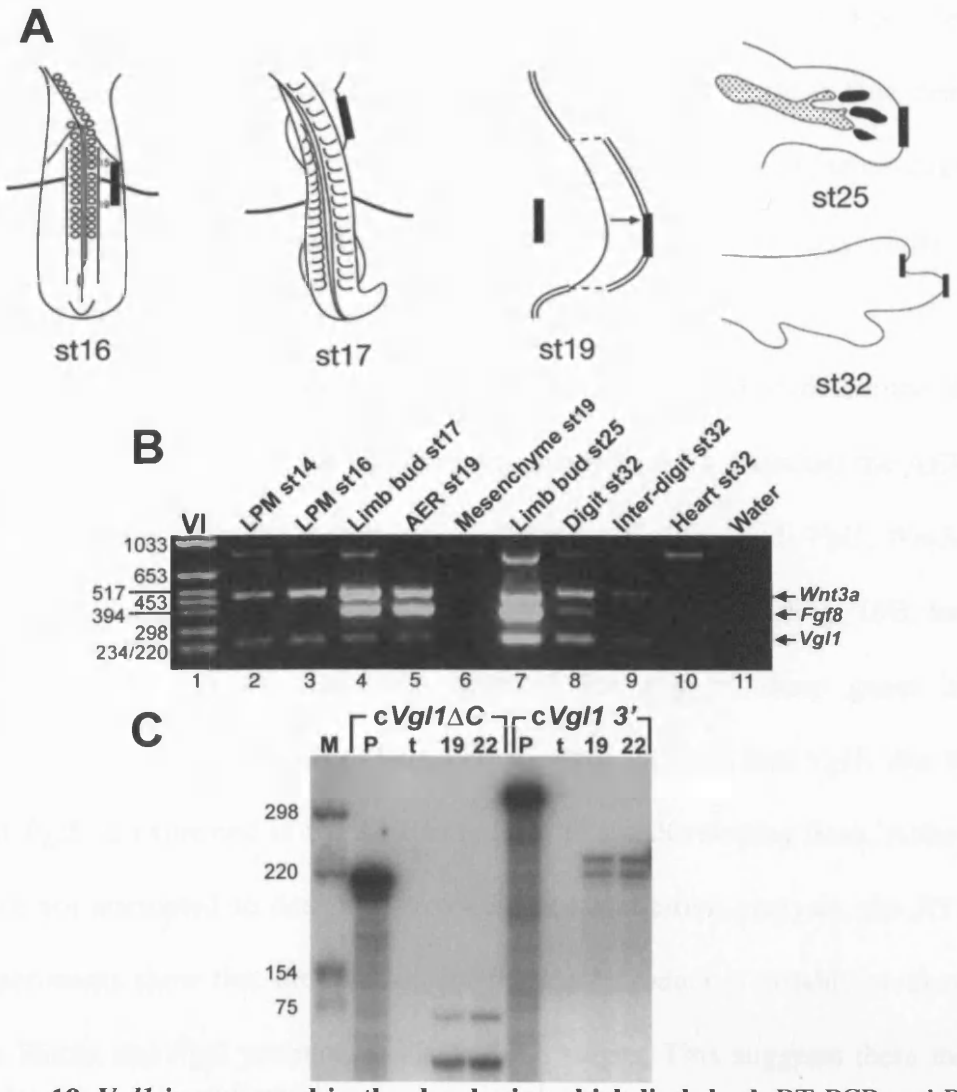

Figure 19. *Vgl1* is expressed in the developing chick limb bud. RT-PCR and RNase protection assay analysis shows that *Vgl1* is expressed in chick limb, from early stages of development. (**A**) Schematic of where the tissue was dissected from to extract RNA for the RT-PCR experiment. Shaded black boxes show where tissue was dissected from; LPM adjacent to somites 15 and 19 of a stage 14 and 16 embryo, a limb bud from a stage 17 embryo, AER and limb mesenchyme from a stage 19 embryo, distal part of a limb from a stage 25 embryo, the distal digit region, interdigit region and heart from a stage 32 embryo. (**B**) RT-PCR with chick RNA using primers for *Wnt3a* (482bp), *Fgf8* (376bp) and *Vgl1* (249bp). *Vgl1* and *Wnt3a* are expressed in the LPM at stages 14 and 16. *Vgl1*, *Wnt3a* and *Fgf8* are expressed in a stage 17 limb bud and stage 19 AER/ectoderm, but not stage 19 limb mesenchyme. *Vgl1*, *Wnt3a* and *Fgf8* are expressed at high levels in stage 25 limb bud and the digit of a stage 32 limb, but at low levels of the interdigit area of a stage 32 limb. No expression is seen in a stage 32 heart or water control. (**C**) RNase protection assay demonstrating *Vgl1* (c*Vgl1*Δ*C* and c*Vgl1 3'*) is expressed in stage 19 and stage 22 limb buds. LPM=lateral plate mesoderm.

RT-PCR is a much more sensitive method than whole-mount RNA *in situ* hybridisation. In a stage 17 limb bud, the expression of *Fgf8* is first detected, shown by the376bp product produced (Fig. 19B, lane 4). At the same stage, the intensity of the *Wnt3a* product has increased, while the intensity of the *Vgl1* product remains the same (Fig. 19B, lane 4).

To further characterize the expression of *Vgl1* and to determine if it is specifically expressed in the ectoderm or mesenchyme I dissected the AER and ectoderm away from the mesenchyme of a stage 19 limb bud. *Vgl1*, *Wnt3a* and *Fgf8* are all expressed in the AER and ectoderm preparation (Fig. 19B, lane 5). However, there is no expression detected for any of these genes in the mesenchyme preparation (Fig. 19B, lane 6). This suggests that *Vgl1*, like *Wnt3a* and *Fgf8*, is expressed in the AER/ectoderm of the developing limb. Although I have not attempted to design a protocol for quantitative analysis, the RT-PCR experiments show that the intensity of the *Vgl1* product is notably weaker than the *Wnt3a* and *Fgf8* products at all of these stages. This suggests there may be less *Vgl1* transcripts present, compared to *Wnt3a* and *Fgf8*. At stage 25, *Vgl1*, *Wnt3a* and *Fgf8* are all still expressed in the limb bud (Fig. 19B, lane 7). At stage 32 in the chick, the AER of the limb starts to regress and AER marker genes, such as *Fgf8*, are downregulated. The AER regresses first in the interdigit areas of the handplate and then later in the region of the AER that covers the digits. To distinguish if *Vgl1* is downregulated as the AER regresses, ectoderm and mesenchyme was dissected from the interdigit area and the distal most part of the digit of a stage 32 limb. *Vgl1*, *Wnt3a* and *Fgf8* are all expressed in the stage 32 digit preparation from the region overlying the digit (Fig. 19B, lane 8), while the intensity of the bands of these genes is much lower in the interdigit area (Fig.

19B, lane 9). This suggests that *Vgl1*, along with *Wnt3a* and *Fgf8*, is downregulated in the interdigit region as the AER regresses. Expression of *Vgl1*, *Wnt3a* and *Fgf8* are all absent in a stage 32 heart preparation (Fig. 19B, lane 10). This is consistent with previous data showing that *VGL1* is not expressed in foetal heart tissue (Vaudin et al., 1999). No expression is seen in the control RT-PCR that contained only water (Fig. 19B, lane 11).

An RNase protection assay (RPA) was used to confirm the expression of *Vgl1*, as it is a specific and quantitative method of analysis. For the RPA, I used two *Vgl1* radiolabelled probes, c*Vgl1*ΔC and c*Vgl1 3'* (see Materials and Methods for details). Total RNA preparations from stage 19 and 22 limb buds were quantified and equal amounts used to hybridize with each probe. Both *Vgl1* probes produce protected bands in limb buds from stage 19 and 22 embryos, with a slightly stronger band present at stage 22 (Fig. 19B). This data, together with the RT-PCR results, indicate that *Vgl1* is expressed in the developing chick limb from stage 14 and at later stages is expressed in the ectoderm/AER of the limb.

3.10 *Vestigial-like1* is expressed in ectodermal cells of the chick embryo

The RT-PCR and RPA results show that *Vgl1* is expressed in the developing limb, but it may be expressed at very low levels or in a small number of cells. To try to enhance the sensitivity of the whole-mount *in situ* hybridisation protocol I modified it in several ways (see Materials and Methods for details). First, instead of using just one digoxigenin (DIG) labelled probe against *Vgl1*, I used three anti-sense RNA probes that were directed against different regions of

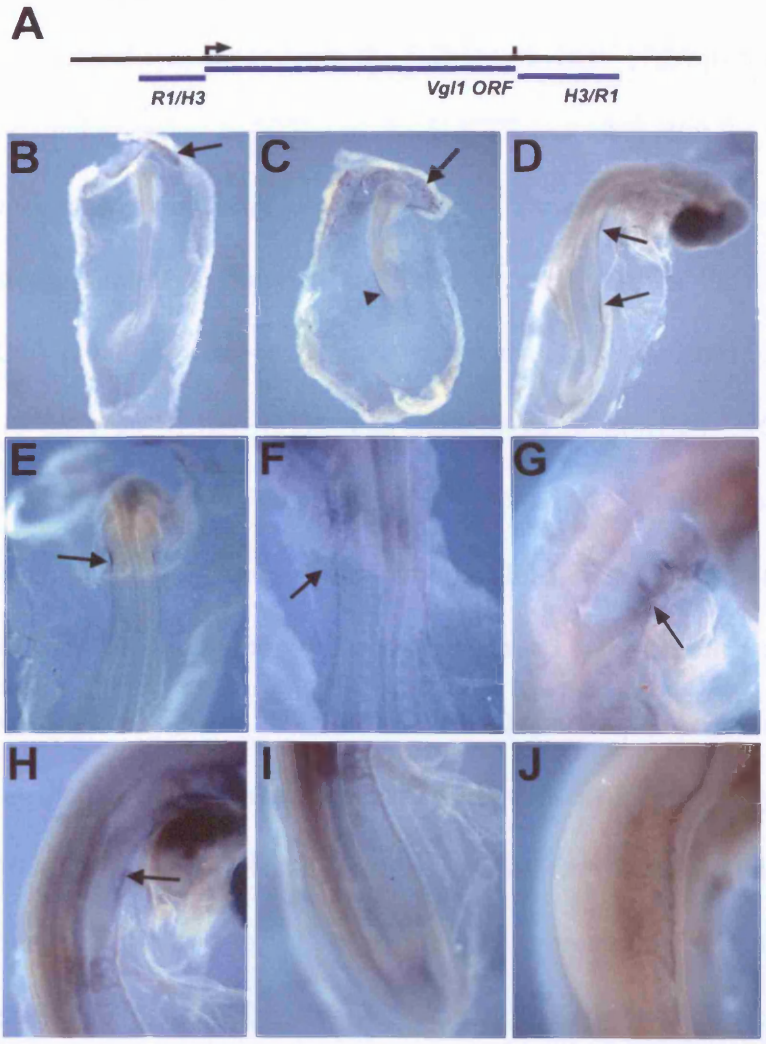

Figure 20. *Vgl1* is expressed in the ectoderm covering the developing chick limb. Whole-mount *in situ* hybridization of *Vgl1* in the developing chick embryo. (**A**) Schematic of the *Vgl1* gene, with the three regions used to make anti-sense RNA *in situ* hybridisation probes shown in blue. The *R1/H3* probe is 180bp of 5' UTR, *Vgl1 ORF* is 729bp of the full protein coding sequence and *H3/R1* is 305bp of 3'UTR. Expression is first detected in the area pellucida and the area opaca, the ectoderm that surrounds the embryo at stage 10 (arrow in **B**), and continues to be expressed there at stage 13 (**C**, arrowhead shows area pellucida expression adjacent to the embryo and arrow shows transcripts in the area opaca). At stage 15, *Vgl1* transcripts are detected in the ectoderm covering the embryo including the limb-forming region and trunk (**D**, arrows show detail in **E** and **F**). At stage 16, expression of *Vgl1* is seen in the distal region of the pharyngeal arches (arrow in **G**). Low levels of *Vgl1* expression in the forelimb-forming (**H**, arrow) and hindlimb-forming region (**I**) of a stage 16 embryo. (**J**) At stage 21, *Vgl1* transcripts are detected in the ectoderm of the limb. All views are dorsal, except (**F**) and (**G**) are right lateral, (**I**) is ventral.

the mRNA. One probe was designed against 180bp of UTR 5' of the initiator methionine, a second was made from the full-length ORF (729bp) template, and a third was complementary to 305bp of the 3' UTR just after stop the codon (Fig. 20A). Second, to enhance the sensitivity of the probes, I increased the amount of digoxigenin-conjugated UTP in the labelling mix used to make the *Vgl1* probes. The DIG RNA labelling mix we routinely use is made up of a ratio 35% labelled DIG-UTP to 65% unlabelled UTP. The percentage of labelled DIG-UTP was increased, and a mix of 60% labelled DIG-UTP and 40% unlabelled UTP was used (see Material and Methods for details). Third, the probes were purified using ProbeQuant G-50 columns to remove unincorporated labelled nucleotides. This reduces the amount of background that can occur due to unincorporated DIG-UTP in the probe preparation that is not washed out of embryonic tissue when developing the whole-mount *in situ* hybridisation. The protocol was also modified to prevent damage to cells that might be more sensitive to proteinase K treatment, such as ectodermal cells, by reducing the concentration and time of incubation in this enzyme.

When this procedure was followed, using no proteinase K treatment, a signal was detected for *Vgl1* in chick embryos (Fig. 20). *Vgl1* transcripts are detected at stage 10 and stage 13 in the area pellucida and the area opaca, the ectoderm that surrounds the embryo (Fig. 20B and 20C arrows). At stage 13, weak expression is seen in the ectoderm adjacent to the trunk of the embryo (Fig. 20C arrowhead). At stage 15, *Vgl1* expression can be detected over the dorsal surface of the embryo, including the LPM of the limb-forming regions (Fig. 20D). Higher magnification of the embryo at this stage shows there is expression along much of the dorsal surface of the trunk that decreases at the

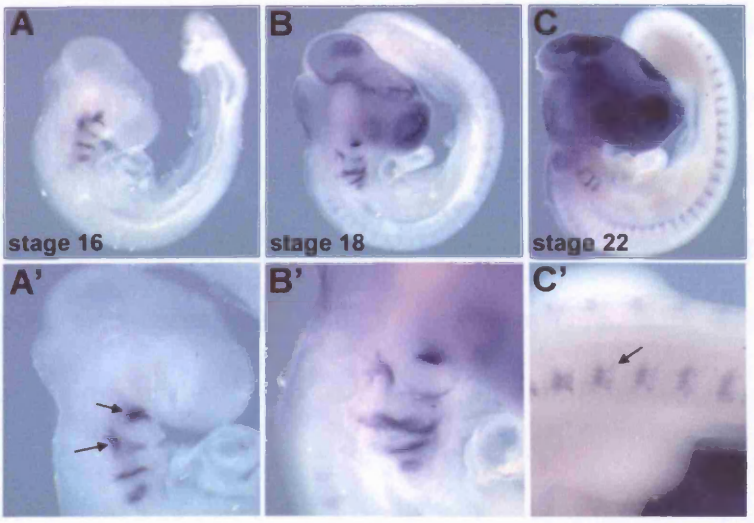

Figure 21. *Vgl2* is expressed in the pharyngeal arches and somites of chick embryos. (**A**) At stage 16, *Vgl2* expression is detected in the pharyngeal arches, (**A'**) close-up of pharyngeal arches (arrows). (**B**) By stage 18, transcripts increase in the pharyngeal arches (**B'** detail), and start to be detected in the somites. (**C**) At stage 22, *Vgl2* expression is still found in the pharyngeal arches and increase in the somites. (**C'**) Detail of somite expression, indicated by arrow. Right lateral views in all cases.

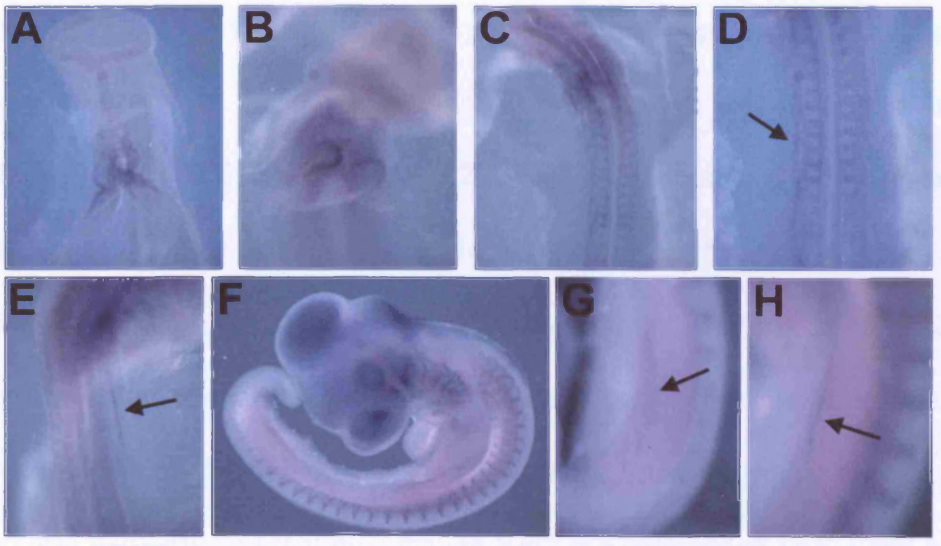

Figure 22. *DTEF1* is expressed in the developing heart and limb ectoderm. (**A**) Expression of *DTEF1* in the developing heart of a stage 10 embryo. At stage 14, expression is still in the heart (**B**), in the borders of the somites and adjacent in the lateral plate mesoderm (LPM) (**C** and detail **D**, arrow marks expression in the adjacent LPM). (**E**) At stage 16, *DTEF1* transcripts are detected in the ectoderm overlying the LPM of the limb-forming region. (**F**) Expression in the somites of a stage 20 embryo. Detail of stage 20 hindlimb (**G**) and forelimb (**H**) with expression of *DTEF1* in the AER/ectoderm. (**A**, **B**) ventral views, (**C**, **D**, **E**) dorsal views, (**F**) left lateral, (**G**, **H**) distal view of limb.

head (Fig. 20E and 20F). *Vgl1* transcripts are detected in the distal region of pharyngeal arches of stage 16 embryos (Fig. 20G). At stage 16, low levels of expression are also seen over the limb-forming region of the forelimb (Fig. 20H) and hindlimb (Fig. 20I). The expression of *Vgl1* is still present in a stage 21 limb bud, and appears to be expressed in the ectoderm (Fig. 20J). This low level staining over regions of the torso was not seen in control probes, such as *Wnt3a* and *Fgf8*.

Whole-mount *in situ* hybridization for *Vestigial-like2* (*Vgl2*) was performed using a chick EST (ChEST976p9) as a template to make an anti-sense ribo-probe. *Vgl2* expression is observed from stage 16 in the pharyngeal arches, where it is confined to the posterior edge of each arch (Fig. 21A and 21A'). At stage 18, *Vgl2* expression in the pharyngeal arches appears more robust and remains restricted to the posterior side. Transcripts are just detectable in the somites (Fig. 21B and 21B'). By stage 22, *Vgl2* expression begins to decrease in the pharyngeal arches, while transcript levels increase in the somites, being more prominent dorsally (Fig 21C and 21C'). Analysis by others (Maeda et al., 2003) have shown that the expression in the somites is confined to the myotome, and expression later in the limb buds is restricted to the muscle forming regions. This report also demonstrated that mammalian Vgl2 is a cofactor of TEF-1 and MEF2 transcription factors and promotes skeletal muscle differentiation (Mielcarek et al., 2002; Maeda et al., 2003). Since I have not detected *Vgl2* at early stages of vertebrate limb development, and it appears to be only involved in the developing muscle of the limb, I have not carried out any further characterization of this gene.

3.11 *DTEF1* is expressed in the heart and ectodermal cells of the chick embryo

Drosophila vestigial and vertebrate *vestigial-like* genes have been shown to interact with members of the Transcription Enhancer Factor (TEF) family of transcription factors and that this complex activates the expression of target genes (Vaudin et al., 1999; Maeda et al., 2003). To study if any members of the TEF's are expressed in the developing vertebrate limb, I obtained EST clones for the three identified chick *TEF* genes, *NTEF1* (ChEST332b16), *RTEF1* (ChEST905i10) and *DTEF1* (ChEST371b16), from the chick BBSRC EST database (http://www.chick.umist.ac.uk) and performed whole-mount *in situ* hybridisation.

I identified one of these genes, *DTEF1*, that is expressed in a similar fashion to *Vgl1* in the vertebrate limbs. *DTEF1* is first expressed at stage 10 in the developing heart of a chick embryo (Fig. 22A). At stage 14, expression is still strong in heart (Fig. 22B), and can be seen at the borders of the developing somites and in the adjacent LPM (Fig. 22C and 22D detail). At stage 16, *DTEF1* transcripts are detected in the limb-forming region of the forelimb and hindlimb (arrow in Fig. 22E). At stage 20, the expression of *DTEF1* persists in the somites, and weak expression is observed in the AER of the forelimb and hindlimb, while expression is downregulated in the heart (Fig. 22F, and detail 22G and 22H).

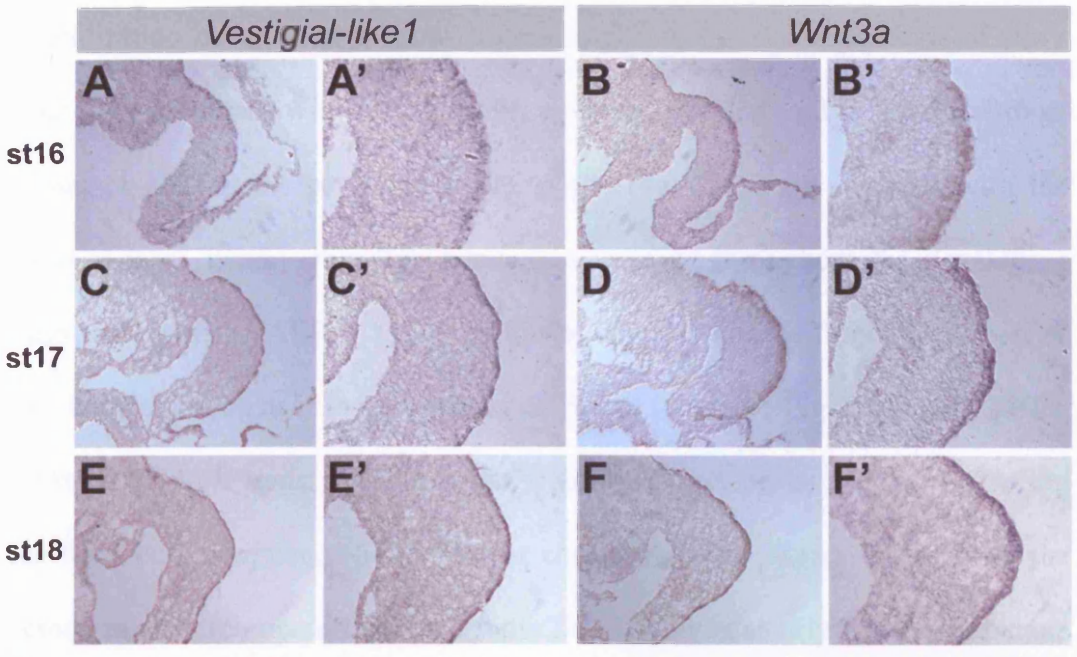

Figure 23. *Vestigial-like1* is expressed in a sub-population of limb ectoderm cells. Frozen cryostat section *in situ* hybridisation on chick limb buds processed with *Vestigial-like1* (*Vgl1*) and *Wnt3a* probes. At stage 16, *Vgl1* is expressed in the limb ectoderm (**A** and **A'** detail), as is *Wnt3a* (**B** and **B'** detail). At stage 17, *Vgl1* is expressed in a sub-population of cells in the distal part of the limb ectoderm, including the ectoderm of the forming AER (**C** and **C'** detail), while *Wnt3a* is expressed throughout the limb ectoderm and forming AER (**D** and **D'** detail). At stage 18, *Vgl1* expression is clearly seen in just the most distal cells of the limb ectoderm (**E** and **E'** detail), while *Wnt3a* is still expressed throughout the AER and dorsal and ventral ectoderm of the limb (**F** and **F'** detail). (**A**, **B**, **C**, **D**, **E**, **F**) 20X magnification, (**A'**, **B'**, **C'**, **D'**, **E'**, **F'**) 32X magnification.

3.12 *Vestigial-like1* is expressed specifically in the periderm

Whole-mount *in situ* hybridisation with *Vgl1* and *DTEF1* probes have shown they appear to be expressed in the ectoderm of the limb-forming region and ectoderm of the limb bud. To confirm this, I carried out RNA *in situ* hybridization on cryostat sections. Interestingly, in transverse sections of early limb buds processed with a *Vgl1* probe, expression is detected in the distal-most subset of cells at the periphery of the AER (Fig. 23). This contrasts with the expression of *Wnt3a* (Fig. 23), which is expressed throughout the developing limb ectoderm and AER. At stage 16, expression of *Vgl1* is throughout most of the limb ectoderm, as is the expression of *Wnt3a* (compare Fig. 23A' with 23B'). At stage 17, *Vgl1* transcripts are in the superficial layer of the ectoderm covering the limb bud, compared to *Wnt3a* that continues to be expressed in all of the ectoderm cells (compare Fig. 23C' with 23D'). This is clearly observed at stage 18, where *Vgl1* expression is still only in a sub-population of the outermost ectoderm cells overlying the limb bud, while *Wnt3a* is expressed throughout the ectoderm and maturing AER cells of the limb (compare Fig. 23E' with Fig. 23F').

The ectoderm originates as a single layer that forms two layers, an outer layer, called the periderm, and a basal layer. The section *in situ* hybridisation data suggests that *Vgl1* could be specifically expressed in the periderm. To analyse this further, I counterstained section *in situ* hybridisations that had been processed with *Vgl1*, *Fgf8* and *DTEF1* with DAPI nuclear stain. The outer periderm cells have thin, squamous cell morphology, while the ectoderm cells underneath have an irregular, columnar epithelium morphology

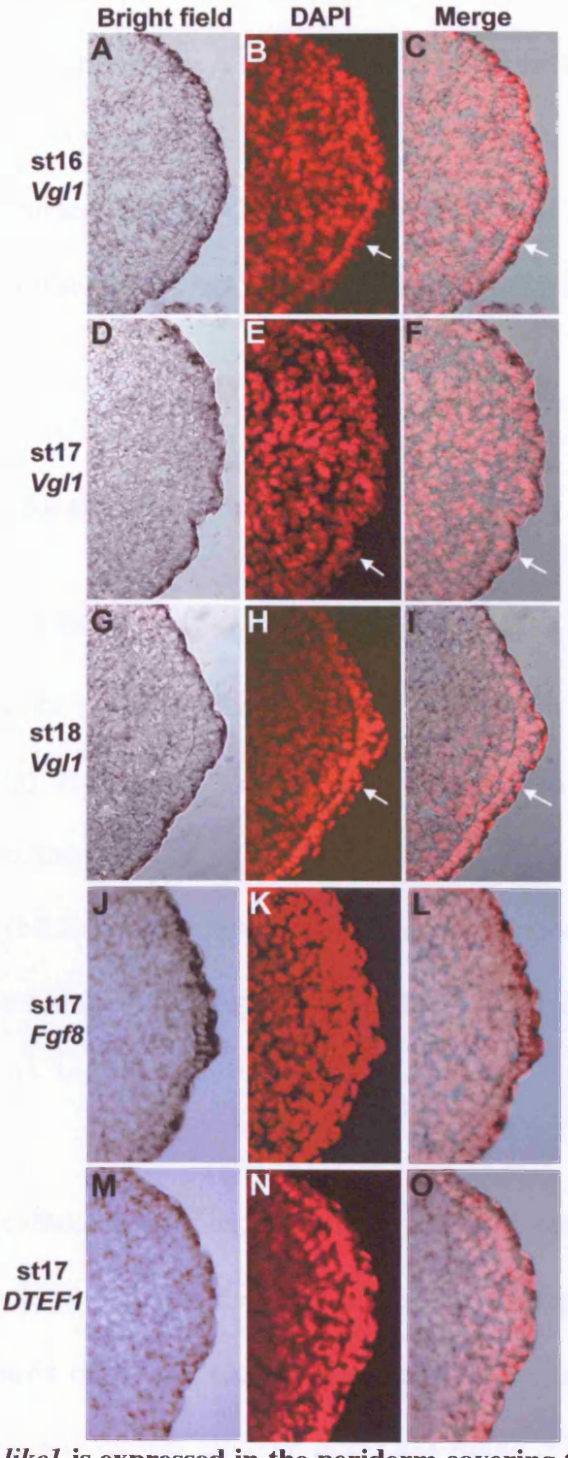

Figure 24. *Vestigial-like1* is expressed in the periderm covering the developing limb bud. At stage 16 (**A**, **B**, **C**), stage 17 (**D**, **E**, **F**) and stage18 (**G**, **H**, **I**) *Vestigial-like1* is expressed in the outermost layer of the ectoderm, the periderm. This is in comparison to *Fgf8*, which is expressed in the pre-AER cells at stage 17 (**J**, **K**, **L**). At stage 17, *DTEF1*, a potential *Vgl1* co-factor, is also expressed in the periderm covering the limb ectoderm. Bright field (**A**, **D**, **G**, **J**, **M**), DAPI nuclear stain (**B**, **E**, **H**, **K**, **N**), merge of bright field and DAPI. (**C**, **F**, **I**, **L**, **O**) All 40X magnification, just showing the distal tip of the limb bud. White arrows indicate cells expressing *Vgl1* in the periderm.

compared to the columnar epithelial cells underneath (Fig. 24A-24I). Most likely these cells represent the periderm. A comparable stage 17 section processed with *Fgf8* shows there is expression in the outer layer of cells and the columnar epithelial cells underneath (Fig. 24J-24L). At stage 17, *DTEF1* is only expressed in the cells on the surface of the ectoderm, in an apparently identical fashion to *Vgl1*.

3.13 Vestigial-like1 localises to the nucleus

Results from work on *Drosophila* have demonstrated that *vestigial* is a nuclear, transcriptional activator protein (Vaudin et al., 1999; Halder and Carroll, 2001; MacKay et al., 2003). However, *vg* is normally expressed in the cytoplasm and only translocates to the nucleus on binding to *sd*, which contains a nuclear localization signal (NLS). A putative NLS and nuclear export signal have been identified in the C-terminal domain of the Vestigial-like2 sequence (Maeda et al. 2002).

To determine the cellular localization of the Vestigial-like1 protein an eGFP fusion construct (*pcDNA-λ-hinge-eGFP*) was generated (Fig. 25A). Studies of the cellular localization of the protein will provide clues to the function of Vgl1. Once *Vestigial-like1* was cloned into the *pcDNA-λ-hinge-eGFP* construct (Fig. 25B) the cellular localization of Vestigial-like1 protein can be visualized by observing where the GFP is in the cell.

Cos-1 and DF1 cells were transfected with either the *Vestigial-like1-eGFP* fusion construct or a control *eGFP* construct. The eGFP protein does not

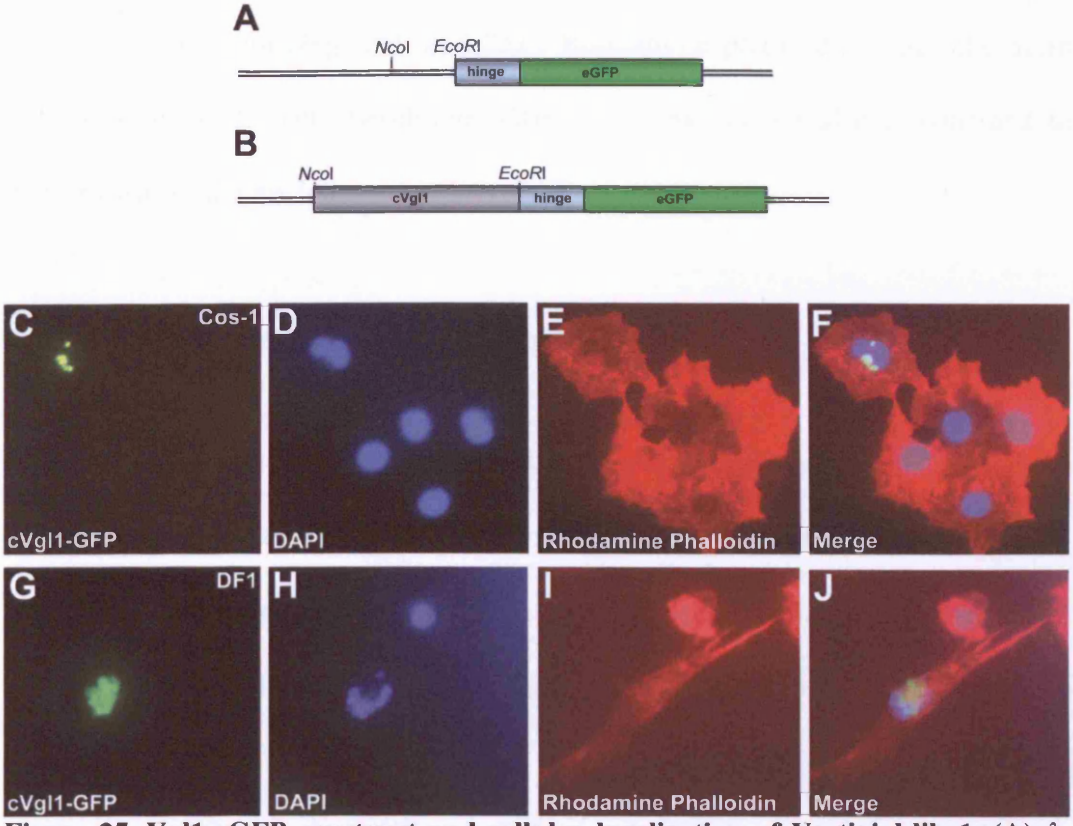

Figure 25. Vgl1-eGFP construct and cellular localization of Vestigial-like1. (**A**) *λ-hinge* and *eGFP* were cloned into *pSlax* so that the gene of interest could be cloned into the *Nco*I/*Eco*RI site, and produce an in-frame fusion construct (see Materials and Methods for details). (**B**) Full-length chick *Vestigial-like1* was cloned into the *Nco*I/*Eco*RI site of *pSlax-λ-hinge-eGFP*. The c*Vgl1-λ-hinge-eGFP* fragment was digested using *Cla*I, blunt-ended with a klenow fill-in, and then ligated into the *pcDNA* vector. The *pcDNA-cVgl1-λ-hinge-eGFP* construct was transfeced into Cos-1 and DF1 cells. (**C**, **G**) Vgl1-eGFP fluorescence in Cos-1 and DF1 cells respectively. (**D**, **H**) DAPI staining has been used as a nuclear stain and (**E**, **I**) Rhodamine Phalloidin to identify the actin cytoskeleton. (**F**, **J**) Merge of Vgl1-eGFP with DAPI and Rhodamine Phalloidin staining.

have a nuclear localization signal, so as expected, Cos-1 and DF1 cells transfected with *eGFP* express GFP throughout the cytoplasm (data not shown). In both the Cos-1 and DF1 transfected cells there is localisation of the Vestigial-like1-eGFP fusion construct in the nucleus, shown by the co-localization with the DAPI, nuclear stain (Fig. 25F and 25J). Rhodamine phalloidin stains the actin cytoskeleton of the cell membrane. Often Vestigial-like1-eGFP is confined to regions within the nucleus.

3.14 Retroviral constructs of chick *Vestigial-like1*

To analyze the role of *Vestigial-like1* (*Vgl1*) in the developing limbs, I used the chick retroviral system to misexpress various forms of *Vgl1*. I produced RCAS viruses of full-length *Vgl1* (*Vgl1-FL*), two putative dominant-negative forms *Vgl1ΔC* and *Vgl1-Engrailed*, and a putative dominant-active form, *Vgl1-VP16*$_4$ (Fig. 26).

Vgl1-ΔC is a truncated form of *Vestigial-like1* that contains the scalloped-binding domain (SDB), but with a large portion of the C terminal removed (see Materials and Methods for details and Fig. 26). The *Vgl1-Engrailed* construct contains *Vgl1-ΔC*, with the *Drosophila Engrailed* repression domain fused in-frame at the C terminus (Jaynes and O'Farrell, 1991). The putative dominant-active form, *Vgl1-VP16*$_4$, contains four VP16 activation domains, separated by λ hinges, fused to *Vgl1-ΔC* (Ohashi et al., 1994). I have misexpressed these constructs in the ectoderm of the developing chick limb. For Vestigial to activate gene transcription it must bind to Scalloped, which contains a DNA binding domain. Since it has shown that human *VESTIGIAL-LIKE1* (*TONDU*) can

substitute for *vestigial* in wing formation, it has been proposed that Vestigial-like1 may act in a similar fashion with the vertebrate orthologues of Scalloped, the TEF's. Misexpressing the *Vgl1-ΔC* construct is predicted to act as a dominant-negative as it will bind to, and sequester the endogenous TEF's, but will not activate transcription of target genes. The *Vgl1-Engrailed* construct is predicted to act in a similar fashion to *Vgl1-ΔC*, but should actively repress transcription of target genes via the *Engrailed* repression domain. The $VP16_4$ domain is a herpes simplex virus activation domain that has been shown, when multimerised, acts synergistically to increase the potency of transcriptional activators (Ohashi et al., 1994). The *Vgl1-*$VP16_4$ form is therefore predicted to activate transcription of *Vestigial-like1* target genes.

3.15 Misexpression of putative dominant-negative *Vestigial-like1* in the developing chick limb

To enable infection of the limb ectoderm, the retroviral supernatants were injected underneath the vitelline membrane of stage 10 embryos over the future limb-forming region of the lateral plate mesoderm. This method has previously been used successfully to infect the ectoderm of limb buds (Laufer et al., 1997). The injected embryos where then allowed to develop to the desired stage, harvested and analysed.

To confirm that I was infecting the ectoderm of the limb and to check the viral spread, embryos were injected with *Vgl1-FL* virus and then processed by whole-

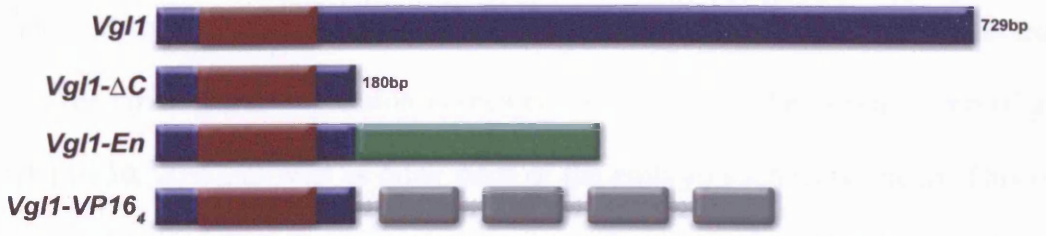

Figure 26. *Vestigial-like1* retroviral constructs. The full-length chick *Vestigial-like1* (*Vgl1*) retroviral construct contains all 729bp of the protein coding sequence. The truncated *Vgl1-ΔC* construct contains the first 180bp, which contains the scalloped binding domain (SBD), shaded in red. The *Vgl1-Engrailed* (*Vgl1-En*) and *Vgl1-VP16$_4$* constructs contain the same 180bp as the *Vgl1-ΔC* construct fused to the either the *Drosophila Engrailed* repression domain, shaded green, or *VP16* activation domains, shaded grey. (*Vgl1*, *Vgl1-ΔC* and SBD drawn to scale, *Engrailed* and *VP16$_4$* not to scale).

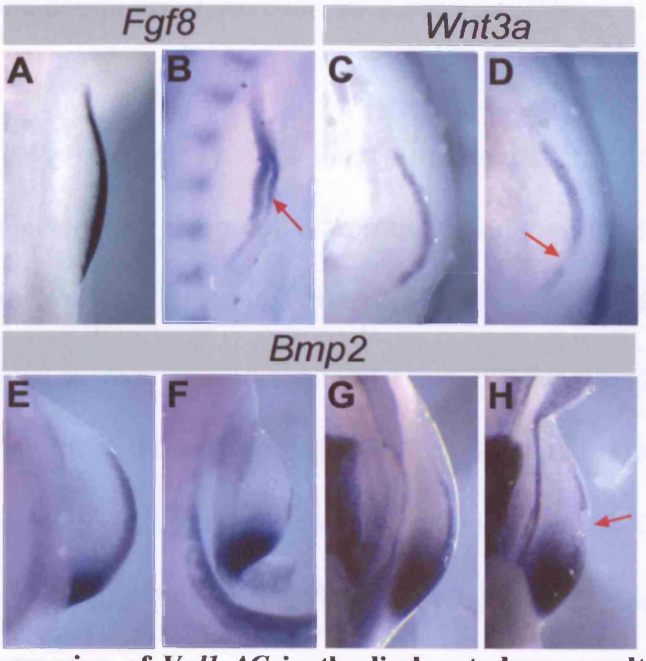

Figure 27. Misexpression of *Vgl1-ΔC* in the limb ectoderm results in gaps in the AER and limb truncations. Control limb buds (**A**, **C**, **E**, **G**), *Vgl1-ΔC* infected limb buds (**B**, **D**, **F**, **H**). There is a large stripe of *Fgf8* expression missing in the AER of a stage 19 *Vgl1-ΔC* infected limb bud (**B**), compared to the control limb (**A**). In a stage 20 limb, there is a gap in the expression of *Wnt3a* (**D**), compared to the control (**C**). Decreased *Bmp2* expression in the AER of a stage 20 forelimb (**F**) and hindlimb (**H**), compared to the control (**E**) and (**G**) respectively. Note the smaller size of the limb bud in the injected limb (**F**), compared the contra-lateral control (**E**). (**A**, **B**, **E**, **F**) dorsal views, (**C**, **D**, **G**, **H**) ventral views.

mount *in situ* hybridisation with an *RCAS* probe. This probe is specific for the retroviral transcript and enables the detection of cells that have been infected with the virus. *RCAS* expression is seen covering most of the injected limb (Fig. 29E) (6/30; 20%), as well as other parts of the embryo such as the heart. This is presumably due the spread of the virus after injection. A transverse section of one of these limb buds clearly shows that the virus has infected the ectoderm, and no infected cells are found in the mesenchyme (arrowheads in Fig. 29F). This is consistent with observations by others that the RCAS virus cannot infect cells across the basement membrane between ectoderm and mesenchyme in the limb (Laufer et al., 1997). However, the *RCAS* staining in the ectoderm is patchy, demonstrating that not all ectoderm cells have been infected.

To determine if *Vgl1* is involved in the formation or function of the AER, embryos were injected with the putative dominant-negative viral construct *Vgl1-ΔC* and processed for gene molecular markers of the AER. I first analysed the expression of *Fgf8*, a gene that is required for AER function and normal PD outgrowth of the limb. Following injection of *Vgl1-ΔC* into the ectoderm overlying the prospective limb region there is a decrease in the levels of *Fgf8* in the AER of a stage 19 limb bud (Fig. 27B) (24/112; 23%), compared to a control limb (Fig. 27A). There is a stripe of *Fgf8* expression missing in the injected limb, suggesting that there is a gap in the AER. A stage 20 limb bud injected with *Vgl1-ΔC* and processed for *Wnt3a*, a gene required for AER formation and maintenance, has a gap in the expression in the AER, compared to an uninjected limb (compare Fig. 27D with 27C) (12/56; 21%). *Vgl1-ΔC* injected embryos processed with *Bmp2* have similar gaps in the expression in the AER in fore- and

hindlimbs (Fig. 27E-27H) (5/28; 18%). The injected limbs display gaps in the AER and normal proximal-distal outgrowth is truncated, compared to uninjected controls (compare Fig. 27F with 27E). AER removal experiments in the chick and deletion of *Fgf* genes from the AER of mouse embryos has demonstrated the importance of this structure. These experiments have shown that signals emanating from the AER, namely the FGFs, are required for AER function and removal of these genes results in proximal-distal truncations of the limb. The gaps in the expression of AER marker genes and the truncated limbs following the misexpression of the putative dominant-negative *Vgl1* construct are consistent with a disruption in AER function, and suggests that AER formation or maintenance has been impaired.

Misexpression of *Vgl1-Engrailed* (*Vgl1-En*) at stage 10, a second putative dominant-negative construct, and harvested at stage 19 shows a decrease in *Fgf8* expression along a large part of the AER (Fig. 28B) (28/88; 32%), compared to a control uninjected limb (Fig. 28A). At later stages (st 22), expression of *Fgf8* is absent in a central stripe at the distal tip of the AER (Fig. 28D) (10/57; 19%). Embryos injected with *Vgl1-En* and processed with *Wnt3a* (17/62; 27%) and *Bmp2* (14/58; 24%) probes have gaps in their expression in the AER, consistent with the observed disruption in *Fgf8* expression in the ridge. At stage 20, *Wnt3a* is expressed in the AER along the anterior-posterior length of the distal tip of the limb (Fig. 28E). A *Vgl1-En* injected forelimb has a patch of *Wnt3a* expression missing at the posterior end of the AER (Fig. 28F), compared to the contra-lateral control (Fig. 28E). *Bmp2* is also normally expressed throughout the AER (Fig.

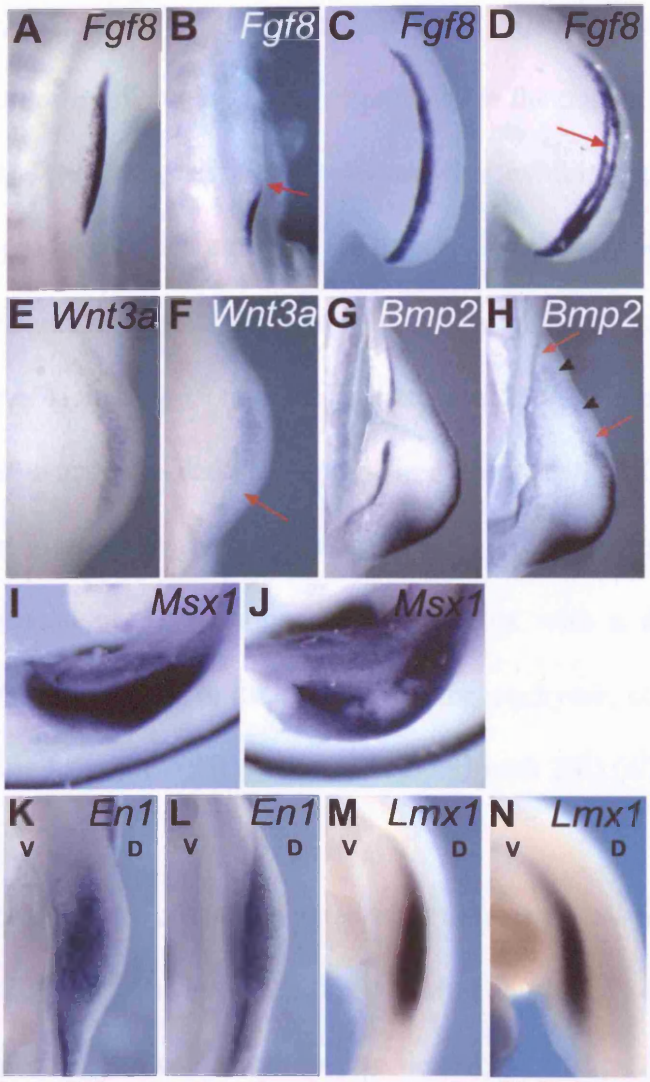

Figure 28. Infection of the putative dominant-negative *Vgl1-Engrailed* in the limb ectoderm results in gaps in the expression of markers of the AER. Control limbs buds (**A**, **C**, **E**, **G**, **I**, **K**, **M**), *Vgl1-Engrailed* (*Vgl1-En*) injected limbs (**B**, **D**, **F**, **H**, **J**, **L**, **N**). Stage 18 *Vgl1-En* injected limb bud has a large gap in the expression of *Fgf8* in the AER (**B** arrow), compared to a control (**A**). A central stripe of *Fgf8* expression is missing (arrow **D**), compared to the control (**C**). There is a decrease in the expression of *Wnt3a* in a stage 20 forelimb (arrow **F**), compared to a control (**E**). Expression of *Bmp2* in a control hindlimb (**G**). An infected stage 20 hindlimb has gaps in the expression of *Bmp2* (arrows **H**), but some patches of expression are still present (arrowhead **H**). A downregulation of *Msx1* expression in the distal mesenchyme of an injected limb (**J**), compared to a control (**I**). The ectodermal ventral marker *En1* (**L**) and the mesenchymal dorsal marker *Lmx1* (**N**) are unaffected after infection with *Vgl1-En*, compared to control limbs (**K**, **M** respectively). Note the injected limb is truncated (**L**), compared to the contra-lateral control (**K**). (**A**, **B**, **M**, **N**) Dorsal views, (**C**, **D**, **E**, **F**, **G**, **H**, **K**, **L**) ventral views, (**I**, **J**) distal views. D=dorsal, V=ventral.

28G). However, a stage 20 hindlimb that has been injected with *Vgl1-En* has patchy expression of *Bmp2*, with gaps in expression in the posterior region of the ridge (Fig. 28H). This suggests these embryos also exhibit gaps in the AER, similar to those produced when embryos are infected with *Vgl1-ΔC*.

Msx1, a homeobox gene expressed in the distal limb mesenchyme is a sensitive marker of signalling from the AER (Ros et al., 1992). The expression of *Msx1* is dependent on ridge-derived signals, and specifically FGFs can restore *Msx1* expression after AER removal (Vogel et al., 1995; Wang and Sassoon, 1995). Misexpression of *Vgl1-En* results in embryos with a decrease in the expression of *Msx1* expressed in the distal limb mesenchyme, consistent with a defect in signalling from the AER (compare Fig. 28J with 28I) (4/25; 16%).

Disruptions in the AER are often associated with defects in DV patterning of the limb (Laufer et al., 1997; Ahn et al., 2001; Barrow et al., 2003; Soshnikova et al., 2003). Gene molecular markers were used to determine if the DV patterning of the limb buds were affected after injection of the dominant-negative *Vgl1* constructs. *Engrailed1 (En1)* expressed in the ventral ectoderm and *Lmx1* in the expressed dorsal mesenchyme are required for DV patterning of the limb (Chen and Johnson, 1999). Embryos injected with the putative dominant-negative virus, *Vgl1-Engrailed*, exhibited no difference in the expression of either *En1* in the ventral ectoderm (Fig. 28L) (0/85) or *Lmx1* in the dorsal mesenchyme (Fig. 28N) (0/57), compared to the contra-lateral controls (Fig. 28K and 28M, respectively). The normal expression of *En1* and *Lmx1b* in the *Vgl1-Engrailed* injected limbs suggests that DV patterning is unaffected. Note that the injected limb (Fig. 28L) is truncated compared to the contra-lateral control (Fig. 28K) but the border of

En1 expression at the DV boundary appears to be the same in both limbs. This indicates that there is a decrease in ridge-derived signals to the underlying mesenchyme and suggests a disruption in the AER, but that the DV boundary is unaffected.

3.16 Misexpression of full-length and a putative dominant-active *Vestigial-like1* in the developing chick limb

An embryo injected with a putative dominant-active form of *Vestigial-like1*, *Vgl1-VP16*$_4$, has a truncated limb, compared to the uninfected control limb (Fig. 29B). This smaller limb bud has ectopic expression of *Fgf8* on the dorsal and ventral sides of the limb (Fig. 29B') (2/54; 4%). This indicates that normal AER function has been disrupted and AER-like cells are found in the dorsal and ventral ectoderm, based on the expression of *Fgf8* (Fig. 29B and 29B'). Misexpression of *Vgl1-VP16*$_4$ also results in limb buds that display a loss of *Fgf8* expression in the AER, similar to the phenotypes produced after injection of the putative dominant-negative constructs (shown with arrows in Fig. 29C) (7/54; 13%). After injection of the *Vgl1-FL* virus, a small number (2/62; 3%) of the embryos have a decrease in the expression of *Fgf8* (arrow in Fig. 29D).

3.17 Misexpression of the *Vgl1* constructs result in an early AER defect

The gaps produced in the AER after infection with the various *Vgl1* constructs could be due to an early defect in AER formation, or a later disruption in the maintenance of the AER. To try to distinguish between the two, embryos were either injected at stage 10 and harvested early during AER formation at stages 16

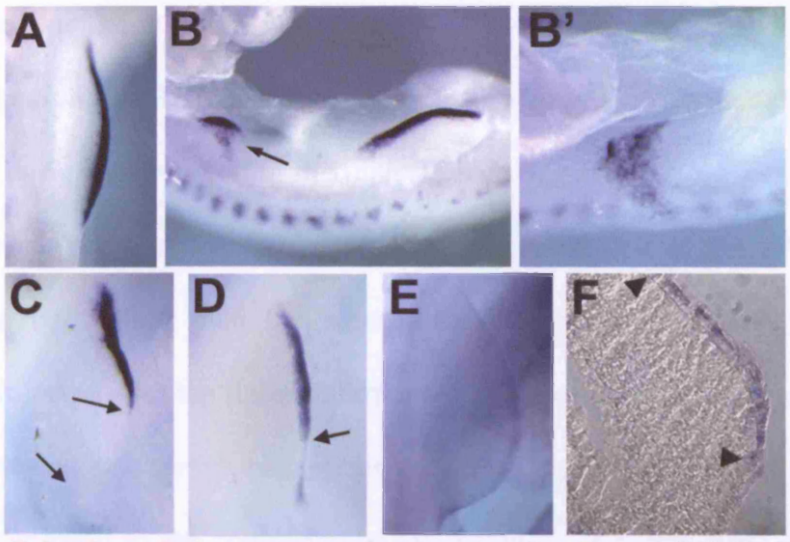

Figure 29. Injection of the putative dominant-active form of *Vgll*, *Vgll-VP16$_4$*, results in disruption in the AER. (**A**) *Fgf8* expression in a control limb. A limb bud injected with *Vgll-VP16$_4$* is truncated and *Fgf8* expressing cells are found dorsally and ventrally (**B**), and detail (**B'**). (**C**, arrows) A *Vgll-VP16$_4$* injected limb that has a large part of *Fgf8* expression missing from the posterior of the AER. (**D**, arrow) A limb injected with *Vgll-FL* also has part of *Fgf8* expression lost from the posterior of the AER. (**E**) A limb injected with *Vgll-FL* and then processed by *in situ* hybridisation with an *RCAS* probe. (**F**) A 10μm transverse wax microtome section of one of these limbs, showing infection of the limb ectoderm, indicated with the arrowheads. All dorsal views of limbs, except (**B**) right lateral view and (**B'**) distal view.

and 17, or they were injected after the AER had started to form at stage 16 and harvested at stage 21.

To analyse whether the embryos injected at stage 10 and harvested early had an AER defect they were processed for *Fgf8* and *Wnt3a*. Misexpression of *Vgl1-En* at stage 10 and harvested at stage 17 had a decrease in *Fgf8* expression, compared to the contra-lateral control (compare Fig. 30A with 30B) (12/76; 16%). The expression domain in the injected limb is smaller along the AP axis and thinner along the DV axis. A section of this embryo clearly demonstrates the reduction in *Fgf8* expression in the injected side of the limb (Fig. 30C, 30D and 30E). The ectoderm of the *Fgf8* expressing pre-AER cells of the infected limb appears to be thinner than the control side (compare Fig. 30D with 30E). Embryos injected with the putative dominant-negative *Vgl1-En* virus at the same stage, harvested at stage 16 and processed with *Wnt3a* have identical expression patterns compared to the contra-lateral control (Fig. 30F and 30G) (0/89). This data suggests that the defects in the AER caused by the misexpression of the *Vgl1* constructs, resulting in gaps in the AER, occur early in limb development when *Fgf8* is first expressed but after the onset of *Wnt3a* expression.

Misexpression of *Vgl1-En* in the limb ectoderm at stage 16, after AER induction, did not affect the expression of *Fgf8* in stage 21 embryos (Fig. 30H and 30I) (0/86). This suggests that *Vgl1* is not involved in the maintenance of the AER once it has formed. Analysis with the *RCAS* RNA *in situ* hybridisation probe of limb ectoderm injected with *Vgl1-En* at stage 16 and harvested at stage 21 shows the viral infection is throughout the limb ectoderm, in a similar pattern to embryos injected at stage 10.

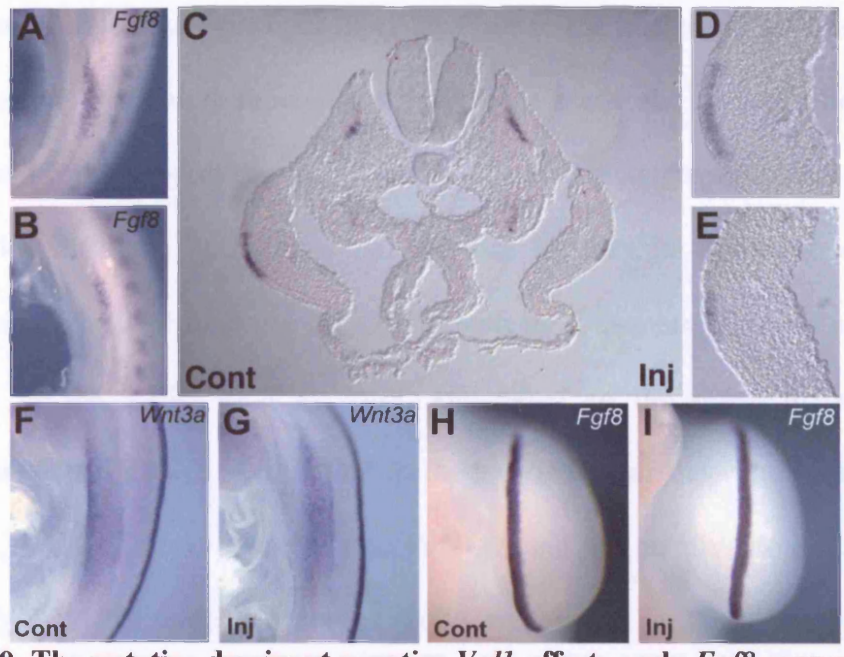

Figure 30. The putative dominant-negative *Vgll* affects early *Fgf8* expression, but not *Wnt3a* expression. *Fgf8* expression in a contra-lateral control limb at stage 17 (**A**), which is decreased in the *Vgll-En* injected side (**B**). The difference in *Fgf8* expression is clearly seen in a 10μm transverse wax vibratome section of this embryo (**C**), and at higher magnification the control (**D**) and the injected side (**E**). The expression of *Wnt3a* in a stage 16 embryo in a contra-lateral control limb (**F**) is the same in an *Vgll-En* injected limb (**G**). The expression of *Fgf8* is identical in a stage 21 contra-lateral control limb bud (**H**) as a limb injected with *Vgll-En* after AER formation at stage16 (**I**). (**A**, **B**, **F**, **G**, **H**, **I**) distal views of limbs. (**C**) 20X magnification, (**D**, **E**) 40X magnification.

I have shown by RT-PCR and RNA *in situ* hybridisation that *Vgl1* and a potential co-factor, *DTEF1*, are expressed during vertebrate limb development. Further, both *Vgl1* and *DTEF1* appear to be expressed in the outer layer of ectoderm cells, the periderm. By using a Vestigial-like1-eGFP fusion construct I have demonstrated that Vestigial-like1 localises to the nucleus in DF1 and Cos-1 cells. Various *Vgl1* viral supernatants have been made and misexpressed in the ectoderm of the prospective chick limb. The two putative dominant-negative forms, *Vgl1ΔC* and *Vgl1-Engrailed*, produce notches in the AER and limb truncations. These phenotypes are also shown by a decrease in gene molecular markers of the AER, such as *Fgf8*, and *Msx1* in the distal mesenchyme. However, no difference is observed in the expression of the ventral and dorsal markers, *En1* and *Lmx1* respectively. *Vgl1-FL* and the putative dominant-active virus, *Vgl1-VP16*$_4$, infected embryos produce truncated limbs. Misexpression of the *Vgl1-VP16*$_4$ virus also produces a limb bud with a broad patch of *Fgf8*-expressing cells on the dorsal and ventral sides of the bud.

4. Discussion

The vertebrate orthologues of two *Drosophila* genes that are required for wing morphogenesis have been studied for their potential roles in vertebrate limb development. These are *Notch1*, a vertebrate orthologue of *Notch*, and a vertebrate orthologue of *vestigial*, *Vestigial-like1*. I will first discuss my *Notch1* results, followed by my *Vestigial-like1* results and I will conclude with a general discussion of my work.

4.1 *Notch1* appears not to be required for the development of the limb skeleton, musculature or vasculature

Notch signalling has been implicated in cartilage/bone, muscle and vascular development (Delfini et al., 2000; Hayes et al., 2003; Kopan et al., 1994; Kuroda et al., 1999; Limbourg et al., 2005; Nofziger et al., 1999; Sciaudone et al., 2003; Shawber et al., 1996; Tezuka et al., 2002; Watanabe et al., 2003; Vargesson et al., 1998). The activity of the mesenchymal *Prx1-Cre* line I have used is detectable in the forelimb bud by E9.5 and by E11.5 will have been active in all limb mesenchyme cells (Logan et al., 2002). Therefore, it is predicted to delete *Notch1* function in all progenitors of the limb cartilage, bone, muscles and vasculature. My *in vivo* results using the *Prx1-Cre* line in combination with a conditional allele of *Notch1* demonstrate that *Notch1* is not required for the formation of any of the derivatives of the developing limb mesenchyme. Subsequently, *Notch1*$^{lox/lox}$; *Prx1-Cre* mutant mice develop to adulthood apparently normal. The lack of phenotype observed in the *Notch1*$^{lox/lox}$; *Prx1-Cre* mutants could be due to redundancy with other *Notch* genes and the upregulation of *Notch2/3/4* in the limb mesenchyme after the deletion of *Notch1*.

Although in my expression analysis I was unable to detect transcripts of *Notch2-4* by whole-mount *in situ* hybridisation in the limb mesenchyme, they may still be present at low levels. Recently published work has confirmed my studies on *Notch1* function in the limb and demonstrated that Notch2 signalling is also not required in the limb mesenchyme (Pan et al., 2005). An antibody against the activated form of Notch1 showed there are low levels of Notch signalling in the medial mesenchyme of E11.5 limbs. *Notch1* and *Notch2* function was deleted in the limb mesenchyme using the *Prx1-Cre*. In these *Notch1*$^{-/-}$ *Notch2*$^{-/-}$ compound mutants the low level of activated Notch1 antibody staining is absent from the limb mesenchyme. This demonstrates that *Notch1* is being deleted and the low level mesenchymal Notch1 signalling is blocked. However, identical to my results, no phenotype was observed in the forelimbs or hindlimbs of these *Notch1*$^{-/-}$ and *Notch2*$^{-/-}$ single mutants or the *Notch1*$^{-/-}$; *Notch2*$^{-/-}$ double mutant.

The *Presenilin* genes, *Presenilin1*/*Presenilin2*, form a component of the γ-secretase complex that is required for cleavage of the intracellular domain of Notch and is essential for Notch signalling (Brunkan and Goate, 2005). Mice that have both *Presenilin* genes conditionally deleted using the *Prx1-Cre* line are therefore null for γ-secretase activity and result in the disruption of all Notch signalling in the limb mesenchyme. These *Presenilin* double knockout mice have subtle skeletal defects (Pan et al., 2005). The digits of the forelimbs appear clenched, while some of the distal phalanx of hindlimbs are missing. In a severe case, nearly all of the digits are missing and the metatarsal is deformed. As no phenotype is observed when *Notch1* and *Notch2* are deleted from the limb mesenchyme, these distal limb defects could be a function of Presenilin that is

independent of Notch signalling. Presenilin is involved in a γ-secretase-independent function in somite differentiation (Huppert et al., 2005). Presenilin could have a similar role in limb development effecting endochondral differentiation (Pan et al., 2005). An alternative explanation is that, the phenotype that results following deletion of *Presenilin1/2* is caused by preventing Notch3 and/or Notch4 signalling in the limb mesenchyme, although I could not detect expression of either gene by RNA whole-mount *in situ* hybridisation. Conditional knockouts of *Notch3* and *Notch4* in combination with the *Prx1-Cre* could be used to test their requirement in the limb mesenchyme and to determine if the phenotype after the deletion of *Presenilin* in the limb mesenchyme is Notch dependent. The expression pattern of *Jagged1* and a downstream target of Notch, *Hes1*, in the distal limb mesenchyme suggest that this could be a site of active Notch signalling. *Jagged1* null mice die at pre-limb bud stages due to vascular defects, preventing the analysis of this gene during vertebrate limb development (Xue et al., 1999). *Jagged1* function could be analysed during limb development by deleting it in the limb mesenchyme using mice carrying a conditional allele of *Jagged1* and the *Prx1-Cre*. Most *Hes1* conventional knockout mice die by E15.5, with a few surviving to just after birth (Ishibashi et al., 1995). No limb phenotype has been reported for these mutant mice, but their limb bone, muscle and vasculature could be analysed in detail to determine if *Hes1* is involved in the development of any of these mesenchymal derivatives.

4.2 *Notch* signalling mediated by *Jagged2* regulates the size of the AER

Notch1 and *Jagged2* are co-expressed within the *Fgf8*-expressing cells that constitute the AER. Previous results describing the disruption of *Jagged2* (Jiang et al., 1998; Sidow et al., 1997) and my own results following the conditional deletion of *Notch1* in the limb ectoderm using the *Brn4-Cre* line produce almost identical phenotypes; expansion of the *Fgf8*-expressing cells in the AER, resulting in syndactyly of the digits. Together, these results suggest that *Jagged2* is signalling through *Notch1* to control the size of the AER. Furthermore, this signalling is occurring in a population of cells that express both ligand and receptor components of the signalling circuit.

The only differing feature in the phenotype of the *Notch1* and *Jagged2* mutants is that osseous fusions of the digits are observed in the conventional *Jagged2* knockout (Jiang et al., 1998; Sidow et al., 1997). These osseous fusions are never seen in my *Notch1* mutant. This milder phenotype is consistent with recently published data in which *Notch1* was deleted in the AER and ectoderm of the limb using a different Cre line, *Msx2-Cre* (Pan et al., 2005). The *Msx2-Cre* line is expressed in a similar manner to the *Brn4-Cre* line in the AER and ectoderm; Cre activity occurs prior to AER formation in the hindlimb, but after AER formation in the forelimb, with high levels of activity in the ventral ectoderm and low levels in the dorsal ectoderm. In the *Notch1*$^{lox/lox}$; *Msx2-Cre* conditional knockouts, soft tissue syndactyly was observed between digits 2, 3 and 4, similar to the *Notch1*$^{lox/lox}$; *Brn4-Cre* mutants I have analysed (Pan et al., 2005).

The difference in the phenotype between the *Notch1* and *Jagged2* mutants is most likely because, although I could never detect it by RNA whole-

mount *in situ* hybridisation, *Notch2* is also expressed in the AER and may compensate for the loss of *Notch1*. Conditional knockout mice for *Notch1* and *Notch2* in the ectoderm and AER have a more severe phenotype than deletion of *Notch1* alone, and the double knockout phenocopies the *Jagged2* mutant (Pan et al., 2005). Deletion of *Notch2* alone using the *Msx2-Cre* does not produce a limb phenotype, suggesting that *Notch1* is the primary receptor acting in the AER (Pan et al., 2005). *Notch2* may not normally signal or only signals at low levels in the AER, but after deletion of *Notch1* in these cells *Notch2* may partially rescue the syndactyly phenotype.

4.3 Timing of Notch signalling disruption can explain some, but not all forelimb/hindlimb differences

Unexpectedly, removal of all Notch signalling from the AER and ectoderm using the double *Presenilin* conditional knockout produces a similar, but less severe forelimb and hindlimb phenotype than the *Notch1*$^{-/-}$; *Notch2*$^{-/-}$ double knockout and the *Jagged2* mutants (Pan et al., 2005). Most of the *Presenilin* mutant embryos display soft tissue fusions, with only a few having osseous fusions. Since *Presenilin1* mRNA and protein have relatively long half-lives, cleavage and activation of Notch1 and Notch2 could occur after the initiation of the *Msx2-Cre* (Pan et al., 2005). This prolonged Notch signalling in the AER and ectoderm could result in a less severe phenotype than the *Notch1*$^{-/-}$; *Notch2*$^{-/-}$ double knockout and *Jagged2* mutants. This suggests an early function for Notch1/Notch2 signalling before, during or just after AER formation (Pan et al., 2005). The absence of antibody staining against the activated form of Notch1 demonstrates that all Notch signalling is lost in the *Presenilin* double knockout

embryos by E11.5 (Pan et al., 2005). This demonstrates that the extended period of Notch signalling in the *Presenilin* double knockout mice is required for a function in the AER prior to E11.5. Analysis of *Fgf8* expression in AERs of the *Notch1* and *Jagged2* mutant hindlimbs shows that an increase in the number of ridge cells is observed by E11.5. At E10.5 no difference was seen in *Fgf8* expression in the *Notch1* and *Jagged2* mutant hindlimbs. This work suggests that Jagged2 mediated activation of Notch1/Notch2 regulates a process after AER induction and a ridge has begun to form, but before E11.5.

In the *Notch1*$^{lox/lox}$; *Brn4-Cre* mutants and in all of the deletions of components of Notch signalling using the *Msx2-Cre* the hindlimb is more severely affected than the forelimb. In both of these Cre lines, Cre is active in the forelimb after the AER has started to form, but before the AER has formed in the hindlimb. This results in the complete removal of the targeted gene in the hindlimb AER, while in the forelimb there is transient expression in the forming AER, and only subsequently is the gene deleted. The early, short pulse of Notch signalling in the forming forelimb AER could be responsible for a milder phenotype than the hindlimbs, suggesting that *Notch1* may have a function in the AER prior to the initiation of Cre activity. My analysis of the *Brn4-Cre* using the Z/AP reporter has shown that Cre activity is not present throughout all of the forelimb AER, even at E12.5. This demonstrates that in the *Notch1*$^{lox/lox}$; *Brn4-Cre* mutant forelimb *Notch1* is not completely deleted from the AER. The undeleted *Notch1* conditional allele in the *Brn4-Cre* mutant forelimb AER may lead to the less severe phenotype. However, in both the *Jagged2* null and the *sm* mutant, the hindlimbs are also more severely affected than the forelimbs. The *sm* mutant is

thought to be a *Jagged2* hypomorph. In these mutants the digits of the forelimbs have only soft tissue syndactyly, while the digits of the hindlimbs are often fused by bone or cartilage (Gruneberg, 1956; Sidow et al., 1997). This indicates that while the timing and activity of the Cre could be involved in the difference in the hindlimb versus forelimb phenotype in the *Notch1*; *Brn4-Cre* and *Msx2-Cre* mutants, it is unlikely to be the only explanation. There could be other factors, such as the regulation of genes that compensate for the loss of Notch signalling in the forelimb, but not the hindlimb. Although the molecular mechanism is yet to be explained it appears that the forelimb is not as sensitive as the hindlimb to the loss of Notch signalling in the AER.

4.4 Notch1 signalling regulates apoptosis within the AER

High levels of cell death have been observed in the AER relative to the levels of apoptosis in the underlying mesenchyme and the dorsal and ventral ectoderm of the limb (Sun et al., 2002). My results implicate *Notch1* in the regulation of apoptosis of AER cells, since following disruption of *Notch1* signalling the number of cells undergoing apoptosis is reduced.

Notch signalling has been implicated in protecting cells from undergoing apoptosis in many different cellular contexts (for review see Miele and Osborne, 1999). However, few examples have been reported in which *Notch1* positively regulates apoptosis. Constitutive activation of the Notch signalling pathway in early neural progenitors results in the induction of apoptosis and a decrease in the progenitor population. In the complementary experiment, loss of Notch signalling in a *Notch1* conditional knockout or in *Presenilin* mutant mice leads to reduced apoptosis of the neural progenitor cells (Yang et al., 2004).

Overexpression of NICD also selectively induces apoptosis in B cells (Morimura et al., 2000) and erythroid cells (Ishiko et al., 2005). Similarly, in *Drosophila*, Notch signalling can trigger apoptosis in cells that are specified incorrectly in either the dorsal or ventral compartment of the wing imaginal disc (Milan et al., 2002), although activation of the Notch pathway itself is not sufficient to kill cells. My results indicate that Notch signalling is needed to control cell number in the AER. These results do not demonstrate that Notch signalling itself is sufficient to cause cell apoptosis in the AER leaving open the possibility that other factors may be required, in conjunction with Notch, for the clearing of cells via this apoptotic mechanism.

The ability of Notch1 to regulate apoptosis in the AER could be tested by expressing active NICD in these cells. This experiment has been performed, where transgenic mice express a constitutively active form of Notch1 under the control of the *Msx2* promoter (Pan et al., 2005). Consistent with the *Notch1* and *Jagged2* loss-of-function mutants the hindlimbs are more severely affected than the forelimbs. Some hindlimbs exhibit complete loss of zeugopod and autopod, while others have only a single digit missing. The forelimbs are less affected, with soft tissue syndactyly and a few with osseous fusions of the digits. The hindlimb phenotypes could be explained by the overexpression of Notch signalling in the AER causing increased apoptosis, resulting in a smaller AER and limb truncations. However, it is difficult to fully understand these phenotypes as the AER of these animals was not shown and no molecular markers of the limbs were analysed.

4.5 Regulation of AER-derived signals is critical for normal limb formation

My results highlight the need to control AER size, since syndactyly results if this process fails. As a result of less apoptosis in the AER, there are increased levels of signalling from the hyperplastic ridge and this leads to a downregulation of *Hoxa13* in the interdigits. This in turn leads to lower expression, or lack of expression, of BMPs in cells of the interdigital mesenchyme. Lower levels of BMPs, which normally positively regulate interdigital apoptosis, lead to decreased programmed cell death in this region and subsequent syndactyly. Alterations to the patterning of the limb vasculature that are seen in the *Notch1*$^{lox/lox}$; *Brn4-Cre* mutants could also account for the formation of syndactyly.

Application of exogenous sources of FGFs or BMPs, as well as inhibitors of these signalling pathways to the interdigit area of the chick limb have shown that FGFs and BMPs control interdigital apoptosis. These observations suggest that both signalling pathways have pro-apoptotic effects (Ganan et al., 1998; Montero et al., 2001). However, it has also been reported that administration of FGFs in the chick limb can antagonise the BMP induced apoptosis in the limb mesenchyme, resulting in the formation of soft tissue syndactyly (Buckland et al., 1998; Ganan et al., 1996; Macias et al., 1996). These results suggest that, in my mutant hindlimbs, increased FGF signalling from the hyperplastic ridge leads to a decrease in the level of *Hoxa13* expression in the mesenchyme. Consequently, the level of BMP expression is lowered leading to a reduction in interdigit-programmed cell death and syndactyly. In the chick, levels of *Hoxa13* expression decrease when the AER is removed, which can be restored with application of an FGF bead. In addition, by varying the concentration of FGF

applied after AER removal it was demonstrated this induction of *Hoxa13* expression is dose-dependent (Vargesson et al., 2001). When FGF4 is applied to a limb bud it is unable to activate the expression of *Hoxa13* early, or expand its domain of expression. Instead, exogenous FGF inhibits the expression of *Hoxa13*, compared to the contra-lateral control. This suggests there are physiological thresholds, and when there is not enough FGF *Hoxa13* expression is not initiated and when there is too much FGF signalling *Hoxa13* expression is inhibited (Vargesson et al., 2001). This is consistent with my results, and suggests there is fine balance of FGF signalling required for the correct expression of *Hoxa13*.

Significantly, I do not observe any difference in the timing of *Fgf8* expression in the AER and expression is downregulated in the regressing AER at the appropriate time during development. This indicates the defects observed result from inappropriate levels of FGF signalling rather than FGF signalling being maintained over an extended period of limb development. Interestingly, in the chick, application of an FGF or Shh bead at the distal tip of a limb prolongs FGF signalling in the overlying apical ridge and produces digits with additional or elongated phalanges. This suggests that FGF signalling from the AER is responsible for the extent of growth of the phalanges (Sanz-Ezquerro and Tickle, 2003). This is distinct from the phenotype in *Notch1*$^{lox/lox}$; *Brn4-Cre* mutants in which the timing of FGF expression is normal. Furthermore, the phenotypes I observe following disruption of *Notch1* signalling in the AER are distinct from those produced when BMP signalling from the ridge is impaired. Members of the BMP family have been implicated in the regression of the AER, as well as

interdigit programmed cell death of the limb. In the chick, misexpression of the BMP antagonist *Noggin* results in limbs with syndactyly and tissue overgrowth (Pizette and Niswander, 1999). In these limb buds, sites of tissue overgrowth correlate with parts of the AER that fail to regress. In addition, the expression of *Fgf8* is prolonged in the regions of ectopic distal outgrowth that correlates with an increase in proliferation in the distal mesenchyme of the limb. This suggests the failure in AER regression and extended FGF expression is responsible for the tissue overgrowth (Pizette and Niswander, 1999). In the mouse, deletion of *Bmpr1a* from the limb ectoderm leads to a failure of AER formation and dorsal transformation of ventral limb structures (Ahn et al., 2001). However, mice in which BMP signalling from the ridge is disrupted with *Noggin* result in severely malformed limbs that have syndactyly similar to the *Notch1* mutants (Wang et al., 2004). Importantly, the limbs of the transgenic *Noggin* mice also have post-axial polydactyly and dorsal transformation of ventral structures. The domain of *Fgf8*-expressing cells in the AER of these mutants is expanded in a similar way to that seen in the *Notch1* mutant limbs. However, in addition to an expansion of the domain of *Fgf8*, which presumably leads to increased levels of FGF signalling, expression of *Fgf8* also persists longer than normal in the mutant AER. Consistent with the chick experiments, these results suggest the extended period of *Fgf8* expression caused by *Noggin* expression in the AER, rather than perturbation of BMP signalling directly, leads to the post-axial polydactyly. Together, these data suggest that the defects I observe in my mutant hindlimbs are due to an increase in the level of FGF signalling from the AER rather than an extension of the period of FGF signalling.

Interestingly, human mutations in *FGFR2* have been shown to cause syndactyly strikingly similar to the fused digits observed after deletion of *Notch1* in the AER. In one pedigree, a double mutation in *FGFR2* results in individuals with medially deviated first digits, partially separate fifth digits and complete cutaneous syndactyly of the central three digits. These mutations are thought to alter the binding specificity and affinity of *FGFR2* expressed in the limb mesenchyme for its ligands, resulting in changes in the level of signalling. The changes in mesenchymal FGF signalling in the *FGFR2* patients could be similar to the increased level of FGF signalling observed from the hyperplastic AER to the underlying mesenchyme after deletion of *Notch1* from the ridge. This alteration in mesenchymal FGF signalling could be responsible for the smiliar phenotypes observed in these mutants. Further work, such as mice carrying the appropriate mutations in *Fgfr2*, will help determine if these phenotypes are occurring through a common mechanism.

4.6 Why do cells in the AER undergo apoptosis when this structure is playing a critical role as a signalling centre of the developing limb bud?

Apoptosis is occurring prior to regression of the AER, indicating that programmed cell death is taking place at stages when FGF signalling from this structure is essential for proximal-distal outgrowth. In the chick there are apoptotic cells in the AER at stage 18HH (Todt and Fallon 1984). This observation indicates cells are being cleared from the AER by apoptosis as soon as the ridge has formed and that apoptosis of AER cells is not only required to remove cells during the degeneration of the ridge. Classical embryological and complementary gene deletion experiments have highlighted the importance of

the AER during vertebrate limb development (Barrow et al., 2003; Saunders, 1998; Soshnikova et al., 2003; Summerbell, 1974). Therefore one may predict that it would be necessary to have tight regulation of the size of this structure to regulate the level of ridge-derived signals. During development, programmed cell death is often used as a method to regulate the size of a population of cells (reviewed in Conlon and Raff, 1999). Programmed cell death can be induced in specific cells within the embryo. This can ensure there is a tightly controlled mechanism to regulate the correct number of cells in a specific tissue or progenitor pool. In addition, nearly all cells rely on extracellular cell survival cues to protect them from apoptosis. If a cell fails to receive enough cell survival factor a proteolytic cascade is activated involving members of the caspase family, resulting in cell death.

Cell death has been demonstrated to control the number of cells in a region of the vertebrate limb that is required for patterning, and suggests that apoptosis is a conserved mechanism to regulate levels of signalling in the developing embryo. Programmed cell death has been shown to be important in controlling the number of *Shh*-expressing cells in the zone of polarising activity (ZPA) of the vertebrate limb bud (Sanz-Ezquerro and Tickle, 2000). This is a group of posterior mesenchymal cells that acts as a signalling centre to pattern the anterior-posterior axis of the limb. Increasing the level of Shh signalling in the posterior of the limb bud leads to a reduction in the level of *Shh* expression and an increase in apoptosis in the posterior necrotic zone, a region of high cell death normally found next to the *Shh* expression domain. Conversely, reducing the number of *Shh*-expressing cells in the polarising region leads to an increase in *Shh* expression and a decrease in cell death in the posterior necrotic zone.

Further, during normal limb development *Shh*-expressing cells contribute to the posterior region of cell death and directly blocking cell death increases the number of *Shh*-expressing cells. This suggests that Shh-induced cell death in the posterior mesenchyme of the limb bud could be a mechanism to control the number of cells in the ZPA and hence the level of signalling from this region of the limb bud.

Apoptosis in the *Drosophila* retina occurs as a result of Notch signalling blocking EGFR-dependent cell survival cues (Yu et al., 2002). Removal of Notch function from the retina results in a reduction in the number of apoptotic cells. An unknown signal is thought to regulate low levels of Notch activation in the retina. Therefore, Notch signalling occurs in only a small number of cells, resulting in the limited antagonism of the EGFR cell survival signalling and triggering apoptosis. A similar process could be taking place in the AER. Limited activation of Notch signalling in the AER may antagonise a cell survival cue, such as FGFs expressed in the ridge. Similar to the *Drosophila* retina, this would result in some of the cells in the AER undergoing apoptosis. Alternatively, cell death in the AER could be taking place in a similar fashion to that triggered by Notch signalling in the wing imaginal disc, where it triggers apoptosis in cells that are misspecified in their dorsal-ventral position. Blocking Notch activation with the use of a dominant-negative receptor or a dominant-negative form of Mastermind, a NICD/CSL co-factor, prevents this apoptosis (Milan et al., 2002). This work illustrates Notch signalling causes cell death in a context-dependent manner, and suggests a combination of signals is needed to designate the cells that are in an incorrect position and direct them to undergo apoptosis. Cell

labelling experiments have demonstrated the AER has compartment boundaries and that loss of these results in the disruption of the ridge. One of these boundaries is at the dorsal extent of the AER and another is at the DV border within the AER (Kimmel et al., 2000). There may be a method to ensure these boundaries are maintained and to control the positional identity of cells within the AER. Notch signalling within the AER could be a component of a mechanism in the AER to ensure that cells that are misspecified in the ridge are removed by apoptosis.

4.7 Functional conservation of Notch signalling between the *Drosophila* wing and the vertebrate limb?

In *Drosophila*, Notch signalling between dorsal and ventral compartments of the developing wing directs outgrowth at the wing margin, a line of cells that are thought to be analogous to the vertebrate AER. The specific expression of the Notch ligands, and modulation of receptor–ligand interaction by Fringe results in the activation of Notch along the DV border (Irvine, 1999; Irvine and Vogt, 1997). Failure of Notch signalling in the wing margin leads to the formation of notches in the wing blade from which the mutant gets its name. In vertebrates, Notch1 and Notch2 signal through the interaction with Jagged2 within the cells of the AER. However, notches are not observed in the mouse AER after deletion of *Notch1*, suggesting that *Notch1* does not play an analogous role in the vertebrate limb to that which *Notch* plays in the fly wing disc. In addition, after the conditional deletion of *Notch1* from the AER this structure forms, but is larger than normal and proximal-distal outgrowth is not disrupted. Nevertheless, there are subsequent subtle digit defects.

There are distinct differences between the activation of the Notch signalling pathway in the *Drosophila* wing margin and the in vertebrate limb. In the wing imaginal disc the two ligands, *Serrate* and *Delta*, are expressed in different domains so that Notch is activated only along the wing margin. Through the differential expression of the Notch ligands, the modulation by Fringe of receptor-ligand affinity, and a feedback loop it is possible to explain how this pattern of activation is established. Dorsally expressed Serrate signals to Notch in ventral cells, and Delta expressed at higher levels ventrally signals to Notch in dorsal cells. Serrate signalling to ventral cells is able to induce the expression of Delta, and Delta signalling to dorsal cells can induce the expression of Serrate, so setting up a positive feedback loop. Later in development, Notch signalling between dorsal and ventral cells ceases and Notch activation at the DV margin is maintained by flanking cells that express Serrate and Delta. These flanking cells at either side of the margin signal to the DV border and sustain Notch signalling, which induces the activation of *wg* and *vg*. Wg then promotes the expression of Serrate and Delta in the flanking cells. This results in the tight regulation of Notch signalling only along the DV border (reviewed in Irvine and Vogt, 1997). At least three Notch ligands are expressed in the vertebrate limb; *Jagged2* in the limb ectoderm and AER, *Jagged1* in the distal mesenchyme, and *Delta-like3* in the medial limb mesenchyme. The expression of these genes, together with the analysis of the conditionally deleted Notch mice has demonstrated that the regulation and the role(s) of Notch signalling is different in the vertebrate limb, compared to the *Drosophila* wing. In the vertebrate limb, the site of Notch activation is not determined by the differential expression of its ligands. A phenotype in the *Notch1* ectoderm/AER

conditionally deleted mice is only visible after the AER has started to form. At this point *Notch1* (and presumably *Notch2*) are co-expressed with *Jagged2* in the ectodermal ridge cells. Although it is not known if the receptor and ligand are expressed on the same cells, they are expressed in the same domain of cells. The mechanism to specify which cells Jagged2 activates Notch1 within the AER to trigger apoptosis has yet to be determined.

4.8 The role of a vertebrate orthologues of *vestigial* in limb development

During the development of the *Drosophila* wing imaginal disc, establishment of Notch activation at the DV boundary activates the expression of a number of genes that initiate outgrowth of the wing. One of these genes, *vestigial* (*vg*), is necessary and sufficient for wing outgrowth in the fly (Kim et al., 1996; Halder et al., 1996; Paumard-Rigal et al., 1998). I have analysed the expression pattern of one of the vertebrate orthologues of *vg*, *Vestigial-like1*, in the developing chick embryo and used a retroviral misexpression approach in the chick to study its function.

4.9 Vertebrate *Vestigial-like1* is expressed in the periderm that covers the developing limb bud

I have used a modified whole-mount *in situ* protocol to demonstrate that during development *Vgl1* expression can be seen in the ectoderm covering the dorsal surface of the trunk including the LPM in the limb-forming region prior to limb outgrowth. Low levels of *Vgl1* transcripts are subsequently detected in the ectoderm covering the limb bud. Transverse sections show that *Vgl1* is expressed

in a sub-population of cells within the AER, compared to *Wnt3a*. Further, by comparing the expression of *Vgl1* to the nuclear stain DAPI, it clearly demonstrates that transcripts are only found in the outermost ectodermal cell layer covering the limb. Previous electron microscopy studies have described this outer layer as simple squamous epithelia, referred to as the periderm (Nakamura and Yasuda, 1979; Todt and Fallon, 1984). Little is known about the periderm and, to date, only a small number of genes have been identified that have restricted expression in this layer of ectodermal cells. It is noteworthy that all of the marker genes identified as being expressed in the periderm are, so far, structural genes that are thought to be involved in the maintenance of cellular structure. These include members of the keratin family that are expressed in many epithelial cell types and form part of the cytoskeleton. Cytokeratin (K5) is expressed from early stages of chick development, prior to stage 8, in the monolayered ectoderm. It continues to be expressed in the periderm cells, until such a point later in development, when this layer is lost (Saathoff et al., 2004). In the mouse, K5 is also expressed in the ectoderm when it is a single layer and in the periderm (Byrne et al., 1994). To date, there is no evidence that *Vgl1* or *TEF*'s can upregulate members of the keratin family or other structural molecules. However, it could be particularly significant that *Vgl1* is the first transcription factor known to have restricted expression in the periderm layer of the ectoderm. A Vgl1-DTEF1 transcription complex could be responsible for specifically upregulating genes restricted to the periderm, such as keratins or cellular adhesion molecules.

Interestingly, my analysis of the expression pattern of members of the TEFs,

potential Vestigial-like co-factors, identified *DTEF1* as having a similar expression pattern to *Vgl1*. *DTEF1* is expressed in the ectoderm covering the limb-forming region and is also expressed in other locations. At stage 20, *DTEF1* is expressed in the AER and ectoderm of the developing limb bud. Sections of a stage 17 embryo show *DTEF1* is expressed in the periderm overlying the forming AER. Human VGL1 physically interacts with all mammalian TEFs in yeast and *in vitro*, and is able to substitute for Vg *in vivo* during *Drosophila* wing development (Vaudin et al., 1999). These data suggests that the two transcription factors I have identified, *Vgl1* and *DTEF1*, could physically interact and regulate the expression of target genes in the periderm.

4.10 What is the periderm?

Studies on the vertebrate periderm have characterised this structure but have revealed little about its function during embryonic development. A number of groups have examined the development and morphology of the periderm (Herken and Schultz-Ehrenburg, 1981; Holbrook and Odland, 1975; M'Boneko and Merker, 1988; Nakamura and Yasuda, 1979). In mouse embryos, the ectoderm is a single layer of cells at E9.5 and by E10.5 the periderm is formed (M'Boneko and Merker, 1988; Nakamura and Yasuda, 1979). By stage 18 in the chick, the wing bud ectoderm is two layers, a simple squamous periderm covering columnar cells (Ede et al., 1974; Todt and Fallon, 1984). The periderm is lost later in development, E18.0 in mice, at the same time the mature epidermis forms, that consists of basal spinous, granular and cornified layers, and no periderm cells are present in the adult (Koster and Koop, 2004). This has led to the proposed model that the periderm acts as an "embryonic skin" that protects

the embryo from the amniotic fluid, but is sloughed off later in development when the underlying epidermis has completed its differentiation (Hardman et al., 1999; M'Boneko and Merker, 1988). This is supported by experiments following the movement of horseradish peroxidase (HRP) used as a tracer after being subcutaneously injected into the chick. The HRP diffuses through the basal cells and stops at the periderm, suggesting these cells have a barrier function. There are many tight junctions between the periderm cells that are thought to be involved in creating this barrier (Saathoff et al., 2004).

4.11 The periderm is necessary for sites of epithelial interaction

In addition to its potential role in protecting the embryo from the amniotic fluid, the periderm may also be involved in other developmental processes. A subset of periderm cells are involved in a process late in embryonic development called temporary epithelial fusions. These are locations within the embryo where the epithelia fuse, but later in development are lost, such as the eyelids (Mazzalupo and Coulombe, 2001). In the case of the eyelid fusions, the periderm migrates over the surface of the cornea (Carroll et al., 1998).

Recently, a role for the periderm has been described in the fusing of the pair of shelves that form the secondary palate (Cuervo and Covarrubias, 2004). This process involves a series of steps including the adhering of the shelves and fragmentation of the adhered regions, resulting in the fusing of the palate. For degeneration and fusion to occur the epithelium that comes in contact must undergo programmed cell death so the mesenchyme can fuse. The point where the palates adhere and fuse has an epithelium made from a basal columnar layer covered by periderm. Cell-labelling experiments showed the periderm cells of

mouse embryos migrate to the apex with the formation of "epithelia triangles" and then die. By inhibiting the migration of the periderm cells with cytochalasin D, which blocks actin polymerisation, cell death in the periderm and underlying epithelial layers is specifically inhibited and fusion does not occur. When the periderm is removed with trypsin treatment, palate shelves adhere and cell death occurs, but epithelial triangles do not form and the secondary palate is much thinner. This work shows that the periderm of the palate shelves must migrate to trigger cell death that is required for correct fusion and formation of the secondary palate. In addition, the removal of the periderm from palate shelves that are cultured but not allowed to fuse exhibit increased cell death, suggesting the periderm is involved in cell survival of the epithelial layer underneath (Cuervo and Covarrubias, 2003).

This provides evidence that the periderm of vertebrate embryos may have functions that are required for specialised epithelial interactions that take place during development. Although no epithelial fusions take place during the formation of the AER, it is clear that that the ectoderm changes its morphology; the AER arises from the cuboidal ectoderm cells that cover the limb bud mesenchyme that differentiate to make the ridge of columnar cells. Little is known about the molecular and physical processes that are involved in the formation of these cells within the ridge. The periderm cells may be required for the differentiation of the columnar epithelial cells that form the AER. The periderm cells overlying the ectoderm of the limb-forming region may be involved in determining the cells that will form the AER. Cell fate-mapping studies in the mouse and the chick have demonstrated that AER progenitor cells originate over a large area of ectoderm of the limb-forming region (Altbaef et al.,

1997; Kimmel et al., 2000; Michaud et al., 1997). Further, not all cells that initially express AER marker genes in the pre-AER ectoderm are found in the mature ridge. This suggests there is a process of cell selection and migration of the pre-AER cells during AER formation. The periderm may play a role in these complex processes that are involved in forming a specialised ridge of cells at the DV border of the limb bud.

4.12 Potential signalling from the periderm

Another potential role for the periderm is the ability of these cells to signal to the columnar epithelial cells of the AER. Although there is no direct evidence to support this idea, recent studies in *Drosophila* imaginal discs have demonstrated that there is signalling between layers of epithelial cells. *Drosophila* imaginal discs are classically thought of as single layers of epithelial cells. The imaginal discs of *Drosophila* are a sheet of epithelial cells that form a sac separated by a disc lumen, on one side is a folded epithelium consisting of columnar cells and on the other are flat squamous cells. The columnar cells form most adult structures, including the wing, hinge and notum and are therefore called the "disc proper". The adjacent squamous cells, known as the peripodial epithelium, contribute little to the adult structure and were thought to be only required late in development during disc metamorphosis (Gibson and Schubiger, 2001). The peripodial epithelium may have analogous functions to the squamous periderm that covers vertebrate embryos.

Recent studies suggest there is communication between the peripodial epithelial cells and the columnar cells of the disc proper. Examination of the peripodial cells has shown they produce microtubules or "translumenal

extensions" that cross the disc lumen to the columnar cells. In the wing imaginal disc the number of microtubules varies, from numerous in the dorsal hinge and notum, to none in the wing blade where the peripodial and columnar epithelium directly contact each other. When the peripodial cells are ablated in the wing and eye disc there are defects in growth and patterning of these discs (Gibson and Schubiger, 2000). The peripodial cells and disc proper cells have their polarity reversed, such that they are orientated with their apical sides facing each other. The apical sides are the sites of signalling activities in epithelial cells, and overexpression of the Notch ligand Delta in the peripodial epithelium induces the activation of Wg in the wing pouch (Pallavi and Shashidhara, 2005). Similar molecular interactions have been observed with other signalling pathways in the wing and eye imaginal discs (Gibson et al., 2002; Pallavi and Shashidhara, 2003; Ramirez-Weber and Kornberg, 2000). For example, if Decapentaplegic (Dpp) function is inhibited in the peripodial epithelium growth is affected in the wing disc (Gibson et al., 2002).

This work has highlighted the importance of the peripodial epithelium during *Drosophila* wing and eye development and has uncovered novel signalling properties between the two epithelial layers. However, there are differences in the expression of *Drosophila* genes in peripodial epithelium of the wing imaginal disc cells and their vertebrate orthologues in the periderm. Wg signalling is not required in the peripodial epithelium and misexpression of Wg in these cells results in the transformation of the squamous peripodial cells into columnar cells and the induction of wing hinge genetic markers. *Wnt3a* is expressed in the columnar AER cells and I have shown that *Wnt3a* is also expressed in the overlying squamous periderm. *vg* is not expressed in peripodial

epithelium, and misexpression of Wg and Vg also leads to the transformation of these cells to a columnar morphology, but genetic markers suggest that they acquire the identity of wing blade. However, it is interesting to speculate whether there could be cellular communication between the squamous periderm cells and the columnar AER cells in the vertebrate limb.

Gap junctions have been observed between the periderm and the epidermal cells underneath in human and rat tissue (Arita et al., 2002; Risek et al., 1995). Gap junctions are intercellular channels that form between regions of membrane of cells in close contact. They connect adjacent cells so that ions and low molecular weight second messengers can pass from one cell to another. This may aid in tissue homeostasis and control cell proliferation and differentiation (Arita et al., 2002). Analysis of the expression of members of connexin proteins, constituents of gap junctions, has demonstrated the presence of a high number of gap junctions in the periderm. These gap junctions could allow the periderm to communicate and developmentally regulate the epidermal layers below. Microvilli present on the surface of the periderm could absorb carbohydrates that are required for epidermal development from the amniotic fluid, which are then transported to the lower epidermal layers through the gap junctions (Arita et al., 2002; Holbrook and Odland, 1975). The periderm covering the limb-forming region may be required to provide signals to the ectoderm of the cells that form the AER. Disruption of the periderm and the signals it may provide, for example to regulate cell proliferation or differentiation, may result in a ridge that is smaller or has gaps. Alternatively, the periderm may be involved in providing a cell survival cue as appears to be the case in the formation of the secondary

palate.

4.13 Nuclear localisation of *Vestigial-like1*

Vg and Sd are nuclear proteins that form a complex to drive the expression of genes required for *Drosophila* wing development. The cellular localisation of Vgl1 has been analysed to determine if it is found in the nucleus and could act as part of a transcription complex. Vg is predicted not to contain a nuclear localisation signal (NLS) and requires the TEA domain of Sd to translocate to the nucleus and activate target genes (Srivastava et al., 2002; Simmonds et al., 1998; Halder et al., 1998). A Vestigial-like1-GFP fusion construct transfected into DF1 and Cos-1 cells localises to the nucleus, as expected for a transcriptional co-factor. Using the PSORT II program on the ExPASy proteomics server (http://us.expasy.org) mouse Vgl1, Vgl2 and Vgl4 are predicted to contain a NLS. Mouse Vgl2 contains a putative NLS in the C-terminal domain, outside of the TEF interaction domain. Vgl2 is incorrectly localised and retained in the cytoplasm following the deletion of the C-terminal domain containing the NLS (Maeda et al., 2002). Mouse Vgl4 nuclear localisation is abolished after the deletion of the domain required for interacting with TEFs, but not the putative NLS. The loss of nuclear localisation suggests that Vgl4 requires a TEF to translocate to the nucleus (Chen et al., 2004). This data suggests that while in some cases the predicted NLS appears to be functional, in others they may not be required for nuclear localisation. PSORT II predicts that chick Vgl1 does not have a NLS, but this program is not exhaustive and Vgl1 may have acquired a NLS. If, on the other hand, Vgl1 were being imported into the nucleus with a co-factor, such as a TEF, it would have to be present in both the Cos-1 and DF1

cells. To test if Vgl1 has a NLS, or if it is translocating to the nucleus with a TEF, the cellular localisation of Vgl1 could be analysed in a cell line that is negative for TEFs. Vgl1 would remain in the cytoplasm if a TEF were necessary for its nuclear transport. In addition, deletion constructs of the Vgl1 protein would enable the determination of which domain is required for nuclear localisation.

4.14 Misexpression of *Vestigial-like1* constructs results in disruption of the AER

To ascertain whether *Vgl1* plays a role in the periderm, and if it is involved in the development of the vertebrate limb, various *Vgl1* retroviral constructs have been injected into chick embryos to infect the ectoderm of the prospective limb bud. Misexpression studies using putative dominant-negative forms of *Vestigial-like1*, *Vgl1-ΔC* or *Vgl1-En*, result in disruption of normal AER formation. Patches of expression of gene molecular markers of the AER, such as *Fgf8*, *Wnt3a* and *Bmp2* are often absent in either gaps or a stripe along middle of the AER. Correlated with the disruption of the AER, lower levels of *Msx1* expression in the distal mesenchyme and limb truncations are observed. Misexpression of the *Vgl1-En* construct does not appear to alter DV patterning, as there is no change in the expression of *Lmx1* or *En1*. This indicates that infection in the limb ectoderm of dominant-negative *Vgl1* has a specific effect on the AER, rather than disrupting the expression of all limb ectoderm genes.

The putative dominant-active form of *Vgl1*, *Vgl1-VP16*$_4$, causes ectopic

expression of *Fgf8* on the dorsal and ventral sides of the limb. This spread of *Fgf8* expression indicates there is an expansion of AER-like cells on the dorsal and ventral sides of the limb bud. Alternatively, the spread of *Fgf8* expressing cells could be due to a disruption in AER formation, so that cells that would normally form the AER have not created a ridge of cells at the distal tip of the limb. Strikingly, both the *Vgl1-VP16$_4$* and *Vgl1-FL* constructs also produce limbs that have disrupted AERs. Similar results are obtained in flies; such that when *vg* or *sd* are overexpressed in the wing disc outgrowth is inhibited (Halder et al. 1998; Simmonds et al., 1998; Varadarajan and VijayRaghavan, 1999; Lui et al, 2000). This could be due to changes in the normal ratio of Vg and Sd within a cell, which could regulate the activity of the Vg-Sd heterotetramer in the wing disc. High levels of Vg or Sd may produce multimeric complexes, so that the normal Vg-Sd complexes that activate target genes are inhibited from forming. An analogous situation could be occurring in vertebrates, so that high concentrations of Vgl1 or TEF have an inhibitory effect on normal development.

Embryos were injected with either of the putative dominant-negative constructs, *Vgl1-En* or *Vgl1-ΔC*, and were left to develop to stage 32, to enable skeletal preparations of the limb to be made. However, many of the embryos died prior to this stage, and none were recovered that had a phenotype (0/82 for *Vgl1-En* and 0/56 for *Vgl1-ΔC*). A common problem with the chick misexpression approach is that embryos die due to heart defects. In my experiments this could be due to the method of infection and the dominant-negative effect of these constructs on TEFs expressed in other tissues. As seen in this study, *DTEF1* is expressed in the developing heart, and the analysis of viral spread with an *RCAS* probe showed

that by stage 21 much of the ectoderm surrounding the limb had been infected. This most likely occurs as the replication-competent virus is injected underneath the vitelline membrane and is free to spread to neighbouring tissues. The dominant-negative *Vgl1* constructs could also infect the heart, disrupting TEF function in the heart and preventing embryos with a limb phenotype surviving to stages when the limb skeleton has formed.

4.15 The *Vestigial-like1* constructs disrupt AER formation

To determine if misexpression of the *Vestigial-like1* constructs affects AER formation or maintenance, I injected embryos at different stages of limb development. Embryos injected at stage 10 with the dominant-negative *Vgl1* retroviral construct, *Vgl1-En*, have a decrease in the level of *Fgf8* expression at stage 17 in pre-AER cells. This downregulation of *Fgf8* is just after its expression in the pre-AER cells is initiated. Transverse sections show the region of *Fgf8* expressing cells is smaller and the ectoderm appears thinner in the injected side. However, embryos injected at the same stage and processed for *Wnt3a* expression at stage 16 show no difference in the level or domain of expression. This indicates that the dominant-negative *Vgl1* retroviral construct is not affecting the induction of ectodermal *Wnt3a* expression by mesenchymal *Fgf10*. It suggests there is a disruption in the induction of *Fgf8* expression. Embryos injected with *Vgl1-En* at stage 16, which is after the initiation of *Wnt3a* expression and AER induction, and analysed at stage 21 do not have gaps or patches with reduced levels of *Fgf8* expression in the AER. This indicates the putative dominant-negative constructs are not producing gaps in the AER by

affecting the maintenance of the ridge. After misexpression of the dominant-negative *Vgl1* constructs the levels of AER marker gene expression is decreased, although *Wnt3a* expression is induced normally. This indicates that the ridge is induced, but cells do not fully differentiated into mature AER cells or there is a decrease in the number of cells within the ridge and *Fgf8* expression is lost. Taken together, these results suggest that *Vgl1* and the periderm cells are involved in an early stage in the formation of the mature AER, subsequent to the expression of *Wnt3a* in the pre-AER cells.

4.16 Caveats to the chick retroviral misexpression approach

The spread of the *Vgl1* retroviruses throughout both the periderm and the columnar layers of the limb ectoderm is a caveat to the interpretation of my misexpression experiments. I have shown that at early stages of limb development *Vgl1* and *DTEF1*, a potential co-factor, are only expressed in the outer cells of the limb bud, the periderm. However, when I misexpress the replication competent retroviruses the amount of ectodermal infection can vary and in some cases only the periderm is infected, whereas in others all of the ectoderm is infected. Therefore, viral infection would result in the ectopic misexpression of *Vgl1* constructs in parts of the ectoderm where it is not normally expressed. The proposed model for the retroviral constructs to act is by binding to a co-factor and either inhibiting or activating transcription. It would be predicted that if the co-factor, likely to be *DTEF1*, is only expressed in the periderm the Vgl1 constructs will not be able to have a dominant-active/negative effect in the ectoderm where its co-factor is not expressed. However, I cannot be sure the ectopic expression of the *Vgl1* constructs does not interact with other co-

factors and effect the transcription of genes that are not normal targets of Vgl1. When I inject the dominant-negative *Vgl1* constructs I do not observe disruptions in the expression of AER marker genes when I inject after AER induction, suggesting the disruptions I see in AER formation are a specific effect of the *Vgl1* constructs. To overcome the misexpression throughout the AER, electroporation of the *Vgl1* constructs into the limb could be used to try to target only the periderm cells. Alternatively, an antisense morpholino could be used to knock-down Vgl1 in the periderm overlying the developing limb bud. Morpholinos in chick embryos have recently been used successfully *in ovo* in combination with Pluronic F-127 gel (BASF Corp) to knock-down myosin heavy chain 6 in the developing heart (Ching et al., 2005). Pluronic gel is liquid at 0-4°C, but sets when dropped onto the embryo at physiological temperature, moulding around the embryo and remains in place for at least 12 hours (Becker et al., 1999; Becker and Mobbs, 1999). This method could be used to specifically knock-down genes expressed in the periderm to test their requirement in the periderm, and study if there is an effect on AER formation/maintenance.

Misexpression of the *Vgl1* retroviral constructs results in between 20-30% of embryos with a downregulation in gene markers and AER disruptions. A similar percentage of injected embryos stained with the *RCAS* RNA whole-mount *in situ* hybridisation probe in the limb ectoderm. This suggests that the targeting of the virus when injecting the embryos could partly determine the percentage of embryos that have a phenotype.

4.17 A role for *Vgl1* and the periderm in vertebrate limb development

Gaps in the AER produced by misexpression of the dominant-negative *Vgl1* retroviral constructs suggest that *Vgl1* and the periderm may be involved in AER formation. A study of the periderm overlying the mouse forelimb describes differences in the periderm that covers the dorsal and ventral surface of the limb, compared to the periderm that covers the AER (Nakamura and Yasuda, 1979). Scanning electron microscopic (SEM) observations have shown that at E10.5 the periderm cells of the forelimb are thin and long that run the length of the AP axis of the AER, compared to the periderm on the dorsal and ventral surface that are flatter and rounder. The periderm overlying the AER also contains a larger number of microvilli than the periderm covering the rest of the limb ectoderm. Transmission electron microscopy studies showed that an E9.5 forelimb consists of a single layer of ectoderm. At Ell.5, the periderm cells overlying the ridge are rounder with more cytoplasmic organelles, compared to the periderm cells of the dorsal and ventral ectoderm. The increased number of cellular organelles of the periderm covering the AER potentially indicates that these cells are more metabolically active (Nakamura and Yasuda, 1979). However, no other data supporting the idea that the AER periderm cells have increased metabolic activity than other periderm cells has been described. SEM studies of the periderm of the chick limb bud have shown it to be slightly different to the mouse. The ridge periderm cells have an irregular shape and are larger than the cells overlying the dorsal and ventral ectoderm. Microfilaments and microtubules in both basal and periderm are more frequent in the cells of the AER (Ede et al., 1974). However, the significance of these differences, if any, has yet to be determined.

To date, the only evidence the periderm has a role in vertebrate limb development is from the administration of 2-methoxyethanol, a known teratogen. The methoxyacetic acid (MAA), a metabolite of 2-methoxyethanol, has been shown in rats to induce ventral duplications of the autopod (Scott et al., 1987). In these rats the periderm is damaged and often absent from the limb bud. It was thought that a high level of MAA in the extra-embryonic fluid damaged the periderm. Rats given 2-methoxyethanol also display many other limb malformations such as ectrodactyly, syndactyly and shortened skeletal elements. Although it was not clear why these malformations are being induced, it was proposed that it was due to a regenerative effect of the embryo trying to repair the periderm (Scott et al., 1987). Similar experiments in mice also result in a wide variety of limb malformations induced by MAA, including ectrodactyly and syndactyly. In these mice no damage is seen in the periderm, but there is extensive apoptosis in the mesenchyme and AER (Rasjad et al., 1991a; Rasjad et al., 1991b). This may be due to species differences or in the protocol for administration of MAA.

Recent proteomic analysis using 2D gel electrophoresis has demonstrated the expression of laminin binding protein p40 (LBP-p40) is downregulated in MAA forelimb buds (Ruyani et al., 2003). LBP-p40 is involved in protein synthesis and loss of this protein causes cell death in the limb bud. In addition, LBP-p40 is also a precursor for LBP, which has been implicated in AER formation (De Arcangelis et al., 1999; Ruyani et al., 2003). Hence, it appears that the effects of MAA on limb development are complex, and in this context it is hard to distinguish what the significance of periderm loss is.

It is interesting that *Vgl1*, a putative transcription factor, is expressed in the ectoderm from early stages of development and is subsequently found specifically in the periderm. *Vgl1* could be involved in the development of the periderm cells, and misexpression of the dominant-negative *Vgl1* constructs may prevent this layer of cells forming. If the periderm were completely absent it would affect the proposed protective role of the periderm and the forming AER could be damaged, resulting in gaps in the expression of AER markers. This effect would have to be specific to the columnar epithelium of the AER, as no downregulation of either dorsal or ventral ectoderm markers is seen. Electron microscopy could be used to study the periderm and establish if these cells are missing after injection of the *Vgl1* constructs. Alternatively, *Vgl1* could be involved in another function of the periderm. After misexpression of the dominant–negative *Vgl1* the periderm may be impaired form carrying out a function that is required for the formation of the AER, such as signalling to the underlying ectoderm or epithelial interactions that may be required to make the ridge. Electron microscopic analysis of injected embryos could identify if *Vgl1* is involved in periderm development by analysing changes in the morphology of these cells. A group has successfully removed the periderm using trypsin washes and demonstrated this layer of cells is required for the correct fusion of the secondary palate (Cuervo and Covarrubias, 2003). If this protocol could be modified, or another method devised, to remove the periderm from the limb bud it would be possible to test the requirement of these cells in AER formation. My section *in situ* hybridisation data has shown that signalling molecules, such as *Wnt3a* and *Fgf8*, are expressed in the AER and the overlying periderm. To test if these, and other genes expressed in the periderm, are required for the formation

and function of the AER they could be deleted specifically from the periderm. By using homologous recombination cloning, *Cre-GFP* could be substituted for exon 1 of *Vgl1* in a BAC that contained the regulatory region of *Vgl1*. This could be used to produce a *Vgl1-Cre* line. This line would express GFP and Cre in cells where *Vgl1* is normally expressed and could be used to delete genes of interest from the periderm if suitable conditional alleles are available.

This study of *Vgl1* has uncovered a potentially novel role for the periderm during vertebrate development. It suggests that the periderm covering the developing limb bud is involved in the formation of the AER and subsequently limb outgrowth. *Vgl1* could be regulating a number of different cellular processes in the periderm such as; cell adhesion, cell signalling or cell survival that could affect AER formation. This work indicates that the periderm may have a more complex role during development, as has recently been identified for the formation of the palate. The periderm may commonly be used during development to aid in specialised epithelial interactions. Further work on *Vgl1* and the periderm will help to identify the function of these cells during AER formation and may uncover other roles for the periderm during development.

4.18 *VGL1* is a candidate gene for Split Hand Foot Malformation 2

The congenital limb abnormality split-hand/split-foot malformation (SHFM), also known as ectrodactyly, is characterised by a cleft of the hands and/or feet with loss of digits. In humans five loci have been identified that cause SHFM, called SHFM1-5. Linkage analysis has mapped the locus that causes SHFM2 to a 5.1Mb region on Xq26 and *VGL1* is a candidate gene as it lies within this region. No mutations are present in the exons and exon/intron boundaries of 19

candidate genes, including *VESTIGIAL-LIKE1* (Faiyaz-Ul-Hauqe, 2005). However, the possibility remains that a mutation could be in a regulatory region of the *VESTIGIAL-LIKE1* gene.

Studies of the genes involved in SHFM, and mouse models that display SHFM-like phenotypes have demonstrated that the AER is disrupted in these malformations. This is particularly significant as I observe disruptions in the AER after misexpression of the *Vgl1* constructs in the developing limb. Mutations in the *TP63* gene that codes for p63, result in SHFM4. Analysis of *Tp63* knockout mice has revealed that an AER forms, but is not maintained so that at birth the forelimbs lack the radius and autopod and the hindlimbs are absent (Mills et al., 1999; Yang et al., 1999). It is thought p63 is required for proliferation of the ridge cells, although the mechanism by which it carries out this function has yet to be determined. The mouse mutant *Dactylaplasia* (*Dac)* is phenotypically similar to SHFM3 and it has been mapped to 10q24, the locus responsible for causing this malformation. A *Dac* mutation has been fine-mapped to a disruption in *Dactylin*, a member of the F-box/WD40 gene family. The F-box/WD40 family are adapter proteins that target proteins for degradation by the ubiquitin pathway (Sidow et al., 1999). In addition, several patients with SHFM3 have been shown to have a significant decrease in the levels of *DACTYLIN* (Basel et al., 2003). Mice carrying *Dac* mutations have an increased level of cell death in the AER, and subsequently there is loss of the central part of the ridge. This results in heterozygous mutants missing the central digits and monodactyly in homozygous mutants (Seto et al., 1997). A third mouse model of SHFM, the $Dlx5^{-/-}$; $Dlx6^{-/-}$ double knockout, displays a severe defect of the central digits of the hindlimbs. This phenotype is characteristic of SHFM1 and maps to the same

locus. The middle part of the AER in *Dlx5*$^{-/-}$ *Dlx6*$^{-/-}$ mutants degenerates prior to E11.5, so the level of *Fgf8* expression in the ridge is reduced. Although no difference was observed in the level of apoptosis in the AER, there is a decrease in the level of proliferation of cells within the ridge (Merlo et al., 2002; Robledo et al., 2002).

These mouse models have demonstrated that the major cause of the SHFM phenotype is disruptions to the AER, and specifically that ectrodactyly is a result of the failure in maintenance of the central domain of the ridge. SHFM is caused by mutations that disrupt normal gene expression, which is best modelled by the misexpression of my dominant-negative *Vgl1* constructs. When I misexpress these dominant-negative *Vgl1* viruses in chick embryos I see an early effect on AER formation, rather than a later defect in maintenance of the ridge. It would be expected that an early defect in AER formation would result in more severe truncations of the limbs, which is not seen in most cases of SHFM. However, after misexpression of the *Vgl1* constructs I never observe embryos that completely lack an AER, but instead have gaps in the expression of AER gene markers. These partial disruptions in the AER could be a result of unequal infection of virus in the limb ectoderm. A similar effect could be occurring in SHFM if there was a mutation in a regulatory sequence required for *Vgl1* expression so that only part of the AER is disrupted. *Vgl1* in the periderm may be having an indirect effect on the formation of AER, such as protection from the amniotic fluid, which produces irregular disruptions in the AER. Thus, it is possible that mutations in the *Vgl1* gene or a regulatory sequence could result in the formation of an AER but with gaps in the ridge. This disrupted AER may be sufficient for outgrowth of the limb, but result in the absence of digits. Further

analysis of the role of *Vgl1* and the locus of SHFM2 will help to identify if Vgl1 is responsible for this malformation.

4.19 Concluding Remarks

During evolution many genes and regulatory mechanisms are conserved so that their function and expression pattern has remained largely unaltered. A good example of this is *Pax6*, that has been called an 'eye selector gene'. *Pax6* is a transcription factor required for normal eye development in a diverse array of animals, including flies and mammals (reviewed in Kozmik, 2005). *Drosophila melanogaster* has been intensively studied and many of the genes and molecular pathways involved in *Drosophila* development have been discovered and analysed. Although there are many differences between the fly wing and the vertebrate limb, it is becoming increasingly apparent they share the use of a large number of genes and molecular pathways (Shubin et al., 1997; Tabin et al., 1999). Vertebrate orthologues of *Drosophila* genes required for normal wing development have been analysed and some have, in a number of examples equivalent, important roles in vertebrate limb development. A good example is the *Drosophila* gene *wg* that is required for proximal-distal wing outgrowth at the DV boundary. The related vertebrate members of the same gene family, *Wnt3a* in the chick and *Wnt3* in the mouse, are required for the formation of the AER and subsequently the distal growth of the limb bud.

My results show that certain roles for the vertebrate orthologues of *Notch* and *vestigial* have been conserved, but they do not appear to be playing equivalent roles in both the fly and vertebrates. There are some parallels in the function of *Drosophila vg* and *Notch* and their vertebrate orthologues during

limb development. The role of Notch signalling regulating apoptosis in the wing imaginal disc and in the AER may be a conserved function, but it has yet to be determined how and why Notch signalling is triggering programmed cell death in the ridge. Misexpression of dominant-negative *Vgll* constructs in the vertebrate limb results in gaps in the AER, comparable to gaps produced in the *Drosophila* wing of *vg* mutants. *Vgll* appears be involved in AER formation, but precisely how this is occurring and if it is a direct effect of Vgl1 is still not clear. Deletion of Notch1 function from the AER results in the expansion of this structure. In contrast, knockdown of Vgl1 function in limb bud ectoderm by misexpression of dominant-negative retroviral constructs leads to gaps in the AER. This work demonstrates that although *Notch1* and *Vgll* are expressed in the vertebrate limb they appear to be involved in different cellular processes.

In *Drosophila*, Notch signalling is activated at the DV boundary and is required for initiating the outgrowth of the wing, in part, by inducing the expression of *vestigial*, which is also essential for wing development. This is distinct from the role of *Notch1* regulating apoptosis in the AER and *Vgll* that has been recruited to perform a function in the periderm. In addition, the expression of *Vgll* in the periderm of the chick is earlier than the expression of *Notch1* in the limb ectoderm. This indicates that the epistatic relationship between *Notch* and *vg* is not conserved in the vertebrate limb, although it is still possible that *Vgll* expression in the periderm is induced by Notch signalling. Phylogenetic analysis of animals from flies to vertebrates demonstrates that the intermediate animals do not have comparable structures to the *Drosophila* wing and the vertebrate limb (Shubin et al., 1997; Tabin et al., 1999). This indicates that the *Drosophila* wing and the vertebrate limb are not homologous structures.

A fundamental difference is that the *Drosophila* wing is derived primarily from a single layer of ectoderm, while the vertebrate limb consists of mesoderm covered with an ectodermal layer. The development of the vertebrate limb requires interactions between the mesenchyme and overlying ectoderm, and the majority of patterning takes place in the mesenchymal tissue (Tickle, 2003). Many of the genes and molecular pathways that are utilized in the fly wing and vertebrate limb appear to be conserved, but there are many differences in the structure and morphology of these appendages. These differences have most likely occurred over many years, so that they have become divergent structures (Shubin et al., 1997; Tabin et al., 1999). It appears that, although the expression of *Notch1* in the AER is conserved with the expression of *Notch* in the margin of the wing disc, its function in proximal-distal outgrowth has not been conserved. *Vgl1* expression and function does not seem to be conserved as it is expressed in the periderm, nevertheless more work must be done to determine the role of the periderm in AER and vertebrate limb development. Although the role of *Notch1* and *Vgl1* in vertebrate limbs does not appear to be fully analogous, compared to the *Drosophila* wing, the analysis of these orthologues has uncovered two genes that appear to be required for normal vertebrate limb development. This work further establishes the comparative biology of studying vertebrate orthologues of *Drosophila* genes as a good approach to identify genes that are important for vertebrate development.

References

Agarwal, P., Wylie, J. N., Galceran, J., Arkhitko, O., Li, C., Deng, C., Grosschedl, R. and Bruneau, B. G. (2003). Tbx5 is essential for forelimb bud initiation following patterning of the limb field in the mouse embryo. *Development* **130**, 623-33.

Ahn, K., Mishina, Y., Hanks, M. C., Behringer, R. R. and Crenshaw, E. B., 3rd. (2001). BMPR-IA signaling is required for the formation of the apical ectodermal ridge and dorsal-ventral patterning of the limb. *Development* **128**, 4449-61.

Akiyama, H., Chaboissier, M. C., Martin, J. F., Schedl, A. and de Crombrugghe, B. (2002). The transcription factor Sox9 has essential roles in successive steps of the chondrocyte differentiation pathway and is required for expression of Sox5 and Sox6. *Genes Dev* **16**, 2813-28.

Altabef, M., Clarke, J. D. and Tickle, C. (1997). Dorso-ventral ectodermal compartments and origin of apical ectodermal ridge in developing chick limb. *Development* **124**, 4547-56.

Altabef, M., Logan, C., Tickle, C and Lumsden A. (2000). *Engrailed-1* misexpression in chick embryos prevents apical ectodermal ridge formation but preserves segregation of dorsal and ventral compartments. *Developmental Biology* **222**, 307-316.

Arita, K., Akiyama, M., Tsuji, Y., McMillan, J. R., Eady, R. A. and Shimizu, H. (2002). Changes in gap junction distribution and connexin expression pattern during human fetal skin development. *J Histochem Cytochem* **50**, 1493-500.

Baena-Lopez, L. A., Pastor-Pareja, J. C. and Resino, J. (2003). Wg and Egfr signalling antagonise the development of the peripodial epithelium in Drosophila wing discs. *Development* **130**, 6497-506.

Barolo, S., Stone, T., Bang, A. G. and Posakony, J. W. (2002). Default repression and Notch signaling: Hairless acts as an adaptor to recruit the corepressors Groucho and dCtBP to Suppressor of Hairless. *Genes Dev* **16**, 1964-76.

Barrick, D. and Kopan, R. (2006). The Notch transcription activation complex makes its move. *Cell* **124**, 883-5.

Barrow, J. R., Thomas, K. R., Boussadia-Zahui, O., Moore, R., Kemler, R., Capecchi, M. R. and McMahon, A. P. (2003). Ectodermal Wnt3/beta-catenin signaling is required for the establishment and maintenance of the apical ectodermal ridge. *Genes Dev* **17**, 394-409.

Basel, D., DePaepe, A., Kilpatrick, M. W. and Tsipouras, P. (2003). Split hand foot malformation is associated with a reduced level of Dactylin gene expression. *Clin Genet* **64**, 350-4.

Becker, D. L., McGonnell, I., Makarenkova, H. P., Patel, K., Tickle, C., Lorimer, J. and Green, C. R. (1999). Roles for alpha 1 connexin in morphogenesis of chick embryos revealed using a novel antisense approach. *Dev Genet* **24**, 33-42.

Becker, D. L. and Mobbs, P. (1999). Connexin alpha1 and cell proliferation in the developing chick retina. *Exp Neurol* **156**, 326-32.

Bessho, Y. and Kageyama, R. (2003). Oscillations, clocks and segmentation. *Curr Opin Genet Dev* **13**, 379-84.

Boulet, A. M., Moon, A. M., Arenkiel, B. R. and Capecchi, M. R. (2004). The roles of Fgf4 and Fgf8 in limb bud initiation and outgrowth. *Dev Biol* **273**, 361-72.

Bray, S. (1999). Drosophila development: Scalloped and Vestigial take wing. *Curr Biol* **9**, R245-7.

Brunkan, A. L. and Goate, A. M. (2005). Presenilin function and gamma-secretase activity. *J Neurochem* **93**, 769-92.

Buckland, R. A., Collinson, J. M., Graham, E., Davidson, D. R. and Hill, R. E. (1998). Antagonistic effects of FGF4 on BMP induction of apoptosis and chondrogenesis in the chick limb bud. *Mech Dev* **71**, 143-50.

Byrne, C., Tainsky, M. and Fuchs, E. (1994). Programming gene expression in developing epidermis. *Development* **120**, 2369-83.

Campbell, S., Inamdar, M., Rodrigues, V., Raghavan, V., Palazzolo, M. and Chovnick, A. (1992). The scalloped gene encodes a novel, evolutionarily conserved transcription factor required for sensory organ differentiation in Drosophila. *Genes Dev* **6**, 367-79.

Capdevila, J. and Izpisua Belmonte, J. C. (2001). Patterning mechanisms controlling vertebrate limb development. *Annu Rev Cell Dev Biol* **17**, 87-132.

Carroll, J. M., Luetteke, N. C., Lee, D. C. and Watt, F. M. (1998). Role of integrins in mouse eyelid development: studies in normal embryos and embryos in which there is a failure of eyelid fusion. *Mech Dev* **78**, 37-45.

Chen, H. and Johnson, R. L. (1999). Dorsoventral patterning of the vertebrate limb: a process governed by multiple events. *Cell Tissue Res* **296**, 67-73.

Chen, H., Lun, Y., Ovchinnikov, D., Kokubo, H., Oberg, K. C., Pepicelli, C. V., Gan, L., Lee, B. and Johnson, R. L. (1998). Limb and kidney defects in Lmx1b mutant mice suggest an involvement of LMX1B in human nail patella syndrome. *Nat Genet* **19**, 51-5.

Chen, H. H., Mullett, S. J. and Stewart, A. F. (2004). Vgl-4, a novel member of the Vestigial-like family of transcription cofactors, regulates alpha 1-adrenergic activation of gene expression in cardiac myocytes. *J Biol Chem.*

Ching, Y. H., Ghosh, T. K., Cross, S. J., Packham, E. A., Honeyman, L., Loughna, S., Robinson, T. E., Dearlove, A. M., Ribas, G., Bonser, A. J. et al. (2005). Mutation in myosin heavy chain 6 causes atrial septal defect. *Nat Genet* **37**, 423-8.

Cho, K. O., Chern, J., Izaddoost, S. and Choi, K. W. (2000). Novel signaling from the peripodial membrane is essential for eye disc patterning in Drosophila. *Cell* **103**, 331-42.

Choi, H. S., Choi, B.Y., Cho, Y.Y., Mizuno H., Kang B. S., Bode A.M., Dong Z. (2005) Phosphorylation of histone H3 at serine 10 is indispensable for neoplastic cell transformation. *Cancer Res* **65**, 5818-27

Church, V. L. and Francis-West, P. (2002). Wnt signalling during limb development. *Int J Dev Biol* **46**, 927-36.

Cohn, M. J., Patel, K., Krumlauf, R., Wilkinson, D. G., Clarke, J. D. and Tickle, C. (1997). Hox9 genes and vertebrate limb specification. *Nature* **387**, 97-101.

Compagni, A., Logan, M., Klein, R. and Adams, R. H. (2003). Control of skeletal patterning by ephrinB1-EphB interactions. *Dev Cell* **5**, 217-30.

Conlon, I. and Raff, M. (1999). Size control in animal development. *Cell* **96**, 235-44.

Corson, L. B., Yamanaka, Y., Lai, K. M. and Rossant, J. (2003). Spatial and temporal patterns of ERK signaling during mouse embryogenesis. *Development* **130**, 4527-37.
Crossley, P. H. and Martin, G. R. (1995). The mouse Fgf8 gene encodes a family of polypeptides and is expressed in regions that direct outgrowth and patterning in the developing embryo. *Development* **121**, 439-51.
Crossley, P. H., Minowada, G., MacArthur, C. A. and Martin, G. R. (1996). Roles for FGF8 in the induction, initiation, and maintenance of chick limb development. *Cell* **84**, 127-36.
Cuervo, R. and Covarrubias, L. (2004). Death is the major fate of medial edge epithelial cells and the cause of basal lamina degradation during palatogenesis. *Development* **131**, 15-24.
Cygan, J. A., Johnson, R. L. and McMahon, A. P. (1997). Novel regulatory interactions revealed by studies of murine limb pattern in Wnt-7a and En-1 mutants. *Development* **124**, 5021-32.
De Arcangelis, A., Mark, M., Kreidberg, J., Sorokin, L. and Georges-Labouesse, E. (1999). Synergistic activities of alpha3 and alpha6 integrins are required during apical ectodermal ridge formation and organogenesis in the mouse. *Development* **126**, 3957-68.
de Celis, J. F. (1999). The function of vestigial in Drosophila wing development: how are tissue-specific responses to signalling pathways specified? *Bioessays* **21**, 542-5.
de Celis, J. F. and Bray, S. (1997). Feed-back mechanisms affecting Notch activation at the dorsoventral boundary in the Drosophila wing. *Development* **124**, 3241-51.
Delanoue, R., Legent, K., Godefroy, N., Flagiello, D., Dutriaux, A., Vaudin, P., Becker, J. L. and Silber, J. (2004). The Drosophila wing differentiation factor vestigial-scalloped is required for cell proliferation and cell survival at the dorso-ventral boundary of the wing imaginal disc. *Cell Death Differ* **11**, 110-22.
Delanoue, R., Zider, A., Cossard, R., Dutriaux, A. and Silber, J. (2002). Interaction between apterous and early expression of vestigial in formation of the dorso-ventral compartments in the Drosophila wing disc. *Genes Cells* **7**, 1255-66.
Delfini, M., Hirsinger, E., Pourquie, O. and Duprez, D. (2000). Delta 1-activated notch inhibits muscle differentiation without affecting Myf5 and Pax3 expression in chick limb myogenesis. *Development* **127**, 5213-24.
Deregowski, V., Gazzerro, E., Priest, L., Rydziel, S. and Canalis, E. (2006). Notch 1 overexpression inhibits osteoblastogenesis by suppressing Wnt/beta-catenin but not bone morphogenetic protein signaling. *J Biol Chem* **281**, 6203-10.
Deshpande, N., Chopra, A., Rangarajan, A., Shashidhara, L. S., Rodrigues, V. and Krishna, S. (1997). The human transcription enhancer factor-1, TEF-1, can substitute for Drosophila scalloped during wingblade development. *J Biol Chem* **272**, 10664-8.
Dreyer, S. D., Zhou, G., Baldini, A., Winterpacht, A., Zabel, B., Cole, W., Johnson, R. L. and Lee, B. (1998). Mutations in LMX1B cause abnormal skeletal patterning and renal dysplasia in nail patella syndrome. *Nat Genet* **19**, 47-50.

Dudley, A. T. and Robertson, E. J. (1997). Overlapping expression domains of bone morphogenetic protein family members potentially account for limited tissue defects in BMP7 deficient embryos. *Dev Dyn* **208**, 349-62.

Dudley, A. T., Ros, M. A., Tabin, C. J. (2002). A re-examination of proximodistal patterning during vertebrate limb development. *Nature* **418**, 539-544.

Duijf, P. H., van Bokhoven, H. and Brunner, H. G. (2003). Pathogenesis of split-hand/split-foot malformation. *Hum Mol Genet* **12 Spec No 1**, R51-60.

Ede, D. A., Bellairs, R. and Bancroft, M. (1974). A scanning electron microscope study of the early limb-bud in normal and talpid3 mutant chick embryos. *J Embryol Exp Morphol* **31**, 761-85.

Faiyaz-Ul-Haque, M., Zaidi, S. H., King, L. M., Haque, S., Patel, M., Ahmad, M., Siddique, T., Ahmad, W., Tsui, L. C. and Cohn, D. H. (2005). Fine mapping of the X-linked split-hand/split-foot malformation (SHFM2) locus to a 5.1-Mb region on Xq26.3 and analysis of candidate genes. *Clin Genet* **67**, 93-7.

Fallon, J. F., Lopez, A., Ros, M. A., Savage, M. P., Olwin, B. B. and Simandl, B. K. (1994). FGF-2: apical ectodermal ridge growth signal for chick limb development. *Science* **264**, 104-7.

Fischer, A., Schumacher, N., Maier, M., Sendtner, M. and Gessler, M. (2004). The Notch target genes Hey1 and Hey2 are required for embryonic vascular development. *Genes Dev* **18**, 901-11.

Fortini, M. E. (2002). Gamma-secretase-mediated proteolysis in cell-surface-receptor signalling. *Nat Rev Mol Cell Biol* **3**, 673-84.

Fromental-Ramain, C., Warot, X., Messadecq, N., LeMeur, M., Dolle, P. and Chambon, P. (1996). Hoxa-13 and Hoxd-13 play a crucial role in the patterning of the limb autopod. *Development* **122**, 2997-3011.

Galceran, J., Farinas, I., Depew, M. J., Clevers, H. and Grosschedl, R. (1999). Wnt3a-/--like phenotype and limb deficiency in Lef1(-/-)Tcf1(-/-) mice. *Genes Dev* **13**, 709-17.

Ganan, Y., Macias, D., Basco, R. D., Merino, R. and Hurle, J. M. (1998). Morphological diversity of the avian foot is related with the pattern of msx gene expression in the developing autopod. *Dev Biol* **196**, 33-41.

Ganan, Y., Macias, D., Duterque-Coquillaud, M., Ros, M. A. and Hurle, J. M. (1996). Role of TGF beta s and BMPs as signals controlling the position of the digits and the areas of interdigital cell death in the developing chick limb autopod. *Development* **122**, 2349-57.

Gavrieli, Y. Y, Sherman, and S. A. Ben-Sasson. (1992). Identification of programmed cell death *in situ* via specific labelling of nuclear DNA fragmentation. *J. Cell Biol.* **119**, 493-501.

Gibson, M. C., Lehman, D. A. and Schubiger, G. (2002). Lumenal transmission of decapentaplegic in Drosophila imaginal discs. *Dev Cell* **3**, 451-60.

Gibson, M. C. and Schubiger, G. (2000). Peripodial cells regulate proliferation and patterning of Drosophila imaginal discs. *Cell* **103**, 343-50.

Gibson, M. C. and Schubiger, G. (2001). Drosophila peripodial cells, more than meets the eye? *Bioessays* **23**, 691-7.

Gruneberg, H. (1956). An annotated catalogue of the mutant genes of the house mouse. *Memo Med Res Counc* **43**, 1-28.

Gunther, S., Mielcarek, M., Kruger, M. and Braun, T. (2004). VITO-1 is an essential cofactor of TEF1-dependent muscle-specific gene regulation. *Nucleic Acids Res* **32**, 791-802.

Guo, Q., Loomis, C. and Joyner, A. L. (2003). Fate map of mouse ventral limb ectoderm and the apical ectodermal ridge. *Dev Biol* **264**, 166-78.

Halder, G. and Carroll, S. B. (2001). Binding of the Vestigial co-factor switches the DNA-target selectivity of the Scalloped selector protein. *Development* **128**, 3295-305.

Halder, G., Polaczyk, P., Kraus, M. E., Hudson, A., Kim, J., Laughon, A. and Carroll, S. (1998). The Vestigial and Scalloped proteins act together to directly regulate wing-specific gene expression in Drosophila. *Genes Dev* **12**, 3900-9.

Hamburger, V. and Hamilton, H. L. (1951). A series of normal stages in the development of the chick embryo. *J. Exp. Morph.* **88**, 49-92.

Hardman, M. J., Moore, L., Ferguson, M. W. and Byrne, C. (1999). Barrier formation in the human fetus is patterned. *J Invest Dermatol* **113**, 1106-13.

Hayes, A. J., Dowthwaite, G. P., Webster, S. V. and Archer, C. W. (2003). The distribution of Notch receptors and their ligands during articular cartilage development. *J Anat* **202**, 495-502.

Herken, R. and Schultz-Ehrenburg, U. (1981). Autoradiographic investigations on the cell kinetics of epidermis and periderm of limb buds from mouse embryos in vitro. *Br J Dermatol* **104**, 277-84.

Himly, M., Foster, D. N., Bottoli, I., Iacovoni, J. S. and Vogt, P. K. (1998). The DF-1 chicken fibroblast cell line: transformation induced by diverse oncogenes and cell death resulting from infection by avian leukosis viruses. *Virology* **248**, 295-304.

Hogan, B., Beddington, R., Constantini, F., and Lacy, E. (1994). Manipulating the mouse embryo: Cold Spring Harbor Press.

Holbrook, K. A. and Odland, G. F. (1975). The fine structure of developing human epidermis: light, scanning, and transmission electron microscopy of the periderm. *J Invest Dermatol* **65**, 16-38.

Hollyday, M., McMahon, J. A. and McMahon, A. P. (1995). Wnt expression patterns in chick embryo nervous system. *Mech Dev* **52**, 9-25.

Huppert, S. S., Ilagan, M. X., De Strooper, B. and Kopan, R. (2005). Analysis of Notch function in presomitic mesoderm suggests a gamma-secretase-independent role for presenilins in somite differentiation. *Dev Cell* **8**, 677-88.

Huppert, S. S., Le, A., Schroeter, E. H., Mumm, J. S., Saxena, M. T., Milner, L. A. and Kopan, R. (2000). Embryonic lethality in mice homozygous for a processing-deficient allele of Notch1. *Nature* **405**, 966-70.

Irvine, K. D. (1999). Fringe, Notch, and making developmental boundaries. *Curr Opin Genet Dev* **9**, 434-41.

Irvine, K. D. and Vogt, T. F. (1997). Dorsal-ventral signaling in limb development. *Curr Opin Cell Biol* **9**, 867-76.

Ishibashi, M., Ang, S. L., Shiota, K., Nakanishi, S., Kageyama, R. and Guillemot, F. (1995). Targeted disruption of mammalian hairy and Enhancer of split homolog-1 (Hes-1) leads to up-regulation of neural helix-loop-helix factors, premature neurogenesis, and severe neural tube defects. *Genes Dev* **9**, 3136-48.

Ishiko, E., Matsumura, I., Ezoe, S., Gale, K., Ishiko, J., Satoh, Y., Tanaka, H., Shibayama, H., Mizuki, M., Era, T. et al. (2005). Notch signals inhibit the

development of erythroid/megakaryocytic cells by suppressing GATA-1 activity through the induction of HES1. *J Biol Chem* **280**, 4929-39.
Iso, T., Hamamori, Y. and Kedes, L. (2003). Notch signaling in vascular development. *Arterioscler Thromb Vasc Biol* **23**, 543-53.
Jacquemin, P. and Davidson, I. (1997). The role of the TEF transcription factors in cardiogenesis and other developmental processes. *Trends Cardiovasc. Med.* **7**, 192-197.
Jacquemin, P., Hwang, J. J., Martial, J. A., Dolle, P. and Davidson, I. (1996). A novel family of developmentally regulated mammalian transcription factors containing the TEA/ATTS DNA binding domain. *J Biol Chem* **271**, 21775-85.
Jaynes, J. B. and O'Farrell, P. H. (1991). Active repression of transcription by the engrailed homeodomain protein. *Embo J* **10**, 1427-33.
Jen, W. C., Gawantka, V., Pollet, N., Niehrs, C. and Kintner, C. (1999). Periodic repression of Notch pathway genes governs the segmentation of Xenopus embryos. *Genes Dev* **13**, 1486-99.
Jiang, R., Lan, Y., Chapman, H. D., Shawber, C., Norton, C. R., Serreze, D. V., Weinmaster, G. and Gridley, T. (1998). Defects in limb, craniofacial, and thymic development in Jagged2 mutant mice. *Genes Dev* **12**, 1046-57.
Jones, C. M., Lyons, K. M. and Hogan, B. L. (1991). Involvement of Bone Morphogenetic Protein-4 (BMP-4) and Vgr-1 in morphogenesis and neurogenesis in the mouse. *Development* **111**, 531-42.
Jouve, C., Palmeirim, I., Henrique, D., Beckers, J., Gossler, A., Ish-Horowicz, D. and Pourquie, O. (2000). Notch signalling is required for cyclic expression of the hairy-like gene HES1 in the presomitic mesoderm. *Development* **127**, 1421-9.
Kadesch, T. (2004). Notch signaling: the demise of elegant simplicity. *Curr Opin Genet Dev* **14**, 506-12.
Kaneko, K. J. and DePamphilis, M. L. (1998). Regulation of gene expression at the beginning of mammalian development and the TEAD family of transcription factors. *Dev Genet* **22**, 43-55.
Kardon, G. (1998). Muscle and tendon morphogenesis in the avian hind limb. *Development* **125**, 4019-32.
Kaufman, M. H. (2001). The Atlas of Mouse Development The Atlas of Mouse Development: Cambridge, UK, Academic Press.
Kawakami, Y., Capdevila, J., Buscher, D., Itoh, T., Rodriguez Esteban, C. and Izpisua Belmonte, J. C. (2001). WNT signals control FGF-dependent limb initiation and AER induction in the chick embryo. *Cell* **104**, 891-900.
Kengaku, M., Capdevila, J., Rodriguez-Esteban, C., De La Pena, J., Johnson, R. L., Belmonte, J. C. and Tabin, C. J. (1998). Distinct WNT pathways regulating AER formation and dorsoventral polarity in the chick limb bud. *Science* **280**, 1274-7.
Kim, J., Johnson, K., Chen, H. J., Carroll, S. and Laughon, A. (1997a). Drosophila Mad binds to DNA and directly mediates activation of vestigial by Decapentaplegic. *Nature* **388**, 304-8.
Kim, J., Magee, J. and Carroll, S. B. (1997b). Intercompartmental signaling and the regulation of vestigial expression at the dorsoventral boundary of the developing Drosophila wing. *Cold Spring Harb Symp Quant Biol* **62**, 283-91.
Kim, J., Sebring, A., Esch, J. J., Kraus, M. E., Vorwerk, K., Magee, J. and Carroll, S. B. (1996). Integration of positional signals and regulation of wing formation and identity by Drosophila vestigial gene. *Nature* **382**, 133-8.

Kimmel, R. A., Turnbull, D. H., Blanquet, V., Wurst, W., Loomis, C. A. and Joyner, A. L. (2000). Two lineage boundaries coordinate vertebrate apical ectodermal ridge formation. *Genes Dev* **14**, 1377-89.
Klein, T. (2001). Wing disc development in the fly: the early stages. *Curr Opin Genet Dev* **11**, 470-5.
Klein, T. and Arias, A. M. (1999). The vestigial gene product provides a molecular context for the interpretation of signals during the development of the wing in Drosophila. *Development* **126**, 913-25.
Knosp, W. M., Scott, V., Bachinger, H. P. and Stadler, H. S. (2004). HOXA13 regulates the expression of bone morphogenetic proteins 2 and 7 to control distal limb morphogenesis. *Development* **131**, 4581-92.
Koelzer, S. and Klein, T. (2006). Regulation of expression of Vg and establishment of the dorsoventral compartment boundary in the wing imaginal disc by Suppressor of Hairless. *Dev Biol* **289**, 77-90.
Kopan, R., Nye, J. S. and Weintraub, H. (1994). The intracellular domain of mouse Notch: a constitutively activated repressor of myogenesis directed at the basic helix-loop-helix region of MyoD. *Development* **120**, 2385-96.
Koster, M. I. and Roop, D. R. (2004). Genetic pathways required for epidermal morphogenesis. *Eur J Cell Biol* **83**, 625-9.
Kozmik, Z. (2005). Pax genes in eye development and evolution. *Curr Opin Genet Dev* **15**, 430-8.
Kuroda, K., Tani, S., Tamura, K., Minoguchi, S., Kurooka, H. and Honjo, T. (1999). Delta-induced Notch signaling mediated by RBP-J inhibits MyoD expression and myogenesis. *J Biol Chem* **274**, 7238-44.
Lai, E. C. (2004). Notch signaling: control of cell communication and cell fate. *Development* **131**, 965-73.
Lallemand, Y., Nicola, M. A., Ramos, C., Bach, A., Clement, C. S. and Robert, B. (2005). Analysis of Msx1; Msx2 double mutants reveals multiple roles for Msx genes in limb development. *Development* **132**, 3003-14.
Laufer, E., Dahn, R., Orozco, O. E., Yeo, C. Y., Pisenti, J., Henrique, D., Abbott, U. K., Fallon, J. F. and Tabin, C. (1997). Expression of Radical fringe in limb-bud ectoderm regulates apical ectodermal ridge formation. *Nature* **386**, 366-73.
Lawson, N. D., Scheer, N., Pham, V. N., Kim, C. H., Chitnis, A. B., Campos-Ortega, J. A. and Weinstein, B. M. (2001). Notch signaling is required for arterial-venous differentiation during embryonic vascular development. *Development* **128**, 3675-83.
Le Borgne, R., Bardin, A. and Schweisguth, F. (2005). The roles of receptor and ligand endocytosis in regulating Notch signaling. *Development* **132**, 1751-62.
Lei, L., Xu, A., Panin, V. M. and Irvine, K. D. (2003). An O-fucose site in the ligand binding domain inhibits Notch activation. *Development* **130**, 6411-21.
Limbourg, F. P., Takeshita, K., Radtke, F., Bronson, R. T., Chin, M. T. and Liao, J. K. (2005). Essential role of endothelial Notch1 in angiogenesis. *Circulation* **111**, 1826-32.
Liu, X., Grammont, M. and Irvine, K. D. (2000). Roles for scalloped and vestigial in regulating cell affinity and interactions between the wing blade and the wing hinge. *Dev Biol* **228**, 287-303.
Liu, Z. J., Shirakawa, T., Li, Y., Soma, A., Oka, M., Dotto, G. P., Fairman, R. M., Velazquez, O. C. and Herlyn, M. (2003). Regulation of Notch1 and

Dll4 by vascular endothelial growth factor in arterial endothelial cells: implications for modulating arteriogenesis and angiogenesis. *Mol Cell Biol* **23**, 14-25.

Lobe, C. G., Koop, K. E., Kreppner, W., Lomeli, H., Gertsenstein, M. and Nagy, A. (1999). Z/AP, a double reporter for cre-mediated recombination. *Dev Biol* **208**, 281-92.

Logan, M. (2003). Finger or toe: the molecular basis of limb identity. *Development* **130**, 6401-10.

Logan, M., Martin, J. F., Nagy, A., Lobe, C., Olson, E. N. and Tabin, C. J. (2002). Expression of Cre Recombinase in the developing mouse limb bud driven by a Prxl enhancer. *Genesis* **33**, 77-80.

Logan, M. and Tabin, C. (1998). Targeted gene misexpression in chick limb buds using avian replication-competent retroviruses. *Methods* **14**, 407-20.

Loomis, C. A., Harris, E., Michaud, J., Wurst, W., Hanks, M. and Joyner, A. L. (1996). The mouse Engrailed-1 gene and ventral limb patterning. *Nature* **382**, 360-3.

Loomis, C. A., Kimmel, R. A., Tong, C. X., Michaud, J. and Joyner, A. L. (1998). Analysis of the genetic pathway leading to formation of ectopic apical ectodermal ridges in mouse Engrailed-1 mutant limbs. *Development* **125**, 1137-48.

Lubman, O. Y., Korolev, S. V. and Kopan, R. (2004). Anchoring notch genetics and biochemistry; structural analysis of the ankyrin domain sheds light on existing data. *Mol Cell* **13**, 619-26.

Lyons, K. M., Pelton, R. W. and Hogan, B. L. (1989). Patterns of expression of murine Vgr-1 and BMP-2a RNA suggest that transforming growth factor-beta-like genes coordinately regulate aspects of embryonic development. *Genes Dev* **3**, 1657-68.

M'Boneko, V. and Merker, H. J. (1988). Development and morphology of the periderm of mouse embryos (days 9-12 of gestation). *Acta Anat (Basel)* **133**, 325-36.

Ma, L., Benson, G. V., Lim, H., Dey, S. K. and Maas, R. L. (1998). Abdominal B (AbdB) Hoxa genes: regulation in adult uterus by estrogen and progesterone and repression in mullerian duct by the synthetic estrogen diethylstilbestrol (DES). *Dev Biol* **197**, 141-54.

Macias, D., Ganan, Y., Ros, M. A. and Hurle, J. M. (1996). In vivo inhibition of programmed cell death by local administration of FGF-2 and FGF-4 in the interdigital areas of the embryonic chick leg bud. *Anat Embryol (Berl)* **193**, 533-41.

MacKay, J. O., Soanes, K. H., Srivastava, A., Simmonds, A., Brook, W. J. and Bell, J. B. (2003). An in vivo analysis of the vestigial gene in Drosophila melanogaster defines the domains required for Vg function. *Genetics* **163**, 1365-73.

Maeda, T., Chapman, D. L. and Stewart, A. F. (2002). Mammalian vestigial-like 2, a cofactor of TEF-1 and MEF2 transcription factors that promotes skeletal muscle differentiation. *J Biol Chem* **277**, 48889-98.

Marshall, C. J. (1995). Specificity of receptor tyrosine kinase signaling: transient versus sustained extracellular signal-regulated kinase activation. *Cell* **80**, 179-85.

Martin, G. R. (1998). The roles of FGFs in the early development of vertebrate limbs. *Genes Dev* **12**, 1571-86.

Mazzalupo, S. and Coulombe, P. A. (2001). A reporter transgene based on a human keratin 6 gene promoter is specifically expressed in the periderm of mouse embryos. *Mech Dev* **100**, 65-9.
Merlo, G. R., Paleari, L., Mantero, S., Genova, F., Beverdam, A., Palmisano, G. L., Barbieri, O. and Levi, G. (2002). Mouse model of split hand/foot malformation type I. *Genesis* **33**, 97-101.
Michaud, J. L., Lapointe, F. and Le Douarin, N. M. (1997). The dorsoventral polarity of the presumptive limb is determined by signals produced by the somites and by the lateral somatopleure. *Development* **124**, 1453-63.
Mielcarek, M., Gunther, S., Kruger, M. and Braun, T. (2002). VITO-1, a novel vestigial related protein is predominantly expressed in the skeletal muscle lineage. *Mech Dev* **119 Suppl 1**, S269-74.
Miele, L. and Osborne, B. (1999). Arbiter of differentiation and death: Notch signaling meets apoptosis. *J Cell Physiol* **181**, 393-409.
Milan, M., Perez, L. and Cohen, S. M. (2002). Short-range cell interactions and cell survival in the Drosophila wing. *Dev Cell* **2**, 797-805.
Mills, A. A., Zheng, B., Wang, X. J., Vogel, H., Roop, D. R. and Bradley, A. (1999). p63 is a p53 homologue required for limb and epidermal morphogenesis. *Nature* **398**, 708-13.
Min, H., Danilenko, D. M., Scully, S. A., Bolon, B., Ring, B. D., Tarpley, J. E., DeRose, M. and Simonet, W. S. (1998). Fgf-10 is required for both limb and lung development and exhibits striking functional similarity to Drosophila branchless. *Genes Dev* **12**, 3156-61.
Minguillon, C., Del Buono, J. and Logan, M. P. (2005). Tbx5 and Tbx4 are not sufficient to determine limb-specific morphologies but have common roles in initiating limb outgrowth. *Dev Cell* **8**, 75-84.
Mitsiadis, T. A., Henrique, D., Thesleff, I. and Lendahl, U. (1997). Mouse Serrate-1 (Jagged-1): expression in the developing tooth is regulated by epithelial-mesenchymal interactions and fibroblast growth factor-4. *Development* **124**, 1473-83.
Montero, J. A., Ganan, Y., Macias, D., Rodriguez-Leon, J., Sanz-Ezquerro, J. J., Merino, R., Chimal-Monroy, J., Nieto, M. A. and Hurle, J. M. (2001). Role of FGFs in the control of programmed cell death during limb development. *Development* **128**, 2075-84.
Moran, J. L., Levorse, J. M. and Vogt, T. F. (1999). Limbs move beyond the radical fringe. *Nature* **399**, 742-3.
Morimura, T., Goitsuka, R., Zhang, Y., Saito, I., Reth, M. and Kitamura, D. (2000). Cell cycle arrest and apoptosis induced by Notch1 in B cells. *J Biol Chem* **275**, 36523-31.
Myat, A., Henrique, D., Ish-Horowicz, D. and Lewis, J. (1996). A chick homologue of Serrate and its relationship with Notch and Delta homologues during central neurogenesis. *Dev Biol* **174**, 233-47.
Nagel, A. C., Wech, I. and Preiss, A. (2001). Scalloped and strawberry notch are target genes of Notch signaling in the context of wing margin formation in Drosophila. *Mech Dev* **109**, 241-51.
Naiche, L. A. and Papaioannou, V. E. (2003). Loss of Tbx4 blocks hindlimb development and affects vascularization and fusion of the allantois. *Development* **130**, 2681-93.

Nakamura, H. and Yasuda, M. (1979). An electron microscopic study of periderm cell development in mouse limb buds. *Anat Embryol (Berl)* **157**, 121-32.

Nam, Y., Sliz, P., Song, L., Aster, J. C. and Blacklow, S. C. (2006). Structural basis for cooperativity in recruitment of MAML coactivators to Notch transcription complexes. *Cell* **124**, 973-83.

Nelson, W. J. and Nusse, R. (2004). Convergence of Wnt, beta-catenin, and cadherin pathways. *Science* **303**, 1483-7.

Niswander, L., Tickle, C., Vogel, A., Booth, I. and Martin, G. R. (1993). FGF-4 replaces the apical ectodermal ridge and directs outgrowth and patterning of the limb. *Cell* **75**, 579-87.

Nobta, M., Tsukazaki, T., Shibata, Y., Xin, C., Moriishi, T., Sakano, S., Shindo, H. and Yamaguchi, A. (2005). Critical regulation of BMP-induced osteoblastic differentiation by delta1/jagged1-activated notch1 signaling. *J Biol Chem.*

Nofziger, D., Miyamoto, A., Lyons, K. M. and Weinmaster, G. (1999). Notch signaling imposes two distinct blocks in the differentiation of C2C12 myoblasts. *Development* **126**, 1689-702.

Noramly, S., Pisenti, J., Abbott, U. and Morgan, B. (1996). Gene expression in the limbless mutant: polarized gene expression in the absence of Shh and an AER. *Dev Biol* **179**, 339-46.

Ohashi, Y., Brickman, J. M., Furman, E., Middleton, B. and Carey, M. (1994). Modulating the potency of an activator in a yeast in vitro transcription system. *Mol Cell Biol* **14**, 2731-9.

Pallavi, S. K. and Shashidhara, L. S. (2003). Egfr/Ras pathway mediates interactions between peripodial and disc proper cells in Drosophila wing discs. *Development* **130**, 4931-41.

Pallavi, S. K. and Shashidhara, L. S. (2005). Signaling interactions between squamous and columnar epithelia of the Drosophila wing disc. *J Cell Sci* **118**, 3363-70.

Pan, Y., Liu, Z., Shen, J. and Kopan, R. (2005). Notch1 and 2 cooperate in limb ectoderm to receive an early Jagged2 signal regulating interdigital apoptosis. *Dev Biol* **286**, 472-82.

Panin, V. M., Papayannopoulos, V., Wilson, R. and Irvine, K. D. (1997). Fringe modulates Notch-ligand interactions. *Nature* **387**, 908-12.

Parr, B. A. and McMahon, A. P. (1995). Dorsalizing signal Wnt-7a required for normal polarity of D-V and A-P axes of mouse limb. *Nature* **374**, 350-3.

Paumard-Rigal, S., Zider, A., Vaudin, P. and Silber, J. (1998). Specific interactions between vestigial and scalloped are required to promote wing tissue proliferation in Drosophila melanogaster. *Dev Genes Evol* **208**, 440-6.

Pereira, R. M., Delany, A. M., Durant, D. and Canalis, E. (2002). Cortisol regulates the expression of Notch in osteoblasts. *J Cell Biochem* **85**, 252-8.

Pizette, S., Abate-Shen, C. and Niswander, L. (2001). BMP controls proximodistal outgrowth, via induction of the apical ectodermal ridge, and dorsoventral patterning in the vertebrate limb. *Development* **128**, 4463-74.

Pizette, S. and Niswander, L. (1999). BMPs negatively regulate structure and function of the limb apical ectodermal ridge. *Development* **126**, 883-94.

Radtke, F., Wilson, A., Stark, G., Bauer, M., van Meerwijk, J., MacDonald, H. R. and Aguet, M. (1999). Deficient T cell fate specification in mice with an induced inactivation of Notch1. *Immunity* **10**, 547-58.

Rallis, C., Bruneau, B. G., Del Buono, J., Seidman, C. E., Seidman, J. G., Nissim, S., Tabin, C. J. and Logan, M. P. (2003). Tbx5 is required for forelimb bud formation and continued outgrowth. *Development* **130**, 2741-51.

Ramirez-Weber, F. A. and Kornberg, T. B. (2000). Signaling reaches to new dimensions in Drosophila imaginal discs. *Cell* **103**, 189-92.

Rancourt, D. E., Tsuzuki, T. and Capecchi, M. R. (1995). Genetic interaction between hoxb-5 and hoxb-6 is revealed by nonallelic noncomplementation. *Genes Dev* **9**, 108-22.

Rasjad, C., Yamashita, K., Datu, A. R. and Yasuda, M. (1991a). Pathogenesis of limb malformations in mice induced by methoxyacetic acid. *Hiroshima J Med Sci* **40**, 101-7.

Rasjad, C., Yamashita, K., Datu, A. R. and Yasuda, M. (1991b). Pattern of limb malformations in mice induced by methoxyacetic acid. *Hiroshima J Med Sci* **40**, 93-9.

Rauskolb, C., Correia, T. and Irvine, K. D. (1999). Fringe-dependent separation of dorsal and ventral cells in the Drosophila wing. *Nature* **401**, 476-80.

Riddle, R. D., Ensini, M., Nelson, C., Tsuchida, T., Jessell, T. M. and Tabin, C. (1995). Induction of the LIM homeobox gene Lmx1 by WNT7a establishes dorsoventral pattern in the vertebrate limb. *Cell* **83**, 631-40.

Riddle, R. D., Johnson, R. L., Laufer, E. and Tabin, C. (1993). Sonic hedgehog mediates the polarizing activity of the ZPA. *Cell* **75**, 1401-16.

Risek, B., Klier, F. G., Phillips, A., Hahn, D. W. and Gilula, N. B. (1995). Gap junction regulation in the uterus and ovaries of immature rats by estrogen and progesterone. *J Cell Sci* **108 (Pt 3)**, 1017-32.

Robledo, R. F., Rajan, L., Li, X. and Lufkin, T. (2002). The Dlx5 and Dlx6 homeobox genes are essential for craniofacial, axial, and appendicular skeletal development. *Genes Dev* **16**, 1089-101.

Rodriguez-Esteban, C., Schwabe, J. W., De La Pena, J., Foys, B., Eshelman, B. and Belmonte, J. C. (1997). Radical fringe positions the apical ectodermal ridge at the dorsoventral boundary of the vertebrate limb. *Nature* **386**, 360-6.

Ros, M. A., Lyons, G., Kosher, R. A., Upholt, W. B., Coelho, C. N. and Fallon, J. F. (1992). Apical ridge dependent and independent mesodermal domains of GHox-7 and GHox-8 expression in chick limb buds. *Development* **116**, 811-8.

Ross, D. A. and Kadesch, T. (2004). Consequences of Notch-mediated induction of Jagged1. *Exp Cell Res* **296**, 173-82.

Rubin, L. and Saunders, J. W., Jr. (1972). Ectodermal-mesodermal interactions in the growth of limb buds in the chick embryo: constancy and temporal limits of the ectodermal induction. *Dev Biol* **28**, 94-112.

Ruyani, A., Sudarwati, S., Sutasurya, L. A., Sumarsono, S. H. and Gloe, T. (2003). The laminin binding protein p40 is involved in inducing limb abnormality of mouse fetuses as the effects of methoxyacetic acid treatment. *Toxicol Sci* **75**, 148-53.

Saathoff, M., Blum, B., Quast, T., Kirfel, G. and Herzog, V. (2004). Simultaneous cell death and desquamation of the embryonic diffusion barrier during epidermal development. *Exp Cell Res* **299**, 415-26.

Sanz-Ezquerro, J. J. and Tickle, C. (2000). Autoregulation of Shh expression and Shh induction of cell death suggest a mechanism for modulating polarising activity during chick limb development. *Dev* **127**, 4811-4823.

Sanz-Ezquerro, J. J. and Tickle, C. (2003). Fgf signaling controls the number of phalanges and tip formation in developing digits. *Curr Biol* **13**, 1830-6.
Sasai, Y., Kageyama, R., Tagawa, Y., Shigemoto, R. and Nakanishi, S. (1992). Two mammalian helix-loop-helix factors structurally related to Drosophila hairy and Enhancer of split. *Genes Dev* **6**, 2620-34.
Sauer, B. (1998). Inducible gene targeting in mice using the Cre/lox system. *Methods* **14**, 381-92.
Saunders, J. W., Jr. (1998). The proximo-distal sequence of origin of the parts of the chick wing and the role of the ectoderm. 1948. *J Exp Zool* **282**, 628-68.
Schaefer-Klein, J., Givol, I., Barsov, E. V., Whitcomb, J. M., VanBrocklin, M., Foster, D. N., Federspiel, M. J. and Hughes, S. H. (1998). The EV-O-derived cell line DF-1 supports the efficient replication of avian leukosis-sarcoma viruses and vectors. *Virology* **248**, 305-11.
Schaeren-Wiemers, N. and Gerfin-Moser, A. (1993). A single protocol to detect transcripts of various types and expression levels in neural tissue and cultured cells: in situ hybridization using digoxigenin-labelled cRNA probes. *Histochemistry* **100**, 431-40.
Schlange, T., Arnold, H. H. and Brand, T. (2002). BMP2 is a positive regulator of Nodal signaling during left-right axis formation in the chicken embryo. *Development* **129**, 3421-9.
Schweisguth, F. (2004). Notch signaling activity. *Curr Biol* **14**, R129-38.
Sciaudone, M., Gazzerro, E., Priest, L., Delany, A. M. and Canalis, E. (2003). Notch 1 impairs osteoblastic cell differentiation. *Endocrinology* **144**, 5631-9.
Scott, W. J., Jr., Nau, H., Wittfoht, W. and Merker, H. J. (1987). Ventral duplication of the autopod: chemical induction by methoxyacetic acid in rat embryos. *Development* **99**, 127-36.
Sekine, K., Ohuchi, H., Fujiwara, M., Yamasaki, M., Yoshizawa, T., Sato, T., Yagishita, N., Matsui, D., Koga, Y., Itoh, N. et al. (1999). Fgf10 is essential for limb and lung formation. *Nat Genet* **21**, 138-41.
Selever, J., Liu, W., Lu, M. F., Behringer, R. R. and Martin, J. F. (2004). Bmp4 in limb bud mesoderm regulates digit pattern by controlling AER development. *Dev Biol* **276**, 268-79.
Seto, M. L., Nunes, M. E., MacArthur, C. A. and Cunningham, M. L. (1997). Pathogenesis of ectrodactyly in the Dactylaplasia mouse: aberrant cell death of the apical ectodermal ridge. *Teratology* **56**, 262-70.
Sharpe, C., Lawrence, N. and Martinez Arias, A. (2001). Wnt signalling: a theme with nuclear variations. *Bioessays* **23**, 311-8.
Shawber, C., Nofziger, D., Hsieh, J. J., Lindsell, C., Bogler, O., Hayward, D. and Weinmaster, G. (1996). Notch signaling inhibits muscle cell differentiation through a CBF1-independent pathway. *Development* **122**, 3765-73.
Shubin, N., Tabin, C. and Carroll, S. (1997). Fossils, genes and the evolution of animal limbs. *Nature* **388**, 639-48.
Sidow, A., Bulotsky, M. S., Kerrebrock, A. W., Birren, B. W., Altshuler, D., Jaenisch, R., Johnson, K. R. and Lander, E. S. (1999). A novel member of the F-box/WD40 gene family, encoding dactylin, is disrupted in the mouse dactylaplasia mutant. *Nat Genet* **23**, 104-7.
Sidow, A., Bulotsky, M. S., Kerrebrock, A. W., Bronson, R. T., Daly, M. J., Reeve, M. P., Hawkins, T. L., Birren, B. W., Jaenisch, R. and Lander, E. S.

(1997). Serrate2 is disrupted in the mouse limb-development mutant syndactylism. *Nature* **389**, 722-5.

Simmonds, A., Hughes, S., Tse, J., Cocquyt, S. and Bell, J. (1997). The effect of dominant vestigial alleles upon vestigial-mediated wing patterning during development of Drosophila melanogaster. *Mech Dev* **67**, 17-33.

Simmonds, A. J., Liu, X., Soanes, K. H., Krause, H. M., Irvine, K. D. and Bell, J. B. (1998). Molecular interactions between Vestigial and Scalloped promote wing formation in Drosophila. *Genes Dev* **12**, 3815-20.

Soshnikova, N., Zechner, D., Huelsken, J., Mishina, Y., Behringer, R. R., Taketo, M. M., Crenshaw, E. B., 3rd and Birchmeier, W. (2003). Genetic interaction between Wnt/beta-catenin and BMP receptor signaling during formation of the AER and the dorsal-ventral axis in the limb. *Genes Dev* **17**, 1963-8.

Srivastava, A., MacKay, J. O. and Bell, J. B. (2002). A Vestigial:Scalloped TEA domain chimera rescues the wing phenotype of a scalloped mutation in Drosophila melanogaster. *Genesis* **33**, 40-7.

Stadler, H. S., Higgins, K. M. and Capecchi, M. R. (2001). Loss of Eph-receptor expression correlates with loss of cell adhesion and chondrogenic capacity in Hoxa13 mutant limbs. *Development* **128**, 4177-88.

Summerbell, D. (1974). A quantitative analysis of the effect of excision of the AER from the chick limb-bud. *J Embryol Exp Morphol* **32**, 651-60.

Sun, X., Mariani, F. V. and Martin, G. R. (2002). Functions of FGF signalling from the apical ectodermal ridge in limb development. *Nature* **418**, 501-8.

Swiatek, P. J., Lindsell, C. E., del Amo, F. F., Weinmaster, G. and Gridley, T. (1994). Notch1 is essential for postimplantation development in mice. *Genes Dev* **8**, 707-19.

Tabin, C., Carroll S.B. and G., P. (1999). Out on a limb: parellels in vertebrate and invertebrate limb patterning and the origin of the appendages. *Am Zool* **39**, 650-663.

Tezuka, K., Yasuda, M., Watanabe, N., Morimura, N., Kuroda, K., Miyatani, S. and Hozumi, N. (2002). Stimulation of osteoblastic cell differentiation by Notch. *J Bone Miner Res* **17**, 231-9.

Tickle, C. (2003). Patterning systems--from one end of the limb to the other. *Dev Cell* **4**, 449-58.

Tickle, C. and Altabef, M. (1999). Epithelial cell movements and interactions in limb, neural crest and vasculature. *Curr Opin Genet Dev* **9**, 455-60.

Tickle, C. and Wolpert, L. (2002). The progress zone - alive or dead? *Nature Cell Biol.* **4E**, 216-218.

Todt, W. L. and Fallon, J. F. (1984). Development of the apical ectodermal ridge in the chick wing bud. *J Embryol Exp Morphol* **80**, 21-41.

Todt, W. L. and Fallon, J. F. (1986). Development of the apical ectodermal ridge in the chick leg bud and a comparison with the wing bud. *Anat Rec* **215**, 288-304.

Varadarajan, S. and VijayRaghavan, K. (1999). scalloped functions in a regulatory loop with vestigial and wingless to pattern the Drosophila wing. *Dev Genes Evol* **209**, 10-7.

Vargesson, N., Clarke, J., Vincent, K., Coles, C., Wolpert, L. and Tickle, C. (1997). Cell fate in the chick limb bud and relationship to gene expression. *Dev* **124**, 1909-1918.

Vargesson, N., Kostakopoulou, K., Drossopoulou, G., Papageorgiou, S. and Tickle, C. (2001). Characterisation of hoxa gene expression in the chick limb bud in response to FGF. *Dev Dyn* **220**, 87-90.

Vargesson, N., Patel, K., Lewis, J. and Tickle, C. (1998). Expression patterns of Notch1, Serrate1, Serrate2 and Delta1 in tissues of the developing chick limb. *Mech Dev* **77**, 197-9.

Vasiliauskas, D., Laufer, E. and Stern, C. D. (2003). A role for hairy1 in regulating chick limb bud growth. *Dev Biol* **262**, 94-106.

Vaudin, P., Delanoue, R., Davidson, I., Silber, J. and Zider, A. (1999). TONDU (TDU), a novel human protein related to the product of vestigial (vg) gene of Drosophila melanogaster interacts with vertebrate TEF factors and substitutes for Vg function in wing formation. *Development* **126**, 4807-16.

Vogel, A., Roberts-Clarke, D. and Niswander, L. (1995). Effect of FGF on gene expression in chick limb bud cells in vivo and in vitro. *Dev Biol* **171**, 507-20.

Vogel, A., Rodriguez, C. and Izpisua-Belmonte, J. C. (1996). Involvement of FGF-8 in initiation, outgrowth and patterning of the vertebrate limb. *Development* **122**, 1737-50.

Wang, C. K., Omi, M., Ferrari, D., Cheng, H. C., Lizarraga, G., Chin, H. J., Upholt, W. B., Dealy, C. N. and Kosher, R. A. (2004). Function of BMPs in the apical ectoderm of the developing mouse limb. *Dev Biol* **269**, 109-22.

Wang, S., Younger-Shepherd, S., Jan, L. Y. and Jan, Y. N. (1997). Only a subset of the binary cell fate decisions mediated by Numb/Notch signaling in Drosophila sensory organ lineage requires Suppressor of Hairless. *Development* **124**, 4435-46.

Wang, Y. and Sassoon, D. (1995). Ectoderm-mesenchyme and mesenchyme-mesenchyme interactions regulate Msx-1 expression and cellular differentiation in the murine limb bud. *Dev Biol* **168**, 374-82.

Watanabe, N., Tezuka, Y., Matsuno, K., Miyatani, S., Morimura, N., Yasuda, M., Fujimaki, R., Kuroda, K., Hiraki, Y., Hozumi, N. et al. (2003). Suppression of differentiation and proliferation of early chondrogenic cells by Notch. *J Bone Miner Metab* **21**, 344-52.

Weinstein, B. M. and Lawson, N. D. (2002). Arteries, veins, Notch, and VEGF. *Cold Spring Harb Symp Quant Biol* **67**, 155-62.

Wilkie, A. O. M., Patey, S. J., Kan, S., van den Ouweland A. M. W., and B. Hamel, C. J. (2002). FGFs, Their Receptors, and Human LimbMalformations: Clinical and Molecular Correlations. *Am J of Med Gen* **112**:266–278.

Williams, J. A., Bell, J. B. and Carroll, S. B. (1991). Control of Drosophila wing and haltere development by the nuclear vestigial gene product. *Genes Dev* **5**, 2481-95.

Williams, J. A., Paddock, S. W. and Carroll, S. B. (1993). Pattern formation in a secondary field: a hierarchy of regulatory genes subdivides the developing Drosophila wing disc into discrete subregions. *Development* **117**, 571-84.

Williams, J. A., Paddock, S. W., Vorwerk, K. and Carroll, S. B. (1994). Organization of wing formation and induction of a wing-patterning gene at the dorsal/ventral compartment boundary. *Nature* **368**, 299-305.

Williams, R., Lendahl, U. and Lardelli, M. (1995). Complementary and combinatorial patterns of Notch gene family expression during early mouse development. *Mech Dev* **53**, 357-68.

Wilson, J. J. and Kovall, R. A. (2006). Crystal structure of the CSL-Notch-Mastermind ternary complex bound to DNA. *Cell* **124**, 985-96.

Xue, Y., Gao, X., Lindsell, C. E., Norton, C. R., Chang, B., Hicks, C., Gendron-Maguire, M., Rand, E. B., Weinmaster, G. and Gridley, T. (1999). Embryonic lethality and vascular defects in mice lacking the Notch ligand Jagged1. *Human Mol Genetics* **8**, 723-30.

Yamada, T., Pfaff, S. L., Edlund, T. and Jessell, T. M. (1993). Control of cell pattern in the neural tube: motor neuron induction by diffusible factors from notochord and floor plate. *Cell* **73**, 673-86.

Yang, A., Schweitzer, R., Sun, D., Kaghad, M., Walker, N., Bronson, R. T., Tabin, C., Sharpe, A., Caput, D., Crum, C. et al. (1999). p63 is essential for regenerative proliferation in limb, craniofacial and epithelial development. *Nature* **398**, 714-8.

Yang, X., Klein, R., Tian, X., Cheng, H. T., Kopan, R. and Shen, J. (2004). Notch activation induces apoptosis in neural progenitor cells through a p53-dependent pathway. *Dev Biol* **269**, 81-94.

Yu, S. Y., Yoo, S. J., Yang, L., Zapata, C., Srinivasan, A., Hay, B. A. and Baker, N. E. (2002). A pathway of signals regulating effector and initiator caspases in the developing Drosophila eye. *Development* **129**, 3269-78.

Zhang, N., Norton, C. R. and Gridley, T. (2002). Segmentation defects of Notch pathway mutants and absence of a synergistic phenotype in lunatic fringe/radical fringe double mutant mice. *Genesis* **33**, 21-8.

Zimmermann, R. C., Hartman, T., Bohlen, P., Sauer, M. V. and Kitajewski, J. (2001). Preovulatory treatment of mice with anti-VEGF receptor 2 antibody inhibits angiogenesis in corpora lutea. *Microvasc Res* **62**, 15-25.